P.D.
539.7
G326
v. 1
no. 3

TECHNICAL PROGRESS REVIEW

POWER REACTOR TECHNOLOGY

Prepared for U. S. ATOMIC ENERGY COMMISSION by the GENERAL NUCLEAR ENGINEERING CORP.

ILLINOIS STATE LIBRARY
JUL 1 - 1958
U. S. Dept. of Documents

JUNE 1958 VOLUME 1 NUMBER 3

TECHNICAL PROGRESS REVIEWS

To meet the needs of industry for concise summaries of current atomic developments, the AEC is publishing this series, Technical Progress Reviews. Issued quarterly, each of the reviews digests and evaluates the latest findings in a specific area of nuclear technology and science.

The three journals currently published in this series are:

Power Reactor Technology, Walter H. Zinn and associates, General Nuclear Engineering Corporation

Reactor Fuel Processing, Stephen Lawroski and associates, Chemical Engineering Division, Argonne National Laboratory

Reactor Core Materials (covering solid material developments), R. W. Dayton, E. M. Simons, and associates, Battelle Memorial Institute

Each journal may be purchased by subscription (domestic, $2.00 a year; foreign, $2.50 a year) or by individual issue (55¢) from the Superintendent of Documents, U. S. Government Printing Office, Washington 25, D. C.

●

Availability of Reports Cited in This Review

Unclassified AEC reports are available for inspection at AEC depository libraries and are sold by the Office of Technical Services, Department of Commerce, Washington 25, D. C.

Unclassified reports issued by other Government agencies or private organizations should be requested from the originator.

Unclassified British and Canadian reports may be inspected at AEC depository libraries. British reports are sold by the British Information Service, 30 Rockefeller Plaza, New York, N. Y.; Canadian reports (AECL series) are sold by the Scientific Document Distribution Office, Atomic Energy of Canada, Ltd., Chalk River, Ontario, Canada.

Classified U. S. and foreign reports identified in this journal as Secret or Confidential may be purchased by properly cleared Access Permit Holders from the Technical Information Service Extension, U. S. Atomic Energy Commission, P. O. Box 1001, Oak Ridge, Tenn. Such reports may be inspected at classified AEC depository libraries.

POWER REACTOR TECHNOLOGY

a review of recent developments *prepared by*

GENERAL NUCLEAR ENGINEERING CORP.

JUNE 1958 VOLUME 1 NUMBER 3

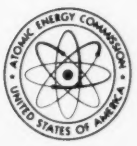

foreword

This quarterly review of reactor development has been prepared at the request of the Division of Information Services of the United States Atomic Energy Commission. Its purpose is to assist interested organizations in the task of keeping abreast of new results in reactor technology for civilian application.

The report is a concise discussion of selected phases of research and development for which there have been significant advances or a heightened interest in the past few months. It is not meant to be a comprehensive abstract of all material published during the quarter, nor is it meant to be a treatise on any part of the subject. The intention is to cover the various areas of reactor development from the general viewpoint of the reactor designer rather than from the more detailed points of view of specialists in the individual areas. However, papers which are thought to be of particular significance or particular usefulness in specialized fields will be mentioned in short notes. In the overall plan of the report, it is intended that various subjects will be treated from time to time and will be brought up to date at that time.

Any interpretation of results which is given represents only the opinion of the editors of the report, who are General Nuclear Engineering Corporation personnel. Readers are urged to consult the original references wherever possible in order to obtain all the background of the work reported and to obtain the interpretation of the results given by the original authors.

W. H. ZINN
General Nuclear Engineering Corporation

P.D.
539.1
G326
v.1
no.3

contents

ii		Foreword
		General Research and Development
1	I	Reactor Physics
17	II	Heat Transfer
20	III	Reactor Dynamics and Safety
24	IV	Fuel Elements
37	V	Other Reactor Materials
		Progress on Specific Reactor Types
42	VI	Liquid Metal Fuel Reactors
56	VII	Fast Reactors: EBR-II

Issued quarterly by the U. S. Atomic Energy Commission. Use of funds for printing this publication approved by the Director of the Bureau of the Budget on November 1, 1957.

SUBSCRIPTIONS

POWER REACTOR TECHNOLOGY is available on subscription for $2.00 per year domestic, $2.50 foreign, 55 cents per copy, through the Superintendent of Documents, U. S. Government Printing Office, Washington 25, D. C.

Integral Experiments and Evaluations

Bucklings for D_2O Moderated Lattices

A number of buckling measurements on clumped fuel elements in D_2O have been reported recently. These measurements, along with those reviewed in the referenced report, indicate that considerable work is in progress to fill the needs for lattice measurements of this type.[1] Most of the measurements so far have been measurements of buckling only, but it is presumed that more detailed measurements of the lattice characteristics will follow.

Buckling measurements on fuel assemblies made up of plates, tubes, and rods have been reported.[2] Some of the measurements were made in exponential facilities of the usual type, whereas others were made in the Savannah River Process Development Pile. The latter measurements require corrections of up to 30 μB, which are not applied in the reference. The plate assemblies were made up of uranium metal plates, 0.180 in. thick, at various spacings. Buckling measurements were made over a range of volumetric ratios of moderator to fuel from ~10 to 60, both with and without D_2O in the fuel-element assembly (thus simulating both D_2O- and gas-cooled reactors). Tubular fuel assemblies with outside diameters of 3.03 and 2.31 in. and wall thicknesses of 0.185 and 0.215 in., respectively, were studied, both singly and in coaxial pairs. The rod clusters were made up of large (1 in. in diameter) uranium metal rods. It is stated that measurements on clusters of smaller rods are planned. Neutron flux traverses were taken for several of the plate lattices. It is stated that the values of the effective absorption cross section of the lattice, the thermal diffusion constant, the diffusion area, and the thermal utilization derived from these measurements agreed well with those calculated on an IBM 650 computer with the P-3 approximation.

Measurements[3] on lattices of clumped natural-uranium dioxide rods in D_2O were made in the Process Development Pile. The rods were made of UO_2 pellets 0.370 in. in diameter with a density of 10.0 g/cm^3. Clusters composed of 13 to 61 rods of two different spacings (0.632 and 0.795 in. center-to-center) were investigated in triangular lattices of spacings 7.00, 9.26, and 10.70 in. Maximum bucklings for 31 and 37 rod clusters occurred at ratios of moderator volume to equivalent uranium metal volume of 40 to 50; the maximum values were between 400 and 500 μB, with the higher values for the smaller clusters (the lattices contained some aluminum).

It was assumed[3] that the values for τ, D_f, and D_s were the same in the test lattice as in the rest of the Process Development Pile. These assumptions, with a P-3 calculation for f and L^2, and an estimate of ϵ from other experimental work, allowed the evaluation of k_∞ and p. The values of k_∞, when plotted as a function of moderator-to-fuel volume ratio, gave a continuous curve, which did not appear to be influenced appreciably by the manner of achieving a given ratio (i.e., whether by using clusters of many rods with a large lattice spacing or clusters of few rods in a smaller lattice spacing) so long as the spacing of the rods in the clusters was held constant. For the rod spacing of 0.632 in., k_∞ rises from a value of ~1.026 at a moderator to equivalent uranium metal volume ratio of 20 to a value of 1.170 when the ratio is increased to 70. Evidently the lower values of buckling which occur for the larger clusters relative to the smaller clusters represent an increase in diffusion length, reflect-

ing the circumstance that it is harder for thermal neutrons to "find" the large widely spaced clusters than the smaller more closely spaced ones.

The Critoph formulation for resonance escape probability was applied to the derived values of p. It was found that this formulation gave a consistent pattern for the results provided the effective energy of resonance absorption was taken to lie in the range from 7 to 20 ev. This range is lower than that used by Critoph to fit the ZEEP data[4] (100 ev). However, the method used for calculating the resonance flux dip in the fuel elements was different from that used by Critoph.

Measurements[5] on clusters of natural-uranium dioxide rods in D_2O are also reported for 0.632-in. center-to-center rod spacing. Buckling measurements were made over a range of volumetric ratios of moderator to equivalent uranium metal from ~20 to 70 for three cases: (1) D_2O-cooled fuel clusters without housing tubes, (2) D_2O-cooled fuel clusters in aluminum housing tubes, and (3) the same clusters with the D_2O in the housing replaced by helium. Substitution of gas cooling for D_2O cooling has comparatively little effect on buckling if the total volume of gas in the lattice is kept small. However, buckling decreases markedly if large volumes of the lattice are occupied by gas.

Reference 6 describes measurements made in the Savannah River exponential facility, the Subcritical Experiment (SE), on natural-uranium metal plate lattices. Earlier measurements of this type have been reviewed in reference 1. The experiments described in reference 6 were done in two phases. During the first phase, a preliminary design fuel assembly was used, whereas the second phase covered measurements on fuel assemblies which resembled more nearly those of a practical mechanical design. The latter differed from the earlier assemblies primarily in the plate spacing and in the amount of nickel plating used between the uranium metal and the aluminum jacket. Also, the average moderator analysis during the two phases was different. The characteristics of the different fuel assemblies (Fig. 1) are compared in Table I-1, and the measured bucklings are given for an equilateral triangular lattice of 7-in. spacing.

The results of the buckling measurements on the two sets of fuel assemblies were in good agreement after appropriate corrections were applied to account for differences in design and moderator purity.

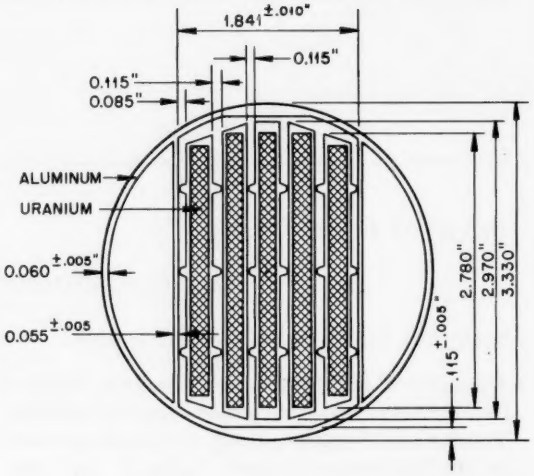

	Uranium length, in.	Uranium width, in.
Center plate	2.728	0.180
Unribbed plates	2.728	0.180
Outside ribbed plates	2.510	0.180
Cladding thickness	0.030	

Figure 1—Uranium plate assembly.

Table I-1 CHARACTERISTICS OF PLATE ASSEMBLIES

	Preliminary design	Later design
Thickness of uranium, in.	0.180	0.180
Cross sectional area of uranium, sq in.	2.38	2.38
Average thickness of electroplated nickel layer, in.	0.0007	0.0002
Cladding (2S aluminum), in.	0.030	0.030
Thickness of D_2O channel between plates, in.	0.140	0.115
Average moderator purity, mole % D_2O	98.97	99.80
Measured buckling, μB	361	425
Corrected buckling,* μB	417	425

*Preliminary design corrected to the same D_2O channel thickness, moderator purity, and nickel content as for later design.

The change in buckling was measured when D_2O was removed from the coolant channels surrounding the plates of the preliminary fuel design. The material buckling was increased by 50 μB. The effect of the orientation of the plate assemblies into positions other than that in which all plates were parallel was also in-

vestigated. However, within the precision of the experiments, no change in buckling was obtained.

During the final phase of the measurements, the 7-in. lattice spacing was increased to study the dependence of material buckling on the volume ratio of moderator to fuel. Starting with a 7-in. spacing, the fuel assemblies were spread apart to increase the moderator-to-fuel volume ratio progressively from 15 : 9 to 69 : 5. A maximum buckling of 492 ± 20 μB was obtained at a moderator-to-fuel volume ratio of 24 : 8. The results of the measurements of material buckling as a function of moderator-to-fuel volume ratio are plotted in Fig. 2. The deviations indicated for the points are estimated standard deviations. The lattice configurations used are shown in Fig. 3.

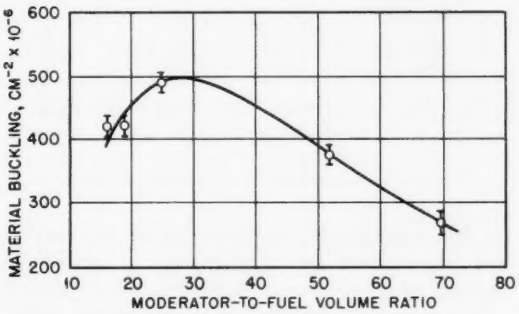

Figure 2 — Effect of moderator-to-fuel ratio on material buckling.

A summary of the calculated and measured parameters for the plate lattices are given in Tables I-2 and I-3.

Measurements[7] of k_∞ for D_2O moderated clusters of UO_2 and plutonium-aluminum rods were made in the Hanford Physical Constants Testing Reactor. The measurement involves the installation of a small section of the unknown lattice at the center of the test reactor and poisoning the central cell with thermal absorber to the point where its reactivity effect is zero. The multiplication constant of the lattice can then be determined from the amount of thermal poisoning required. The function of the unknown lattice cells surrounding the central cell is to convert the neutron spectrum of the test reactor to that which characterizes the unknown lattice.

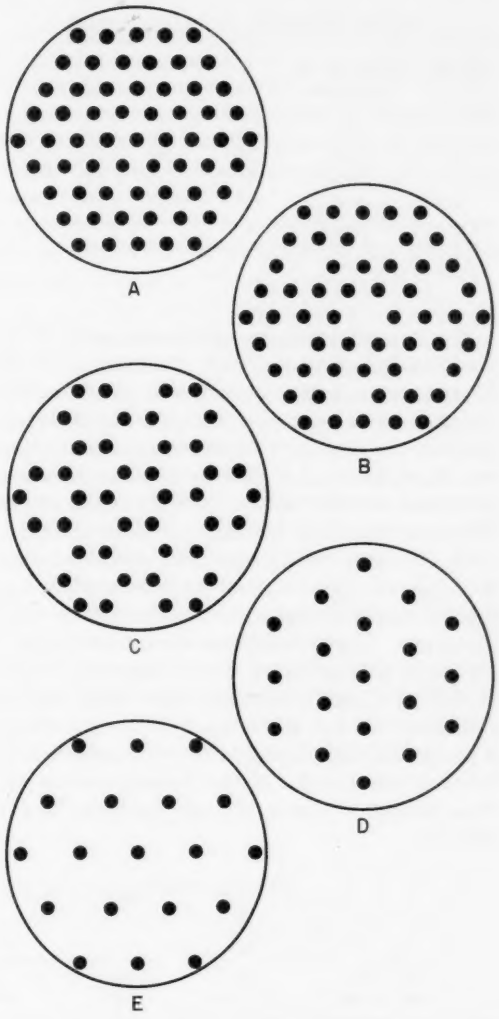

Figure 3 — Arrangement of lattices in the exponential tank for investigating the effect of moderator-to-fuel ratio. A, 15.9; B, 18.8; C, 24.8; D, 51.5; E, 69.5.

Table I-2 COMPARISON OF MEASURED AND CALCULATED PARAMETERS FOR PLATE LATTICES AT A 7-IN. LATTICE SPACING

Parameters	Measured value*	Calculated value (P_3 approximation)
f	0.951	0.953
$(\Sigma_a)_{eff}$, cm^{-1}	0.01056	0.01074
L^2, cm^2	78.8	80.4

*Corrected to moderator purity of 99.80 mole % D_2O and nickel layer 0.0002 in. thick.

Table I-3 SUMMARY OF CALCULATIONS

Lattice No.	Moderator-to-fuel ratio	L^2, cm^2	f	k_∞*	p*
1	15.9	80.4	0.95	1.087	0.835
3	24.8	129.7	0.948	1.126	0.869
4	51.5	291.9	0.929	1.152	0.908
5	69.5	404.4	0.916	1.146	0.916

*Derived from measured bucklings using calculated values of L^2 and f.

The UO_2 fuel rods had diameters of 0.504 in. and density of 10.1 g/cm^3. Clusters of 7 and 19 rods were investigated on 7- and 8-in. triangular lattice spacings. Both air and D_2O were used in the process tube surrounding the cluster. A rather large amount of aluminum was contained in the lattice (roughly equal to the UO_2 in volume). In the case of the 19 rod clusters, the value of k_∞ was also measured when 3 of the 19 rods in a cluster were replaced by plutonium-aluminum rods containing 1.78 wt. % plutonium. This substitution represented a ratio of weight of plutonium in the lattice to weight of U^{235} of 0.142; it increased the "effective enrichment" of the fuel from 0.00714 to 0.00816, if plutonium is assumed to be equivalent to U^{235}. Some of the results of the measurements are summarized in Table I-4 for the 8-in. lattice spacing.

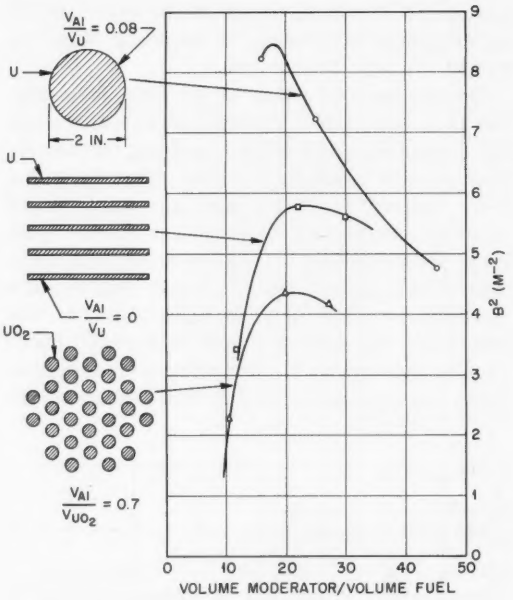

Figure 4 — Volume ratio of moderator to fuel.

as the 2-in. solid rod. However, no correction has been made for differences in aluminum content of lattices or differences in D_2O purity.

For measurements[9,10] on thoria-urania mixtures in D_2O, fuel pellets of roughly $\frac{1}{4}$ in. in diameter were used, composed of 84.28 wt. % thorium, 3.37 wt. % U^{235}, and the remainder oxygen. Reference 9 reports exponential studies in a 5-ft-diameter tank, and reference 10 reports critical experiments in a tank of $6\frac{3}{4}$ ft in diameter. In both cases the fuel was used in simple single rod lattices. The lattices investigated in reference 9 were quite dilute; a rod spacing of $\sim 2\frac{1}{4}$ in. or less would have been supercritical. The experiments therefore do not give much information on the interesting question of resonance absorption. The measurements of reference 10 were made with a much

Table I-4 RESULTS OF MEASUREMENTS

No. of fuel rods per cluster	Coolant	Volume ratios: Moderator / UO_2	Coolant / moderator	Al / UO_2	Pu-Al / UO_2	f	k_∞
19	Air	11.809	0.093	1.004	0	0.898	1.060
19	D_2O	11.809	0.093	1.004	0	0.892	1.048
19	Air	14.023	0.093	1.192	0.1875	0.9039	1.117
19	D_2O	14.023	0.093	1.192	0.1875	0.8982	1.112

It is not possible to summarize the results of all the measurements described in the foregoing paragraphs in this review. A few of the data, however, have been plotted in Fig. 4 to illustrate the effects of fuel subdivision in the lattice and have been compared with earlier measurements on single rod lattices.[8] The bucklings are plotted as functions of the volume ratio of moderator to fuel, where fuel refers to uranium metal or UO_2, as the case may be. Fuel clusters have been selected which contain roughly the same volume of fuel per unit length

more concentrated lattice, having a triangular spacing of $\frac{3}{4}$ in. and giving a moderator-to-fuel ratio of ~13. The buckling of this lattice was determined to be 1.64×10^{-3} cm^{-2}. Criticality was measured at various core diameters, with the height of D_2O adjusted in the tank to the critical value. A core 60 in. high was critical at a radius of 10.71 in. A description of the critical facility used for these measurements is contained in reference 11.

Graphite Lattices

Reference 12 reports buckling measurements on small (4 by 4 by 6 ft) graphite exponential piles using enriched uranium of 1.44 wt. % U^{235} content. The uranium was in the form of hollow slugs with an outside diameter of 1.37 in. and an inside diameter of 0.48 in. A "coolant" annulus was provided around each slug. Bucklings were measured with and without ordinary water in the coolant annulus and in the hollow core of the fuel slug. Lattice spacings from ~5 to 10.5 in. were investigated.

In reference 13 the previously measured values of diffusion length in five Hanford Production Pile moderators and in the Standard Pile, a graphite stack, have been corrected for (1) neutron absorption in the aluminum process tubes, (2) atmospheric nitrogen in the openings of the pile, (3) nitrogen in the graphite pores, (4) neutron streaming in voids, and (5) density of the graphite to reduce these values to diffusion lengths of equivalent solid stacks of graphite of 1.6 g/cm^3 density for comparison purposes. The weighted average value of the diffusion length of four of the piles is 54.19 cm, equal to the value for the Standard Pile. The values of the diffusion length were measured prior to the start-up of the cold piles and do not apply to the operating piles.

A revised value of the macroscopic thermal absorption cross section of reactor grade aluminum of 0.0145 cm^{-1} and a revised microscopic transport cross section of graphite of 4.95 barns was used in the analysis, which yields an apparent thermal absorption cross section for carbon of 3.748×10^{-3} barns at 2200 meters/sec.

Temperature Effects in Graphite Lattices

In designing a nuclear reactor it is necessary to know how the reactivity behaves with changes in temperature. The temperature coefficient of reactivity is due to (1) the dependence of neutron cross section on neutron energy, (2) the dependence of material densities on the temperatures of the materials utilized in the reactor, and (3) the dependence of resonance capture on the temperature of the resonance captor.

Reference 14 reports measurements of buckling as a function of temperature in a graphite exponential pile of $7\frac{1}{2}$-in. lattice spacing. The lattice section of the assembly was a 101-in. cube which was set on six 1- by 2-in. graphite shims on top of a 20-in.-thick graphite base. The pile was loaded with natural-uranium fuel elements of 1.36 in. in diameter by 4 in. in length. This loading gives a uranium volume in the lattice cell of 9.37 cm^3/cm of length, an aluminum volume of 3.31 cm^3/cm, a graphite volume of 347.49 cm^3/cm, and an annular void volume around the slugs of 2.33 cm^3/cm. The density of the graphite utilized in the pile was 1.648 g/cm^3. The exponential pile was heated electrically to a maximum of 460°C.

The material buckling variation with temperature obtained from the experiment is -9.72×10^{-8}cm^{-2}/°C. This results in a temperature coefficient with a pile atmosphere of air of

$$\frac{1}{B_0^2}\frac{\Delta B_m^2}{\Delta T} = -9.92 \times 10^{-4}/°C \qquad \text{(air)}$$

From the critical equation

$$\eta = \frac{(1 + B_m^2 L_t^2)\, e^{B_m^2 \tau}}{\epsilon f_u p}$$

it can be seen that if the dependency of the parameters f_u, p, L_t^2, and τ on the thermal temperature of a reactor can be calculated then the dependency of η on temperature can be determined. The results of the reported calculations of the lattice parameters are reproduced in Table I-5.

A least squares analysis of the k_∞ determined from the experimental bucklings and the calculated lattice parameters result in the temperature coefficient

$$\frac{1}{k_\infty}\frac{\Delta k_\infty}{\Delta T} = -4.58 \times 10^{-5}/°C \qquad \text{(air)}$$

Theoretical corrections were made to the parameters in Table I-5 for the presence of air in the pile. The corrected temperature

coefficients for the air-free pile are

$$\frac{1}{B_0^2}\frac{\Delta B_m^2}{\Delta T} = -9.69 \times 10^{-4}/°C$$

and

$$\frac{1}{k_\infty}\frac{\Delta k_\infty}{\Delta T} = -4.99 \times 10^{-5}/°C$$

Reference 15 reports measurements of the variation of thermal-neutron diffusion length in graphite with temperature, up to 500°C. The observed variation is in good agreement with that predicted by the relation

$$L^2 = (3N\,\sigma_a\,\sigma_{tr})^{-1}$$

where N, σ_a, and σ_{tr} denote, respectively, the density of nuclei, the thermal microscopic absorption cross section, and the thermal microscopic transport cross section and where the transport cross section is assumed constant with temperature and the absorption cross section is assumed to vary as $1/\sqrt{T}$.

An expression was obtained, from the experimental data, relating reactivity change to changes in moderator temperature and fuel exposure. As expected from the Pu^{239} fission cross-section variation with neutron energy in the thermal energy range, the experimental results showed a strong positive increase in graphite coefficient with exposure level. No attempt was made to compare the experimental results with theoretical calculations based on the thermal-neutron equilibrium distribution existing in the pile and on the Pu^{239} cross-section variation with neutron energy. The report discusses and, in some cases, evaluates the possible sources of errors arising in the interpretation of the experimental results.

Small Graphite-moderated Beryllium-reflected Assemblies

Critical experiments on small graphite-moderated beryllium-reflected assemblies, fueled with highly enriched U^{235} foils, are reported in reference 16. Core lengths of ~77 cm were used, with core radii from 31.3 to 48.8 cm. The radial beryllium reflector thickness varied from 12 to 14 cm. Critical masses from 17.4 to 57.5 kg were observed, the larger values being associated with the smaller core radii. The data, including flux distributions and fission distributions, are presented in considerable detail.

Conversion Ratio of PWR Blanket

Reference 17 presents results of experimental measurements of the initial conversion ratio in the natural-uranium oxide blanket of a mock-up critical assembly of the Pressurized Water Reactor (PWR). The experimental values reported were determined on two of the fuel assemblies of the outer blanket. The PWR power-reactor core consists of an annular "seed" region of highly enriched uranium and an inner and outer "blanket" of natural-uranium oxide. It is stated that there is not a large difference between the true PWR design and the mock-up; thus the values of initial conversion ratio in the PWR power reactor can be inferred from the values measured in the critical assembly.

Radiative capture of neutrons in the U^{238} of the natural-uranium blanket results in the production of Pu^{239}, thus giving increased core life. The conversion ratio is expected to vary with position in the blanket because of the neutron flux spectrum variation over the blanket volume. The major variation in flux spectrum arises

Table I–5 RESULTS OF THEORETICAL CALCULATIONS*

Temp., °C	f_u	p	L_t^2	τ	Experimental B_m^2, μB	k_∞	η
20	0.9128	0.8593	188.5	251.9	97.9	1.0542	1.3011
100	0.9166	0.8574	201.6	348.3	90.6	1.0509	1.2946
200	0.9203	0.8553	216.7	346.1	79.7	1.0457	1.2862
300	0.9230	0.8533	230.2	343.6	71.0	1.0414	1.2801
400	0.9249	0.8521	243.3	341.1	60.6	1.0359	1.2726
460	0.9264	0.8511	249.0	340.5	55.5	1.0332	1.2686

* ϵ = 1.0329 for all pile temperatures.

from the nonhomogeneity of composition of the blanket region, mainly due to the water channels between the assemblies of fuel rods. As a result of this nonhomogeneity, large local changes occur in the moderating and absorption properties of the blanket region, and there are rather large local variations in neutron flux spectrum.

The reference describes the experimental techniques used in the measurements and compares the experimental results with theoretical calculations based on four-energy group diffusion theory. Two geometric representations of the critical assembly were used in the calculations: (1) the seed and blanket regions were each separately described as homogeneous mixtures of appropriate composition with the water channels explicitly described as separate regions and (2) the water channels were "smeared out" into the fuel regions so only the grossly different regions of seed, blanket, and external water reflector were differentiated as to composition.

The calculations which explicitly describe the water channels agree fairly well with the experimental results. The smeared out calculation, although it fails to describe the large local variations actually obtained, appears to predict the average value of conversion ratio in the blanket — stated to be ~1.15 — quite well.

The conversion ratio in the blanket alone would be expected to be quite high, since the fuel is natural uranium, and the fuel to moderator ratio is rather high, giving a low resonance escape probability. The net conversion ratio for the entire reactor must take into account the destruction of U^{235} in the highly enriched seed and therefore is much lower. The net conversion ratio is related to the blanket conversion ratio approximately by

Net conversion ratio ≅ (blanket conversion ratio) × (fraction of total power produced in blanket)

The fraction of power generation in the blanket has been estimated[18] to be 0.5 at the beginning of core life and 0.45 after the equivalent of 3000 full-power hours of operation.

Doppler Effect

In fast-neutron reactors it is theoretically possible for the fission resonances of U^{235} to give a positive component to the temperature coefficient of reactivity because of Doppler broadening of the resonances. Doppler broadening of the U^{238} absorption resonances would have an opposite reactivity effect, and it would be expected that the net prompt temperature coefficient would be negative for fast reactors which contain relatively high proportions of U^{238}. Several experiments have been performed[19] in the Argonne fast critical facility, ZPR-III, to investigate the Doppler effect in assemblies simulating EBR-I, which contains a negligible fraction of U^{238} in the core, and EBR-II, which will contain roughly equal fractions of U^{235} and U^{238}.

The over-all temperature coefficients of three assemblies, two of which approximated the EBR-II core composition, were measured. The measured values were negative in both cases. They were then calculated, and the results were compared to the measured values. No Doppler effect was included in the calculations. The agreement between the measured and the calculated temperature coefficients was reasonably good. The third assembly differed from the other two in that the U^{238} was replaced by steel. This change did not result in a marked decrease of the negative temperature coefficient, as would have been the case if Doppler broadening were playing an important part in the coefficient.

The Doppler effect has remained a possible explanation of the positive prompt power coefficient of reactivity in EBR-I, even though bowing of the fuel elements appears to be the most plausible explanation of the effect.[20] The EBR-I was mocked up in ZPR-III, and the assembly was investigated for the Doppler effect. The measured core temperature coefficient (negative) and the calculated (without Doppler effect) temperature coefficient showed little difference. The small difference could be assumed to be due to a small positive Doppler effect. The difference is slightly less than the predicted theoretical Doppler effect for EBR-I. Hence the experiment strongly indicates that the Doppler effect was not the primary cause of the much larger prompt coefficient in EBR-I, and the experimental results are in best agreement with calculated temperature coefficients if a Doppler effect equal to or less than the theoretical value is used.

A direct measurement of the Doppler effect was attempted in an assembly having approximately the EBR-II composition. No effect was seen, but the limits of sensitivity of the experiment were such that it allowed only the deter-

mination of an upper limit of 9×10^{-11} $(\Delta k/k)/g\ U^{235}/°C$ for the Doppler temperature coefficient of reactivity. This is about a factor of 3 greater than the current theoretical predictions.[21,22]

A second experiment to measure the Doppler effect for U^{235} was made in an assembly which was a mock-up of EBR-I. A helical element of U^{235} was first thermally cycled in the assembly with U^{235} as the fuel. The assembly was then reloaded with plutonium as the fuel, maintaining approximately the same geometry, and the element was thermally cycled again. The purpose of the plutonium-fueled assembly was to obtain an estimate of the effects of motions of the heated element due to thermal expansion. The Doppler effect of the uranium resonances of the element interacting with the uranium resonances of the core, and small motions of the element due to expansion, can each produce a small but presumably measurable reactivity change. In order to obtain a true Doppler effect measurement, it is necessary to correct the observed reactivity change on thermal cycling for the effect due to this motion. The experiment was performed first in the uranium-fueled assembly, then in the plutonium-fueled assembly, where any Doppler effect should be very sharply reduced in magnitude. The results indicate the following upper limit for the Doppler effect in the uranium-fueled assembly for the temperature range involved:

$$\frac{\Delta k}{k}\ (\text{Doppler effect}) \leq +\ 1.2 \times 10^{-11}/g\ U^{235}/°C$$

As a result of these experiments, it is considered reasonable at the present time to assume a Doppler coefficient for EBR-II equal to 1.5×10^{-6} $(\Delta k/k)/°C$. Although this is only half the value calculated theoretically in reference 21, it is stated[19] that more recent theoretical work indicates lower values.[23]

Experiments have been performed in the Hanford Test Pile[24] to measure the Doppler coefficient of U^{235} for reactor loadings containing low density concentrations of U^{235}. The Test Pile is a thermal-neutron reactor. The conclusion drawn from the results of these experiments is that the Doppler coefficient of U^{235} at these densities is too small to be measured with the Hanford Test Pile.

The Coupled Fast-Thermal Assembly

In reference 25 measurements related to the coupling of the fast and thermal sections of the Argonne ZPR-V critical assembly are described. ZPR-V is a zero power coupled fast-thermal critical assembly, involving a dilute fast core surrounded by a light water moderated enriched-uranium thermal annulus. The two regions are coupled through an annular natural-uranium isolation blanket. This facility is used in studying some of the properties of dilute fast reactor systems as well as those of coupled fast-thermal power breeders. The fast-thermal reactor is of interest because of the expectation that thermal reactor control characteristics (reasonably long neutron lifetime; sensitivity to thermally absorbing control rods) may be approximated in the reactor while maintaining a conversion ratio which approaches that of a pure fast system.

From the standpoint of reactor control, the quantities of interest in a given fast-thermal system are the effective prompt neutron lifetime and the reactivity sensitivity of the coupled system to changes in the compositions of the fast and thermal sections. These two characteristics have been investigated in the reported work, the reactivity effects being described in terms of the "reactivity fraction" of each region of the reactor. The reactivity fraction of a given region is defined theoretically as the ratio of the spatial integral (over the region) of the neutron production density, weighted with the adjoint flux, to the integral of the adjoint-weighted production density over the total reactor. The measured reactivity fractions for the fast core, the isolation blanket, and the thermal annulus were, respectively, 0.24, 0.14, and 0.61. The measured effective prompt neutron lifetime was 39.0 ± 3.0 μsec.

From the standpoints of conversion ratio and fuel economy, the interesting quantity in a given system is the ratio of the number of fast fissions to the number of thermal fissions. This ratio is stated in the reference in terms of the ratio of the number of neutrons emitted by fast fissions to the number emitted by slow fissions. The measured value of this quantity is 0.43. The fast to thermal fission ratio would be slightly lower than this number.

In a fast-thermal power reactor, it would be expected that the fast core would be made larger relative to the thermal annulus than it is in

ZPR-V. For such a case the reactivity fraction of the fast core, as well as the fast to thermal fission ratio, would be larger. The effective prompt neutron lifetime would decrease, although not necessarily by a large amount.

Alpha Measurements in EBR-I

The results of capture to fission ratio measurements for U^{235} and Pu^{239} at various locations in EBR-I have been reported in reference 26. The number of capture events in the U^{235} and Pu^{239} samples, respectively, were determined by mass spectrometric measurement of the increase in U^{236} or Pu^{240} content of each sample. The number of fissions in each sample was determined by radiochemical assay of the fission product Cs^{137}. The variation of α, both radially and axially, has been determined. These measurements will be very useful in the analysis of fast reactor systems for they represent effective values of α for the type of neutron spectrum characteristic of such systems. The effective energy of the spectrum varies over a wide range in EBR-I, from the center of the core, which is fueled with highly enriched U^{235}, through the natural-uranium inner and outer blankets, which are finally surrounded by graphite. Within this range neutron energy spectra can probably be found which approximate the spectra of most fast reactors of interest for power generation. Measurements of the neutron energy spectrum at various points in EBR-I have been previously reported.[27]

If it is assumed that ν, the number of neutrons emitted per fission, is constant at the thermal value, values of η, the number of neutrons produced per neutron absorbed in the fissionable isotope, can be derived from the α measurements. For Pu^{239} the value of η so derived is near 2.7 at the center of EBR-I and remains above 2.0 throughout the inner blanket and most of the outer blanket. For U^{235} η falls below 2.0 at a point about two-thirds through the inner blanket.

Resonance Absorption in Uranium Rods

Reference 28 reports a measurement of the spatial distribution of U^{238} resonance capture in a 1.3 per cent enriched-uranium metal rod 0.387 in. in diameter. The metal fuel rod was installed as the center rod of a uranium oxide fueled lattice moderated by light water. The U^{238} resonance capture was measured in a cadmium-covered section of the rod as a function of radial position in the rod, using depleted U^{238} foils. The activity observed was the 103-kev X ray emitted in the de-excitation of the excited state of Pu^{239} to the ground state by internal conversion. The distribution in the body of the cylinder was measured by flat metal foils, whereas the distribution near the surface, to a depth of 0.065 in., was measured by a long thin (0.002 in.) spiral foil of natural uranium which was wound onto a section of the cylinder having an appropriately reduced diameter. The distribution of resonance capture was found to be rather flat at depths greater than 40 mils.

If the resonance integral is assumed to have the usual form

$$RI = A\left(1 + \mu \frac{s}{m}\right)$$

the value of μ can be derived from the observed distribution. The value of μ s/m was found to be 0.28. The corresponding value calculated from the results of Creutz et al.[29] would be 0.59. It is stated that this value would drop to 0.52 if a correction were made for the interaction of neighboring rods. The difference shown in this comparison suggests that part of the surface term in the expression is contributing to the volume activation in the small rod used for the tests.

Measurements of this type are of great value as data for the better understanding of resonance absorption in lumped absorbers. For the development of improved theoretical treatments of the problem, detailed measurements of this type are needed in addition to the gross measurements of resonance escape probability in various lattices.

Control Rods

The most widely used method of controlling a reactor is the insertion of a neutron absorbing material into the core region by mechanical means. The neutron absorbing material, or control rod, changes the neutron reproduction factor to a desired level and produces changes in the neutron flux and power distributions. The treatment of these changes is one of the functions of reactor physics. In

some cases it poses complex and difficult problems. For example, the usual control-rod arrangement in an H_2O moderated reactor — an array of cruciform rods in a cylindrical core — is a formidable problem to treat analytically.

The Reactor Control Meeting in Los Angeles, Mar. 6–8, 1957, was devoted mainly to considerations of control-rod physics. The following sections contain a brief discussion of this subject, based on the recently issued unclassified record of the meeting[30] and on articles from the October 1957 Bettis Technical Review.[31] Most of the material is slanted toward the problems of H_2O moderated reactors, but most of the theoretical methods have general applicability.

Geometry

The term "rod" is often a misnomer as applied to the control elements used in a practical reactor design. Most control elements being used in water moderated reactors are thin slabs, or configurations such as the wye and the cross, which may be considered as assemblies of thin slabs. The reason for using thin slabs is that this geometry furnishes a large surface to mass ratio, which gives a high probability of neutron capture without taking up much room in the reactor core.

A method of calculating slab type control rods has been published recently by Hurwitz and Roe.[32] This method is a one-group treatment for a black control rod and involves the calculation of an effective area around the rod within which all neutrons are considered to be captured by the rod. This absorption area in the limit of small thermal diffusion lengths is simply the product of the diffusion length and the effective perimeter, which, in turn, is the geometric perimeter plus a correction for the corners. Once the absorption area is determined, the rod can be eliminated from the calculation, and the absorption area can be treated as a region of zero fission probability or of zero source strength for the thermal-neutron group. This theory has been corrected for the fact that, in general, the flux does not go to zero at the surface of the absorber and has been extended to include gray control rods.[30a] Further extensions of the theory to include more than one energy group have also been made.[33–35]

This method is particularly useful if the rods can be considered as uniformly distributed over the reactor core or if the core can be divided into coaxial regions each of which contains a uniform rod distribution. In its application the method is rather similar to the cell method.[30b] Calculational methods,[30c,30d,36] which are extensions of the Nordheim-Scalettar method,[37] are useful for strong off-center rods installed in patterns which are not easily handled by the absorption area or cell techniques. These methods usually apply only to rods of simple shapes (e.g., circular cylinders). Often more complex shapes can be converted to equivalent cylinders by the absorption area method or by other methods.

Since the relation between neutron absorption in the rod and reactivity is dependent on the rod position, the calculation of a group of partially inserted slab type rods is a three-dimensional problem and no straightforward analytical solution is available, although a three-dimensional machine code (TRIXY) for the IBM 704 has recently been developed for this problem.[38] At present such problems are being solved by calculations assuming all rods in a bank (window shade technique) and by patching together pieces of two-dimensional calculations.

Epithermal Absorption Cross Section

Most of the elements that are considered for control-rod materials have large epithermal resonance absorption cross sections, and it is generally acknowledged that the effect of epithermal absorption may be quite large. For example, a comparison of hafnium and cadmium slabs of the same thickness (~0.100 in.) in a polyethylene moderated critical assembly reveals that hafnium is 25 per cent more effective.[30e] Since cadmium of this thickness is black to thermal neutrons whereas hafnium is somewhat transparent, the difference in their effectiveness is due to the large epithermal resonances in hafnium.

Unfortunately, there are rather large uncertainties regarding the calculation of epithermal absorptions. These uncertainties are caused by various factors, such as incomplete and poor resolution in cross-section measurements, uncertainty in the proportion of each resonance attributed to absorption, and spatial and energy self-shielding effects. Nevertheless, a considerable amount of theoretical calcula-

tion has been performed to derive effective epithermal constants, particularly for application to control-rod regions in digital computer codes.[30f,30g,39] However, most of the applied methods fit constants empirically to experimental measurements in order to avoid uncertainties.

Since the epithermal capture is large in the important cases, the control rod undoubtedly perturbs the existing flux spectrum in the vicinity of the rod. However, most calculations are made without taking into account the epithermal flux depression and are made by assuming that the spectrum is characteristic of the fuel-moderator region, usually of the 1/E variety.

Power Distribution

It is desirable that the control-rod system be so designed that it produces the minimum adverse effect on the reactor power distribution. In a reactor having several strong control rods moved in a bank, the average power density in the control-rod region may be quite small; the heat generation is then confined almost entirely to the rodless region, and the total power capacity of the reactor is reduced. To minimize such effects, the rods should be programmed to utilize the core as effectively as possible for heat transfer. The axial flux distortion can be minimized by operating rods one at a time so that every rod except one is either completely in the core or completely out. Similarly, the radial power distribution can be flattened by a suitable placement of rods with respect to the radial direction.

The development of an optimum rod programming procedure would include a complete study of the reactor throughout its life and possibly would require three-dimensional multiple control-rod calculations. Actual rod programs are usually based on simpler analyses, often primarily on analyses of the condition at start-up, when the reactor is near its maximum reactivity. However, care is necessary in such calculations to ensure that the power distribution does not get worse with reactor operation. Some of the techniques involved in approximating three-dimensional power distributions for reactors containing banks of partially inserted rods are described in references 30b and 40–42.

Control-rod Channels

A troublesome effect which usually accompanies the use of absorbing control rods in H_2O moderated reactors is the thermal-flux peaking in the water channels which are left when the rods are withdrawn. This peaking increases significantly the power density in the fuel elements adjacent to the channel, relative to the power density in elements farther away. Since some of the control rods are almost always installed in regions of the core where the general level of power density is highest, the additional power peaking near these rod channels adds appreciably to the maximum to average power ratio for the core. Control-rod followers composed of low absorption materials can reduce this effect by keeping the water out of the region vacated by the rod. However, the use of followers usually requires a longer and more expensive pressure vessel. The followers can only partially eliminate the peaking effect because adequate mechanical clearances must be maintained. A considerable amount of effort has been made to calculate accurately the water-channel power peaking factors.[30h,30i] The presence of corners in the channels introduces severe mathematical difficulty because of the slow convergence of the more precise solutions for this case.

If the control-rod follower consists of a modified fuel element, the water-channel flux peaking may be largely eliminated. Control rods employing such followers usually have a shape which approximates that of the standard fuel subassemblies used in the reactor core. The absorbing section may be a shell of absorbing material filled with water; the water also serves as the coolant for the fueled section of the rod. In addition to the low energy neutrons which diffuse to the absorbing shell from the external fueled region, neutrons slowed down by the water inside the shell are also captured. The reactivity worth of such a rod can therefore be quite large. Rods of this type are used in the Materials Testing Reactor (MTR) and the Army Package Power Reactor (APPR). References 30j and 30k describe the APPR control rods and their characteristics.

The possibility of an inverted reactivity effect (partial insertion of the control rod causes an increase rather than a decrease of reactivity) under certain conditions with control rods using fuel bearing followers has been pointed out.[43,44]

This condition can occur if a number of strong control rods are operated as a bank. When the bank of rods is partially inserted, the effective position of the core (reactivity-wise) is displaced away from the region occupied by the absorbing sections of the rods and toward the reflector at the opposite end of the core. The movement of fuel toward this more effective end of the reactor (i.e., the insertion of a control rod not included in the original bank of rods) could then result in a reactivity increase. This situation can be avoided by proper programming of the rods.

Coolant and Jacketing Effects

The necessities of cooling the control rod, and, in some cases, of jacketing the absorbing material, introduce other uncertainties. The coolant and cladding both tend to reflect neutrons away from the rod; in addition the coolant, if water, also slows down more neutrons in the vicinity of the rod. These are thin region effects which are difficult to calculate but can conceivably be important.[39]

Variations in Control-rod Worth

Since control-rod worth is a function of the diffusion length in the surrounding medium, a change in temperature, which has a pronounced effect on diffusion length, affects the rod worth. In a practical reactor the composition changes with time as fuel is burned and plutonium is formed. This change also affects the diffusion length and the rod worth. If burn-up of the absorbing material in the rods is appreciable, the blackness of the rods will change with time. Reference 30l is a study of the change of rod worth with temperature and fuel exposure in a graphite moderated reactor.

Experimental Measurements

Experimental measurements of the quantities important for control-rod installations are necessary for evaluating the adequacy of approximations used in calculations. Further, in the final design of a power reactor, such measurements are usually necessary in order to verify the adequacy of control and the power distributions for the specific design. Theoretical extensions of the measurements are, however, usually required because it is impractical to duplicate all operating conditions in the critical assembly. Reports of measurements on critical reactor mock-ups and on operating reactors are contained in references 30j, 30k, 30m, and 30n. Experiments related to the relative effectiveness of different control-rod materials and to the effects of individual control-rod geometry are contained in references 30e, 30g, and 30o. Measurements related to the evaluation of methods for calculating control-rod worths and flux distributions are contained in references 30p, 30q, 30r, and 45.

One of the difficulties in utilizing experimental results for the evaluation and extension of theoretical work is the difficulty of measuring the reactivity worth of control rods or groups of control rods when the worth is very large. The ideal scheme for such a measurement would be to remove the rods suddenly and observe the resulting period of exponential neutron flux increase. This method is, of course, impractical for large reactivity changes. The alternate direct measurement is by the rod-drop method. This method has a number of shortcomings which are related primarily to the changes in flux distribution caused by the insertion of the rods. Measurements of reactivity worth by the rod-drop method, and of the difficulties involved, are discussed in references 30p and 30s.

Other Control Methods

Full control is possible in small reactors by varying the reflector properties and thereby varying the neutron leakage out of the reactor. The method of control is particularly suited for reactors of the fast and intermediate energy variety and is also applicable to small light water reactors. Control is attained by substituting a good reflector, such as beryllium or uranium, for a poor reflector such as a boron compound or air. Complete control by the reflector method is limited to reactors whose size, measured in migration lengths, is small. It can also be used as shim control on larger reactors. A simple type of reflector control for H_2O or D_2O moderated reactors is that in which the thickness of the top reflector is varied. For tube type or calandria type reactors, the method can be extended to variation of the moderator height in the core. This system has been used in the NRX reactor and is planned for other Canadian reactors. The method has

also been proposed for control of a boiling water reactor.[46]

If the moderating or absorbing properties of the moderator can be varied, control of reactivity can be achieved by this method. The possibilities which have been suggested for varying the moderator properties include the use of a separate water moderator system in a water-cooled water-moderated reactor[47] and the use of D_2O-H_2O mixtures in which the H_2O content can be increased as reactor operation proceeds to compensate for reactivity loss.[48] One of the advantages of a system which controls by varying the moderating properties is that excess neutrons can be absorbed in the U^{238} resonances, rather than in parasitic absorbers, and thus can contribute to the production of fissionable isotope.

Chemical poisoning of the moderator may be used as a means of varying the moderator properties; the control is then by parasitic neutron absorption. Boron compounds such as H_3BO_3, $Na_2B_8O_{13}4H_2O$, and $(NH_4)_2B_{10}O_{16}5H_2O$ may be dissolved in the coolant; control is achieved by changing the concentration of the poison. In the continuous use of soluble poisons in power reactors, there are a number of problems related to solubility, stability of the chemical compound, and corrosiveness. Experience with soluble poisons in the BORAX reactors is summarized in reference 30t. The most extensive use of soluble poison in other reactors is for emergency shutdown.

The use of a burnable poison is a means of reducing the initial excess reactivity required for a given fuel lifetime in a reactor of low conversion ratio. The burnable poison is an absorbing material having a microscopic cross section of such magnitude that the material is destroyed by neutron absorption at approximately the proper rate to compensate for fuel burn-up. The poison can be incorporated into the fuel elements or may be contained in separate elements; it must, however, be dispersed rather thoroughly through the reactor core since the self-shielding of the material must be either zero or must have some specifically chosen value which leads to the proper rate of destruction. The considerations in choosing burnable poison arrangements which give good approximations to the desired rates of reactivity compensation are discussed in reference 30u.

Briefly Noted Reports

Reference 49 is a useful compilation of fission-product data. Levels of fission products resulting from thermal fission of U^{235} in reactor fuels are computed over a wide range of reactor operation conditions and decay times. Values for approximately 300 fission products are presented in graphical form together with gross totals of their activities, radiation powers, and thermal-neutron poisoning. The gamma spectrum is further broken into four groups of specified energy ranges, which are suitable for use in shielding design. Tabulations of these properties are arranged as to chain or mass number, element, and as to the rare-gas and rare-earth groups. The calculations assume constant replenishment of U^{235}, constant reactor power operation, and no fission-product separations during irradiation. Properties of individual fission products are summed for each decay chain (mass number), each element (atomic number), the rare gases, and the rare earths over a thermal flux range from 10^{12} to 10^{15} neutrons/cm^2/sec, an irradiation time range from 10^5 to 10^8 sec, and a decay time range from 10^3 to 10^9 sec.

Reference 50 covers computed photon energy radiation rates and photon emission rates from the fission products produced by thermal-neutron fission of U^{235}. Curves are given showing photon energy radiation rates, photon emission rates, and beta rates for a time range of about 46 min to about 300 years after fission, with the relative contributions of the fission-product elements to the total.

Reference 51 is a detailed tabulation of the neutron cross sections of U^{235}—capture, fission, scattering, transport, and total—over the neutron energy range from 0.0252 to 33.7 ev, as calculated from the resonance parameters by the single level Breit-Wigner formula.

Reference 52 contains a collection of neutron cross sections averaged over the calculated Wigner-Wilkins spectrum for a hydrogen moderator containing various ratios of absorber to hydrogen. The absorbers considered are U^{235}, Pu^{239}, a 1/v absorber, and mixtures of the three. The important cross sections are given for U^{235}, U^{233}, Pu^{239}, Pu^{240}, Pu^{241}, Am^{241}, Np^{237}, Xe^{135}, Sm^{149}, indium, hafnium, gadolinium, europium, cadmium, Au^{197}, hydrogen, and a 1/v absorber. The tabulation should prove very useful in calculations of H_2O moderated reactors.

Reference 53 is a tabulation of useful cross sections averaged over the Maxwell-Boltzmann neutron energy spectrum. The range of mean spectrum energy covered is from 0.0253 to 0.24 ev. The averages are based on the cross-section curves of report BNL-325.

Reference 54 is a record of the reports to the AEC Nuclear Cross Sections Advisory Group, which met July 17–18, 1957. Recent results of cross-section measurements are reported.

Reference 55 reports results of exponential experiments on a diphenyl moderated lattice of 1-in.-diameter uranium rods. The transport mean free path of diphenyl is given and bucklings for natural and 0.9124 per cent enriched uranium.

Reference 56 reports a study of the (n,2n) reaction in beryllium, using neutrons from a mock-fission source and from a plutonium-beryllium source. Neither of these sources simulates the true fission spectrum well in the higher energy regions, and the measurements are therefore subject to uncertainties. It is stated, however, that, if fission neutrons are permitted to collide with beryllium before they are degraded below threshold of the reaction by collisions with other materials, the (n,2n) reaction can make a significant contribution to the neutron economy of a reactor.

References

1. *Power Reactor Technology*, Vol. I, No. 2, February 1958. (Available from Superintendent of Documents, U. S. Government Printing Office, Washington 25, D. C.)
2. Power Reactor Studies, Quarterly Progress Report for February, March, and April, 1957, DP-232, July 1957. (Unclassified AEC report.)
3. W. E. Graves, Buckling Measurements with Lattices of Clumped UO_2 Rods in Heavy Water, ANS Second Winter Meeting, October 1957, Paper 7-8.
4. E. Critoph, Comparison of Theory and Experiments for (a) Lattice Properties of D_2O-U Reactors; (b) Central Rod Experiments; (c) Foreign Rod Experiments, CRRP-655, July 26, 1956. (Unclassified Canadian report.)
5. D. F. Babcock, Coordinator Power Reactor Studies, Power Reactor Studies Quarterly Progress Report for May, June, and July, 1957, DP-245, September 1957. (Unclassified AEC report.)
6. T. F. Parkinson, Exponential Measurements on Uranium Plate Lattices, DP-268, January 1958. (Classified AEC report.)
7. R. E. Heineman, F. C. Engesser, et al., Measurements of k_∞ for D_2O Moderated Clusters of UO_2 and Pu-Al Rods, ANS Second Winter Meeting, October 1957, Paper 7-7.
8. E. R. Cohen, Exponential Experiments on D_2O-Uranium Lattices, Paper P/605, Volume 5, pp. 268-278, Proceedings of the International Conference in Geneva, August 1955. (Available from the International Documents Service, Columbia University Press, 2960 Broadway, New York 27, N. Y.)
9. W. J. Sturm, W. C. Redman, and M. Copic, Exponential Studies of a Ceramic Mixture of Thoria and Urania in Heavy Water Moderator, ANS Second Winter Meeting, October 1957, Paper 11-2.
10. W. C. Redman, S. G. Kaufmann, and J. W. Armstrong, Heterogeneous Critical Experiments with ThO_2, UO_2, and D_2O, ANS Second Winter Meeting, October 1957, Paper 2-8.
11. W. C. Redman, J. A. Thie, and L. R. Dates, Hazards Summary Report on the Oxide Critical Experiments, ANL-5715, April 1957. (Unclassified AEC report.)
12. R. C. Lloyd, Enriched Uranium-Graphite Lattices, Nuclear Physics Research Quarterly Report for January, February, and March, 1957, HW-50598, May 31, 1957. (Unclassified AEC report.)
13. M. T. Lee, Re-evaluation of Graphite Diffusion Lengths, HW-51175, June 5, 1957. (Unclassified AEC report.)
14. R. C. Lloyd and C. R. Richey, Temperature Coefficient of a Graphite-Uranium Lattice, HW-51008, June 18, 1957. (Confidential AEC report.)
15. R. C. Lloyd and C. R. Richey, Variation of Graphite Diffusion Length with Temperature, Nuclear Physics Research Quarterly Report for January, February, and March, 1957, HW-50598, May 31, 1957. (Unclassified AEC report.)
16. G. E. Hansen, J. C. Hoogterp, et al., Beryllium-reflected Graphite-moderated Critical Assemblies, LA-2141, October 1957. (Unclassified AEC report.)
17. W. Baer, M. J. Galper, and N. Carbone, Measurements of the Conversion Ratio of the PWR Critical Facility Blanket, *Nuclear Science and Engineering*, 3(2): 113-128 (February 1958).
18. Description of the Shippingport Atomic Power Station, WAPD-PWR-970, June 1957. (Unclassified AEC report.)
19. L. J. Koch et al., Experimental Breeder Reactor II (EBR-II); Hazard Summary Report, ANL-5719, May 1957. (Unclassified AEC report.)
20. *Power Reactor Technology*, Vol. I, No. 1, December 1957. (Available from Superintendent of Documents, U. S. Government Printing Office, Washington 25, D. C.)
21. H. Yamanchi and J. De Felice, Nuclear Development Associates, June 17, 1955. (Unpublished.)
22. G. Goertzel and C. Klahr, Interpretation of an Experiment To Measure Doppler Effect, NDA-14-127, June 29, 1956. (Unclassified AEC report.)

23. A. M. Lane, J. E. Lynn, and J. S. Story, An Estimation of the Doppler Effect in Fast Neutron Reactors, AERE T/M-137, July 1956. (Unclassified British report.)
24. Monte V. Davis, The Doppler Coefficient of U^{235} Fuel Elements, *Nuclear Science and Engineering*, 3(1): 107 (January 1958).
25. B. J. Toppel, The Coupled Aspects of a Fast-Thermal Critical ZPR-V, ANL-5775, October 1957. (Unclassified AEC report.)
26. P. Kafalas, M. Levenson, and C. M. Stevens, Determination of the Ratio of Capture to Fission Cross Sections in EBR-I, *Nuclear Science and Engineering*, 2(5): 657 (September 1957).
27. C. Eggler, C. M. Huddleston, et al., Measurement of Neutron Spectra of the Experimental Breeder Reactor, *Nuclear Science and Engineering*, 1(5): 391 (October 1956).
28. D. Klein, W. Baer, and G. G. Smith, Spatial Distribution of U^{238} Resonance Neutron Capture in Uranium Metal Rods, WAPD-T-640, August 1957. (Unclassified AEC report.)
29. E. P. Wigner, E. Creutz, et al., *Journal of Applied Physics*, 26: 260 (1955).
30. Reactor Control Meeting Held in Los Angeles, March 6–8, 1957, TID-7532(Pt. 1), October 1957. (Unclassified AEC report.)
    a. H. Stevens, Half Group Theoreis for Control Rods, p. 16. Knolls Atomic Power Laboratory, Schenectady, N. Y.
    b. A. F. Henry, Review of Methods Used in Control Rod Analysis for Reactor Design at Bettis, p. 3. Bettis Plant, Pittsburgh, Pa.
    c. T. Auerback, Formulas for Control Rod Worth in Thermal Reactors, p. 11. Brookhaven National Laboratory, Upton, N. Y.
    d. R. E. Lightle, Multiple Control Rod Calculations, p. 49. The Babcock & Wilcox Co., Atomic Energy Division, Lynchburg, Va.
    e. D. R. Bach and S. W. Kitchen, Effects of Rod Shape on Control Rod Worth, p. 138. General Electric Company, Knolls Atomic Power Laboratory, Schenectady, N. Y.
    f. J. H. Smith, The Effect of Epithermal Absorptions on Control Rod Absorption Area, p. 33. Knolls Atomic Power Laboratory, Schenectady, N. Y.
    g. H. P. Iskenderian, Theory and Experiments on Rods Containing Rare Earth Metals, p. 156. Argonne National Laboratory, Lemont, Ill.
    h. J. C. Stewart and N. C. Frances, Variational Calculations of Control Rod and Water Gap Interactions, p. 28. Knolls Atomic Power Laboratory, Schenectady, N. Y.
    i. E. L. Wachspress, Thin Regions in Diffusion Theory Calculations, p. 35. General Electric Company, Knolls Atomic Power Laboratory, Schenectady, N. Y.
    j. F. B. Fairbanks and I. G. Gallagher, APPR-1 Control Rod Experiments and Calculations, p. 87. Oak Ridge National Laboratory, Oak Ridge, Tenn.
    k. A. M. Perry, APPR Control Rods — Theory and Experiment, p. 111. Oak Ridge National Laboratory, Oak Ridge, Tenn.
    l. G. W. Stuart, Dependence of Control Rod Worth on Reactor Temperature and Fuel Exposure, p. 42. Hanford Laboratories Operation, General Electric Company, Richland, Wash.
    m. B. M. Carmichael and M. E. Battat, Control Rod Worths Vs. Temperature in LAPRE-I, p. 125. University of California, Los Alamos Scientific Laboratory, Los Alamos, N. Mex.
    n. D. R. deBoisblanc, Some Control Rod Studies at the MTR, p. 231. Phillips Petroleum Co., Atomic Energy Division, Idaho Falls, Idaho.
    o. R. S. Wick, An Empirical Determination of the Fast Absorption Constants of Control Rods, p. 162. Bettis Plant, Pittsburgh, Pa.
    p. W. H. Hartley and R. T. Bayard, Control Rod Worth Studies on Seed and Blanket Reactors, p. 74. Bettis Plant, Pittsburgh, Pa.
    q. G. A. Price, Lattice Experiments with Thin Black Control Rods, p. 150. Brookhaven National Laboratory, Upton, N. Y.
    r. A. D. Voorhis and T. M. Ryan, Investigation of Absorbing Membranes in Slab Reactors, p. 202. Bettis Plant, Pittsburgh, Pa.
    s. J. H. Brown, Limitations of Scram Transient Calibrations, p. 80. Hanford Atomic Products Operation, Richland, Wash.
    t. J. A. Thie, Chemical Control Experience in Boiling Reactors, p. 216. Argonne National Laboratory, Lemont, Ill.
    u. A. Radkowsky, The General Application of Burnable Poison, p. 179. Naval Reactors Branch, Division of Reactor Development, Washington, D. C.
31. Reactor Physics and Mathematics, in Bettis Technical Review, Vol. 1, No. 4, WAPD-BT-4, October 1957. (Unclassified AEC report.)
32. H. Hurwitz and G. M. Roe, Absorption of Neutrons by Black Control Rods, *Journal of Nuclear Energy*, 2: 85 (1957).
33. R. W. Deutsch, Evaluation of a Bank of Slab Type Control Rods, ANS Second Winter Meeting, October 1957, Paper 3-8.
34. B. Wolfe, Epithermal Effects on Control Element Worth, ANS Second Winter Meeting, October 1957, Paper 10-8.
35. P. Greebler, Control Rod Cell Calculations for Determination of Reactivity and Power Distribution, ANS Second Winter Meeting, October 1957, Paper 10-9.
36. J. Codd and C. A. Rennie, Two Group Theory of Control Rods in a Thermal Reactor, AERE-R/R-818. (Unclassified British report.)
37. R. Scalettar and L. W. Nordheim, Theory of Pile

Control Rods, MDDC-42. (Declassified AEC report.)

38. P. Greebler, TRIXY—A Computer Program for Multigroup Nuclear Reactor Calculations in Three-space Dimensions, KAPL-1549, Aug. 1, 1956. (Unclassified AEC report.)
39. R. W. Dayton, The Effectiveness of Control Rod Materials, BMI-1196, 1957. (Unclassified AEC report.)
40. R. S. Halgas and M. Bender, Half-height Cadmium Slab, WAPD-BT-4, October 1957, p. 15. (Unclassified AEC report.)
41. R. R. Schiff, Synthesis of Three-dimensional Power Distributions for a Nonuniformly Depleted Core, WAPD-BT-4, October 1957, p. 23. (Unclassified AEC report.)
42. J. E. Meyer, Synthesis of Three-dimensional Power Shapes, Flux-weighting Technique, WAPD-BT-4, October 1957, p. 29. (Unclassified AEC report.)
43. H. Hurwitz, Jr., and R. Ehrlich, "Highly Enriched Intermediate and Thermal Assemblies," Progress in Nuclear Energy, Series I, Physics and Mathematics, p. 352, McGraw-Hill Book Company, Inc., New York, 1956.
44. L. O. Herwig and E. R. Sanford, An Inverted Reactivity Effect, WAPD-BT-4, October 1957, p. 72. (Unclassified AEC report.)
45. E. R. Sanford, G. F. Bogar, and H. Z. Glick, Experimental Fission Power Distribution near a Cruciform Water Gap, ANS Second Winter Meeting, October 1957, Paper 14-2.
46. W. C. Ballowe, F. J. Jankowski, and J. W. Chastain, Experimental Study of Reflector Control of a Boiling Water Reactor, ANS Second Winter Meeting, October 1957, Paper 11-7.
47. W. J. Levedahl, A Moderator Controlled Pressurized Water Reactor, ANS Second Winter Meeting, October 1957, Paper 16-7.
48. M. C. Edlund, Theory of Shim Control by Spectral Shift, ANS Third Annual Meeting, June 1957, Paper 7-1.
49. J. O. Blomeke and Mary F. Todd, U^{235} Fission-product Production as a Function of Thermal Neutron Flux, Irradiation Time, and Decay Time. I. Atomic Concentrations and Gross Totals, Part I, Volume I, Aug. 19, 1957. II. Summations of Individual Chains, Elements, and the Rare-Gas and Rare-Earth Groups, ORNL-2127, Dec. 1, 1957. (Unclassified AEC report.)
50. C. F. Miller, Gamma Decay of Fission Products from the Slow-Neutron Fission of U^{235}, USNRDL-TR-187, July 11, 1957. (Unclassified U. S. Navy report.)
51. Devereux L. Kavanagh, U^{235} Cross Sections from a Breit-Wigner Analysis, Volumes I and II, CWR-478, June 10, 1957. (Unclassified AEC report.)
52. Harvey J. Amster, A Compendium of Thermal Neutron Cross Sections Averaged Over the Spectra of Wigner and Wilkins, WAPD-185, January 1958. (Unclassified AEC report.)
53. W. J. Roberts, Maxwell-Boltzmann Averaged Neutron Cross Sections, CWR-400-1, Sept. 30, 1957. (Unclassified AEC report.)
54. C. W. Zabel, Reports to the AEC Nuclear Cross Sections Advisory Group, Idaho Falls, Idaho, July 17–18, 1957, WASH-194, Feb. 14, 1958. (Unclassified AEC report.)
55. M. Carl Walske, editor, Reactor Physics Quarterly Progress Report for April–June 1957, NAA-SR-2058, Jan. 15, 1958. (Unclassified AEC report.)
56. Dwight S. Young (n,2n) Study of Be^{9}, LA-2158, October 1957. (Unclassified AEC report.)
57. G. R. Keepin, T. F. Wimett, and R. K. Zeigler, Delayed Neutrons from Fissionable Isotopes, LA-2118, 1957. (Unclassified AEC report.)

Burn-out Measurements

The uncertainties in the limitation imposed by fuel-element burn-out on maximum heat flux is one of the reasons for the present conservatism in heat removal design for water-cooled reactors. Experimental data[1] are presented on the heat-flux limitation, due to the "boiling-burn-out" phenomenon, for the forced circulation of high-purity water in a 0.192-in. horizontal annulus of 1.43 in. I.D. and 21 ft heated length. The geometry and size of the heat-generating element and flow passage are of a scale comparable to practical heat-transfer configurations for large power reactors, for example, reactors fueled with natural or slightly enriched uranium, moderated by heavy water or graphite, and cooled by light or heavy water. The data are sparse but, nevertheless, thinly cover a broad and interesting range of heat-transfer and flow conditions. Pressures range from 590 to 2010 psia and heat fluxes up to 378,000 Btu/hr/sq ft. Bulk boiling of the water occurs within the annular flow passage and gives outlet steam qualities ranging from 22.7 to 44.4 wt. %. Hence the net steam generation in the flow passage is quite large.

In the experiments the transition from nucleate boiling to film boiling, which leads to the boiling-burn-out condition and which is indicated by an accelerating increase in heater rod temperature for fixed flow and heating conditions, was quite gradual. For heater elements of much smaller heat capacity than those used in the experiments, the transition is much more abrupt, as shown by boiling-burn-out experiments utilizing small thin-walled tubes as the heating elements.[2] On this basis and on the basis of other qualitative arguments, it is concluded[1] that the burn-out heat-flux limit will probably be dependent on heater size, shape, and heat capacity and on coolant passage arrangement. Further, it is probable that the burn-out heat flux for flow through multiple flow passages is different from that obtained at a given mass flow through a single passage, particularly for the case of nonuniform heating of the different flow passages. These considerations must be experimentally investigated before reliable general conclusions on burn-out heat fluxes can be made.

Unfortunately, no pressure-drop data are given for the various flow and heat-generation conditions investigated. These data are required for determining the flow distribution in nonuniformly heated multiple flow passages such as those which exist in power reactors. However, the data represent a useful addition to the existing body of data on burn-out.

Reference 3 presents results of an experimental investigation of burn-out heat flux at conditions of interest in connection with the design of pressurized water reactors. Burn-out was investigated for a wide range of variables, i.e., for various flow-channel sizes, geometries, materials, and positions (vertical or inclined 45 deg) and for both uniform and nonuniform axial heat-flux distributions. The water pressures were 830, 1215, and 2000 psia. Data plots of burn-out heat flux vs. mass velocity are presented to show the effects of the variables tested. As is generally characteristic of burn-out heat-flux data, appreciable scatter of the data is obtained.

As a result of the investigation, an expression is suggested as a design equation for predicting burn-out heat flux at 2000 psia, provided no extrapolation is made to conditions not covered in the tests. Comparisons are made, for the various test conditions, of the experimentally measured values of burn-out heat flux with the values indicated by the design equation. The design equation generally appears to give a safe upper limit to the heat flux for avoiding burn-out, although, for many of the test conditions, the burn-out limit given by the design equation is extremely conservative.

Burn-out tests were also conducted to determine the effect of installing flow channels in parallel with the channel in which the burn-out heat-flux condition is approached. The tests indicate that parallel-channel burn-out is appar-

ently similar to that noted with single channels, although the test data plotted give slightly smaller burn-out heat fluxes for the paralleled channel.

Heat Transfer Under Supercritical Conditions

Pressurized-water type reactors with the coolant water at supercritical pressures (> 3206 psia) have been proposed for ship propulsion[4] and may be of interest for central-station power reactors. A general discussion of the problems involved in the development of a supercritical-water reactor power plant is presented in reference 4. Data are presented in reference 5 on the forced-convection heat-transfer characteristics of supercritical water flowing through heated tubes. Friction pressure-drop data are also presented. These data represent the results of a comprehensive experimental effort on this subject. Pressures range from 4000 to 8000 psia, fluid bulk temperatures from 400 to 1000°F, tube-wall temperatures from 400 to 1400°F, and heat fluxes from 0.1×10^6 to 3×10^6 Btu/hr/sq ft.

Correlation of the heat-transfer data is not possible due to several factors:

1. The fluid properties, such as specific heat, viscosity, and thermal conductivity, which control the heat-transfer rates, are not well known as functions of temperature and pressure in the range of interest. Reference 5 gives the various sources of fluid-property values and compares, for supercritical water at 5000 psia and a range of temperatures, a heat-transfer property based on the data from the various sources.

2. The fluid properties vary considerably with temperature in the usual range of interest. Hence, for large temperature differences between the wall and the bulk fluid, the properties vary considerably across the fluid boundary layer. This property variation across the boundary layer must be accounted for in any correlation of the heat-transfer data. Analyses taking this into account have been made,[6,7] and a comparison of experimental and calculated[7] results are presented in reference 5. The agreement is good at the lower temperatures and gets progressively worse as temperatures are increased, presumably because of incorrect property values in reference 7 at the higher temperatures. The agreement is such as to give confidence in the type of analysis made in references 6 and 7.

3. For large temperature differences which straddle a temperature region, called the pseudocritical temperature region in reference 8, a boiling-like phenomenon appears to occur even though the pressure is above the critical value. As shown by the data presented in reference 8 (data of the reference 5 work), the occurrence of this boiling-like phenomenon is evidenced by an abrupt radical change in tube-wall temperature profile along the length of the heated tube for a quite small change in heat flux to the water. Undoubtedly, a change in heat-transfer mechanism occurs. This phenomenon is accompanied by a loud whistling noise similar to noises heard during subcritical boiling, usually when the heat fluxes approach burn-out values. A qualitative description with several possible explanations for the boiling-like phenomenon are given in reference 8.

Despite the difficulties of correlation, the heat-transfer and friction data of reference 5 are presented in convenient fashion for ready use in calculations.

Briefly Noted Reports

Reference 9 contains a collection of papers presented at the Reactor Heat Transfer Conference of 1956 in New York. The collection contains a number of reports both experimental and theoretical which represent general contributions to the theory and technology of heat transfer. A number of papers on transient heat transfer, both in the reactor core and in the entire primary loop, will be useful in connection with reactor safety and transient analysis. Other papers which may be of direct application for specific reactors are those on burn-out heat flux, heat transfer in circulating fuel reactors, heat transfer with polyphenyl coolants, and in-pile molten metal–water reaction experiments.

References

1. D. J. Foley, J. M. Batch, and L. H. McEwen, Boiling Burnout at High Pressure in Horizontal Annuli, Reactor Heat Transfer Conference of 1956, TID-7529(Pt. 2), November 1957. (Confidential AEC report.)

2. W. H. Lowdermilk and W. F. Weiland, Some Measurements of Boiling Burnout, NACA-RM-E54K10, February 1955. National Advisory Committe for Aeronautics, Washington 25, D. C.
3. R. A. DeBortoli, S. J. Green, H. S. Jacket, J. D. Roarty, A. Weiss, and J. E. Zerbe, Investigation of Burnout Heat Flux, Reactor Heat Transfer Conference of 1956, TID-7529(Pt. 1), Book 1, pp. 205-226, November 1957. (Unclassified AEC report.)
4. T. Fahrner, G. H. Farbman, et al., Supercritical Water Reactor Power Plants, Paper Presented at Symposium (Nuclear Powered Ships for American Ship Operators) Held in Washington, D. C., July 30, 1957, TID-7539, September 1957. (Unclassified AEC report.)
5. D. G. Randal, Some Heat Transfer and Fluid Friction Experiments with Supercritical Water, Reactor Heat Transfer Conference of 1956, TID-7529 (Pt. 3), November 1957. (Secret AEC report.)
6. R. G. Deissler and M. F. Taylor, Analysis of Heat Transfer and Fluid Friction for Fully Developed Turbulent Flow of Supercritical Water with Variable Fluid Properties in a Smooth Tube, NACA-RM-E53B17, April 1953. National Advisory Committee for Aeronautics, Washington 25, D. C.
7. K. Goldmann, Heat Transfer to Water at 5000 Psia Flowing Turbulently in Round Tubes, NDA-10-8, Sept. 23, 1952. Nuclear Development Associates.
8. K. Goldmann, Special Heat Transfer Phenomena for Supercritical Fluids, Reactor Heat Transfer Conference of 1956, TID-7529(Pt. 3), November 1957. (Secret AEC report.)
9. John E. Viscardi, compiler, Reactor Heat Transfer Conference of 1956, Books 1 and 2 (collected papers and reports of a conference held at New York, Nov. 1 and 2, 1956), TID-7529(Pt. 1), Novenber 1957. (Unclassified AEC report.)

Transient Boiling Experiments

The self-limitation of power in water-cooled water-moderated reactors under conditions of sudden large reactivity additions has been demonstrated by the BORAX and SPERT experiments. One of the mechanisms of power limitation is the rapid formation of steam at the fuel-element surfaces, the displacement of water from the reactor core, and the consequent decrease in neutron moderation and reduction of reactivity. Laboratory experiments on the characteristics of transient boiling have been made in the past, and, in fact, it was experiments of this kind which indicated that the self-protection characteristic would be a rapid and effective one and which therefore led to the BORAX experiments. A more recent study of transient boiling has been reported in reference 1. This study was made under conditions which approximate those in the BORAX and SPERT reactors more closely than did previous experiments, and it is therefore of considerable interest for the insights it may give into the transient boiling process in such reactors.

Heat was generated electrically at exponentially increasing rates in platinum and aluminum ribbons immersed in subcooled water. The surface temperature of the ribbons was measured, and the growth of steam bubbles was photographed with a high-speed camera. The effects of water temperature, exponential period (5 to 75 msec), and gas concentration in the water were studied at atmospheric pressure. The following conclusions were drawn from the experimental results.

1. When a metal surface in contact with water which is below the boiling point is heated rapidly, there is a measurable rise in surface temperature above the boiling point before boiling commences. Associated with this "temperature overshoot" is a "delay time."

2. There is no measurable temperature overshoot or delay time when the bulk water temperature is near the boiling point.

3. During that part of an excursion preceding the beginning of boiling, the rate at which the surface temperature rises is too rapid for natural convection to contribute to heat transfer. The stagnant water acts as a semi-infinite solid with regard to heat transfer, and the temperature rise can be computed by transient conduction theory.

4. For exponential increases in the heat generation rate, the temperature overshoot and delay time increase as the bulk water temperature is decreased.

5. The temperature overshoot increases as the exponential period is decreased. Under some conditions the delay time goes through a maximum with variation in period, being small for long periods that have little temperature overshoot and also being small for short periods where the rate of temperature rise is rapid.

6. Once quasi-steady boiling has begun during an excursion, for periods greater than 15 msec with large subcooling, behavior of the system at any instant is not appreciably different than it would be for steady boiling. The critical heat flux (flux at the point of incipient film boiling) for these conditions is not greatly influenced by the transient state of the power.

Qualitatively the results of the experiments appear to be consistent with the observed behavior of the BORAX and SPERT reactors. An attempt to apply the results quantitatively to the reactor behavior would be of interest.

Transient boiling experiments under somewhat different conditions have been reported.[2] Bubble growth was studied photographically at the surface of an 8-mil Nichrome wire which was heated very rapidly by electrical impulses of 1-μsec duration. Delay times in the formation of bubbles were observed, and bubble growth was followed for periods of some 100 μsec after the heating pulse. During the 100-μsec period, an individual bubble was found to attain a diameter of from 0.01 to about 0.05 cm, depending on the degree of subcooling (difference between water temperature and saturation temperature) of the water surrounding the wire. The measurable time delays in bubble formation varied from 0 for saturated water to about 33 μsec for a water temperature of 76°C; at the latter temperature the delay was increasing rapidly with subcooling.

Although these experiments are rather idealized ones, they give the advantage of relatively simple situations which may be subjected to

theoretical analysis. The authors present theoretical curves which fit reasonably well the experimental curves of bubble growth and the measurements of delay times. If the basic processes involved are established in such simplified situations, the application of analysis to the much more complex case of the reactor can be approached with some confidence.

Dynamics of Boiling Water Reactors

It is well known that boiling water reactors, when operated at sufficiently high power densities, are subject to power instabilities. The early BORAX experiments demonstrated that the power densities attainable in the stable operating region are, even with natural-circulation reactors, high enough to make this reactor type interesting as a power reactor. Later results from subsequent BORAX reactors, from Experimental Boiling Water Reactors (EBWR),[3] and from laboratory experiments have indicated that the attainable power densities are higher than the earlier estimates and that in some cases heat conduction and transfer considerations rather than stability may be the limiting factor on attainable power density.[4] Nevertheless, the subject of stability remains an important one and must be more thoroughly understood before the principles of designing boiling reactors for maximum performance can be considered as completely established.

Two recent reports[5,6] describe quantitative experiments on the dynamics of boiling reactors in general and particularly on the characteristics of the boiling reactor instability.

Reference 5 is a measurement of the transfer function of the EBWR under a number of different operating conditions. The transfer function is simply the frequency response of the reactor power, when the reactor is excited by a sinusoidal variation in reactivity. The power response, in both amplitude and phase angle, is measured over a range of oscillation frequencies. The measurements are usually made at amplitudes small enough that the reactor kinetics equations can be linearized. Within the limits of this approximation, the transfer function can be used in a way similar to the use of a frequency analysis of any dynamic system. In the reactor case the gain of the system is ordinarily defined as the ratio of the amplitude of the power oscillation, expressed as a fraction of the average power, to the amplitude of the reactivity oscillation, i.e., gain = $(\Delta P/P)/(\Delta k/k)$. Often, as in reference 5, the gain is expressed in decibels, with zero decibels corresponding to the gain under "zero power" operation, at a frequency which is high enough that the gain is unaffected by the delayed neutrons and low enough that it is independent of the prompt neutron lifetime. Reactors which have relatively short neutron lifetimes (10^{-4} sec or shorter) exhibit such a plateau in their low power amplitude response curve in the frequency region just above 2 radians/sec (see Fig. 5). The absolute value of the gain in this region is just $1/\beta$, where β is the delayed neutron fraction. The measurements on EBWR, at an operating

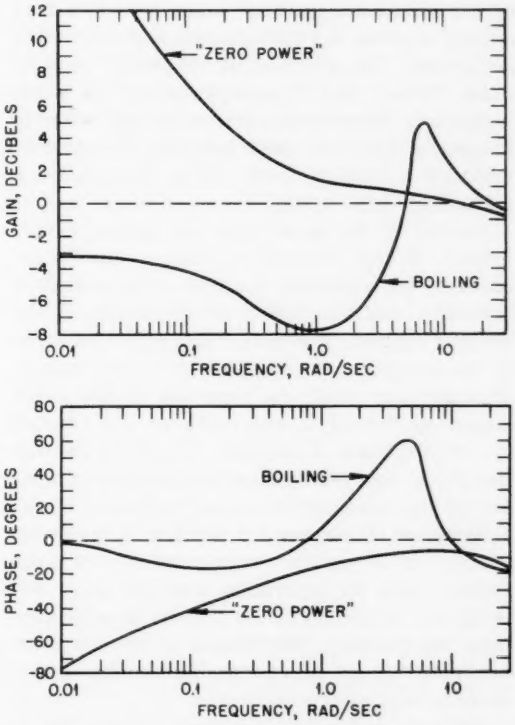

Figure 5—Transfer function of EBWR at zero power and during boiling operation. Boiling curve is from reference 5 and was measured at an operating power of 19.9 Mw (thermal) and at an operating pressure of 550 psi. Zero power curves are calculated curves for a reactor having characteristics which approximate those of EBWR and were supplied by the editor.

power of 19.9 Mw thermal, on this scale exhibit a rather low gain of about −3 decibels at very low oscillating frequencies (0.01 radian/sec). At this frequency the power oscillation of the boiling reactor is essentially in phase with the reactivity oscillation, and the gain at this low frequency is a measure of the power coefficient of reactivity of the reactor. If the gain of the reactor is converted to an absolute magnitude, it appears to represent a power coefficient of reactivity of ~0.084 per cent k_{eff} per Mw (Fig. 5). As the frequency of oscillation is increased, the gain of the reactor decreases, reaching a minimum of about −8 decibels at a frequency of about 1 radian/sec. Further increase of the oscillating frequency causes the gain to rise, and it reaches a peak of ~5 decibels at a frequency of about 8.5 radians/sec and thereafter decreases. The phase shift reaches a peak of about 60-deg lead at approximately the same frequency. These peaks define the approximate frequency region in which instability would presumably occur if the power were increased to a sufficiently high value.

Curves of the same type are given in reference 5 for various operating conditions, covering the variables of power level, operating pressure, and absorption cross section of the reactor coolant. The latter variation was made by the addition of soluble boron to the coolant. This addition would be expected to lower the steam coefficient of reactivity of the reactor for two reasons: (1) because the added absorption of the coolant represents a positive component in the net negative steam coefficient of reactivity and (2) because the addition of the boron results in a greater withdrawal of the shim control rods for operation and therefore results in a reduction of the fast-neutron leakage from the reactor. The effects of the use of an automatic steam bypass on the reactor steam system were also investigated.

Although reference 5 makes no attempt to account for the shape of the frequency response curves, measurements of this type may be expected to lead to a better understanding of boiling reactor dynamics. They also represent a method for predicting the degree of stability of the reactor at higher powers from results of operation at lower powers and therefore form the basis for the safest method of extending the operating power range of the reactor. Finally, the reference points out that, if the curve is continued to relatively high frequencies, of the order 25 to 50 radians/sec, a region is reached in which the oscillations are too rapid for the boiling phenomenon to exert an appreciable self-regulating effect, and the dynamic response of the reactor should be essentially the same as its response at zero power. The high frequency oscillation of the reactivity generator therefore affords an opportunity for the calibration of the reactivity worth of the generator under actual power operation of the reactor. This has not previously been possible in the boiling reactor and indeed is, in general, not possible by other means in any reactor which has a significant power coefficient of reactivity. Once the reactivity generator is calibrated under power operating conditions, it can be used to obtain the absolute power coefficient of reactivity at lower frequencies. The addition of this information is a further aid in the understanding of boiling reactor characteristics.

Reference 6 is a general discussion of boiling reactor instability, based primarily on the BORAX results. Some experimentally determined transfer functions for the BORAX-IV reactor, which is a boiling reactor fueled with uranium-thorium oxide fuel slugs jacketed with aluminum, are given. In this reference an analysis is performed in which the zero power transfer function (which may be either measured or calculated from neutron lifetime and delayed-neutron data) is in effect "divided out" of the measured transfer function to yield the transfer function of the power coefficient of reactivity, i.e., the reactivity feedback which results from the formation of steam in the reactor. This was done for three different operating power levels. It has not yet been possible to explain the resultant feedback responses in terms of the physical characteristics of the reactor. It is stated, however, that this approach, utilizing the more accurate EBWR frequency response data, has allowed the isolation of two characteristic time constants for the power coefficient. It is also stated that there are indications that the use of two time constants may not be sufficient to explain all the observations, particularly in the resonance region.

Briefly Noted Reports

Reference 7 is a detailed report of the examination of the EBR-I core after its accidental meltdown. This information, in a less detailed form, has been previously reviewed.[8]

References

1. M. W. Rosenthal, An Experimental Study of Transient Boiling, *Nuclear Science and Engineering*, 2(5): 640-656 (September 1957).
2. C. E. Fanouff, E. A. McLean, and V. E. Schenner, Some Aspects of Surface Boiling, *Journal of Applied Physics*, 29(1): 80 (January 1958).
3. The Month in the Labs-Argonne, *Nucleonics*, 16(1): 23 (January 1958).
4. W. S. Flinn and M. Petrick, Performance and Potential of Natural Circulation Boiling Reactors (Preprint 98), Session XIV, Nuclear Engineering and Science Conference, American Society of Mechanical Engineers, March 17–21, 1958.
5. J. A. DeShong, Jr., Power Transfer Functions of the EBWR Obtained Using a Sinusoidal Reactivity Driving Function, ANL-5798, January 1958. (Unclassified AEC report.)
6. Joseph A. Thie, Boiling Water Reactor Instability, *Nucleonics*, 16(3): 102 (March 1958).
7. J. H. Kittel, M. Novick, and R. F. Buchanan, The EBR-I Meltdown — Physical and Metallurgical Changes in the Core, ANL-5731, November 1957. (Unclassified AEC report.)
8. *Power Reactor Technology*, Vol. I, No. 2, February 1958. (Available from Superintendent of Documents, U. S. Government Printing Office, Washington 25, D. C.

General Discussion

Most of the published data on fuel elements are concerned with the manufacture and testing of fuel elements which will have a high degree of corrosion resistance in the coolant media and good radiation stability at high burn-ups. To improve these characteristics, there is a strong temptation to incorporate materials of relatively high absorption cross section, which may make for poor neutron economy in the reactor.

In reviewing the material which follows, the reader is referred to the general discussion of fuel-element characteristics as applied to large central-station power reactors given in the first issuance of *Power Reactor Technology*.[1] It covered the relation of fuel elements to fuel cost, fuel-element lifetime, parasitic absorption in fuel elements by additives, and the effect of fuel density of the element.

It is not the intention here to review all reactor fuel materials but to select for review developments in the field of reactor fuel and fuel elements which may have an effect on, or be useful in, the development and design of nuclear power reactors for civilian applications. In general, emphasis will be placed on reviewing and reporting significant data, especially irradiation history, on fuel materials of high fuel content which are the most suitable for large power reactors. However, elements of low fuel content will be reviewed where particular advantages of these fuels are apparent for research reactors or other applications.

Uranium Metal and Alloys of High Uranium Content

Uranium metal as fuel for large power reactors has the advantages of high density, relatively high thermal conductivity, and possibly lower cost compared to oxide and alloyed fuel materials. The main disadvantages are the poor dimensional stability of uranium metal when irradiated to high burn-ups and, in water reactors, its rapid corrosion when jacket failures occur. Since most of the components of the total fuel cost are inversely proportioned to burn-up or, more precisely, to the specific energy production, megawatt days per ton (Mwd/ton), a limitation on burn-up is very serious from the economic point of view.

In the case of alloyed uranium metal, the excellent nuclear performance may be retained while improving the mechanical and corrosion properties if small amounts of alloying materials having low neutron-absorption cross sections are added.

Recent development and testing of elements of this kind is summarized below. In cases involving additives an average macroscopic parasitic absorption cross section ($\overline{\Sigma}_p$) is given for the additives. The value of $\overline{\Sigma}_p$ is computed on the assumption that the alloy has a density of 18.5 g/cm^3 rather than its true density. This cross section can be compared directly with the macroscopic cross section of uranium to give an estimate of the effect on neutron economy, as illustrated in Sec. 3, p. 22, of reference 1.

Natural Uranium

Recently, Argonne National Laboratory (ANL) has reviewed some of the experiments[2] conducted on unalloyed natural uranium up to 1955. Specimens were irradiated to total atom burn-ups as high as 1.82 per cent (15,500 Mwd/ton) at temperatures from 50 to 220°C using the following four methods of fabrication:

1. Rolled at 300°C
2. Rolled at 300°C and quenched from the beta phase
3. Rolled at 300°C and quenched from the beta phase, and recrystallized in the alpha phase
4. Rolled at 600°C

All specimens suffered severe irradiation damage, with the 300°C rolled and beta-quenched uranium showing the best stability. The authors have made the following general conclusions as

a result of the study. In general, the conclusions are still valid today.

1. Uranium growth under irradiation is a function of the fabrication history of the material and the irradiation temperature. In general, the degree of instability under irradiation is directly proportional to the amount of preferred orientation and in particular to the amount of (0 1 0) poles parallel to the rolling direction.

2. Surface roughening of uranium under irradiation is directly related to the preirradiation grain size.

3. Fine-grained highly oriented uranium disintegrates under irradiation by a process of transverse fracturing, whereas coarse-grained randomly oriented material fails by progressively deeper surface damage. Uranium which has been rolled at 300°C and beta quenched should withstand 2 at. % burn-up without disintegrating, particularly if used with diameters comparable to the experimental specimens reported herein.

4. Uranium decreases in density under irradiation at a rate largely independent of prior fabrication history.

5. Uranium increases in hardness when subjected to irradiation.

6. For the materials used in this investigation, a qualitative similarity existed between irradiation growth rates and thermal cycling growth rates.

It was also pointed out in this report that the use of thermal cycling as an indication of the irradiation behavior of fuel materials is probably not applicable to uranium alloys. This was concluded from the results of irradiation experiments with some uranium-zirconium alloys which lengthened under thermal cycling but shortened under irradiation.

Although there has been a recent large increase in the use of oxide type fuel elements in power reactors, the advantages of metallic uranium for fuel elements are not easily overcome. Unalloyed natural-uranium fuel elements having an axial hole have shown excellent external dimensional stability at high temperatures.[3a] Also, uranium specimens alloyed with small amounts of low parasitic absorption materials such as zirconium and niobium show good dimensional stability at relatively high temperatures and burn-ups.[3b]

Development is also continuing on the fabrication of long tubular fuel elements with larger surface to volume ratios using metallic uranium. Nuclear Metals, Inc. has recently reported[4] successful extrusions of uranium tubes 15 ft long, $\frac{1}{4}$ in. thick, with diameters of $2\frac{1}{2}$ to $3\frac{1}{2}$ in. Fabrication of metallurgically bonded zirconium-clad metallic uranium fuel tubes by coextrusion techniques have also been made by NMI.[5] These fuel elements have been made in 29 in. lengths with an outside diameter equal to 2.370 in. and an inside diameter of 1.820 in. using a nominal zirconium-clad thickness of 0.030 in. One of these fuel elements, irradiated to 1500 Mwd/ton in MTR, was reported to have no significant changes. Larger tubes, 15 ft long, an outside diameter of 2.955 in., an inside diameter of 2.445 in., and a zirconium-clad thickness of 0.030 in., were also successfully fabricated. Irradiation of one of these elements to 1700 Mwd/ton resulted in no significant radiation damage.

Uranium-Zirconium

($\bar{\Sigma}_p$ = 0.000195 cm^{-1} per Wt.% Zirconium)

It was previously reported that uranium–2 wt.% zirconium alloys were dimensionally stable to high irradiation burn-ups provided the alpha-beta transformation temperature is not exceeded.[6] However, this alloy has little corrosion resistance in water as low as 100°C. In order to produce a fuel element with better corrosion resistance to hot water, specimens of this alloy were coextruded with Zircaloy-2 tubing and then diffusion heat-treated to produce a corrosion-resistant barrier layer.[7]

Unirradiated samples and samples irradiated to 0.1 wt.% were defected by 0.007-in.-diameter holes drilled through the clad. The samples, after operation in water at 290 and 350°C for several weeks, showed no evidence of core corrosion even though a nonirradiated sample, from which the clad had been stripped, was completely reduced in 1.7 days at 290°C.

It would appear that the barrier obtained by the diffusion heat-treatment is protective for small defects and low irradiations. Samples with larger defects (>0.016-in.-diameter holes) had decreased corrosion lifetimes.

Uranium-Molybdenum

($\bar{\Sigma}_p$ = 0.00257 cm^{-1} per Wt.% Molybdenum)

Attempts at producing radiation damage resistant uranium fuel elements by alloying with less than ~8 wt.% molybdenum have not been successful (references 1, 6, 8, and 9). However, uranium–≥10 wt.% molybdenum have been found to have good dimensional stability at rela-

Table IV-1 CHANGES IN DIMENSIONS AND DENSITY OF CLAD URANIUM-MOLYBDENUM ALLOYS*

Experiment No.	Composition	Max. exposure, Mwd/ton	Max. calc. spec. temp., °C			Diam.	Maximum change in length	Density change
			Surface	Interface	Central			
1 C	U–10.5 wt.% Mo	1,120	62	98	217		Not significant	
	U–12 wt.% Mo	1,120	61	96	213		Not significant	
2 C	U–9 wt.% Mo	5,400	102	210	563		Not significant	
	U–10.5 wt.% Mo	5,400	102	208	555		Not significant	
	U–12 wt.% Mo	5,610	103	210	562		Not significant	
	U–13.5 wt.% Mo	5,610	102	207	555		Not significant	
3 C	U–9 wt.% Mo	9,980	101	207	550		+0.24	
	U–10.5 wt.% Mo	9,980	101	203	542		+0.16	
	U–12 wt.% Mo	10,490	102	207	552		+0.12	
	U–13.5 wt.% Mo	10,490	101	205	547		+0.08	
4 C	U–9 wt.% Mo	27,800	112	238	647		+0.36	−3.4 (Calc.)
	U–10.5 wt.% Mo	28,200	113	240	654	+2.3	+0.24	−3.2 (Calc.)
	U–12 wt.% Mo	28,200	112	238	643		+0.16	−3.6 (Calc.)
	U–13.5 wt.% Mo	28,200	111		634		+0.16	−3.4 (Calc.)
7 C	U–12 wt.% Mo	5,860						−1.3 (Measured)
			(Information not available)					
8 C	U–12 wt.% Mo	10,500						−1.8 (Measured)
5 C†	U–9 wt.% Mo	2,100					+0.07	
	U–10.5 wt.%	2,100					+0.12	

*Data taken from Report WAPD-127, Pt. IV, Tables 6–9 and 12.
†Specimens partially transformed to alpha plus epsilon; all other specimens in the gamma-quenched condition.

Table IV-2 CHANGES IN DIMENSIONS AND DENSITY OF GAMMA-QUENCHED URANIUM-MOLYBDENUM ALLOYS*

Sample No.	Composition	Exposure, Mwd/ton	Estimated central temp., °C	Diameter increase, %	Length increase, %	Density decrease, %
42	U–10.5 wt.% Mo	1600	124	0.3	0.15	0.9
51	U–10.5 wt.% Mo	2800	168	0.5	0.4	1.4
43	U–10.5 wt.% Mo	3000	180	0.3	0.5	1.6
45	U–10.5 wt.% Mo	5350	270	1.1	0.8	2.7
50	U–10.5 wt.% Mo	5500	301	0.8	0.7	2.3
47	U–10.5 wt.% Mo	8500	413	1.6	1.0	3.5
48	U–10.5 wt.% Mo	8800	428	1.1	1.0	4.4
64	U–12 wt.% Mo	1200	141	0.5	0.25	1.1
63	U–12 wt.% Mo	2450	218	0.5	0.5	2.1
61	U–12 wt.% Mo	3500	296	3.2	2.1	6.7
67	U–12 wt.% Mo	3950	157	0.5	0.55	1.6
62	U–12 wt.% Mo	5250	189	1.0	0.9	3.0
65	U–12 wt.% Mo	6100	209	1.2	1.2	4.0
81	U–13.5 wt.% Mo	1350	152	0	0.1	0.5
85	U–13.5 wt.% Mo	2050	101	0	0.2	1.1
83	U–13.5 wt.% Mo	2250	231	0.5	0.25	1.1
86	U–13.5 wt.% Mo	2900	130	0.6	0.45	2.2
84	U–13.5 wt.% Mo	3200	273	1.1	0.6	2.8

*Data taken from Report WAPD-127, Pt. IV, Table 10.

tively high burn-ups.[10] A partial summary of the irradiation data available on these alloys are shown in Tables IV-1 and IV-2 taken from the reference report.[10]

No dimensional changes were observed in bare gamma-quenched uranium-molybdenum alloys for exposures of <1200 Mwd/ton (Table IV-1) and for Zircaloy-2-clad uranium-molybdenum alloys up to 5610 Mwd/ton (Table IV-2). In one of the four specimens of uranium-10.5 wt.% molybdenum alloy irradiated in Experiment 4-C to 28,200 Mwd/ton (Table IV-2), the Zircaloy clad developed longitudinal splits. Because irradiation was in low temperature (100°C max.) water, the clad failure was not attributed to Zircaloy corrosion but to the 4 per cent core volume expansion that occurred in the specimen.

The corrosion of bare uranium-molybdenum alloy specimens in high temperature water (~650°F) occurred at rates of ~0.1 to 0.3 mg/cm^2/hr, no significant difference being noted between the unirradiated and irradiated specimens. However, the time to failure of the specimens by gross cracking due to hydride formation was reduced considerably in the irradiated samples. The specimens exposed to ~1-2000 Mwd/ton failed within one to seven days. Corrosion in the case of Zircaloy-2-clad specimens, because Zircaloy getters the hydrogen produced by the corrosion of the core alloy, was stated to be a function of bond integrity and the diffusion rate of hydrogen into the core alloy. In general, the specimens irradiated to fairly high burn-up (>5000 Mwd/ton) and then corrosion tested by defecting the specimens and exposing them to 650°F static water failed within one to seven days. From the data of in-pile corrosion tests, it appeared that better corrosion life of defected fuel elements while in the reactor can be expected. The explanation offered for the improved corrosion life was an assumption that radiation tends to stabilize the gamma phase or corrosion-resistant phase of uranium-molybdenum alloys. Detailed data on a multitude of tests performed on these alloys are included in the reference report.[10]

Although these alloys appear to have excellent potential for water-cooled reactors with respect to radiation stability and aqueous corrosion resistance, the power reactor designer is confronted with an addition of a large amount of parasitic absorption material in the ~10 wt.% molybdenum ($\bar{\Sigma}_p$ = 0.00257 cm^{-1} per wt.% molybdenum compared to $\bar{\Sigma}_p$ = 0.000195 per wt.% zirconium). This would require the acceptance of a lower conversion ratio and higher enrichment of the fuel, both of which are in the direction of higher costs for power generating reactors.

Uranium-Niobium

($\bar{\Sigma}_p$ = 0.001169 cm^{-1} per Wt.% Niobium)

Lower temperature (~300°F) irradiation studies on uranium-10 wt.% niobium exposed to <1000 Mwd/ton by Bettis Plant[10] also show good dimensional stability of this alloy. Aqueous corrosion testing of a number of uranium-10 wt.% niobium elements clad in Zircaloy-2 and defected after irradiation to ~840 Mwd/ton showed good (no failure in 35 days) corrosion resistance in ~650°F water.[10]

The effect of impurities in uranium-10 wt.% niobium alloys on its corrosion behavior in 680°F water was covered in earlier reports.[6,11]

Again it can be stated that, although these alloys appear to have excellent potentials for power reactors because of their radiation stability and possible corrosion resistance, the amount of parasitic absorption material being added will most certainly lower the conversion ratio obtainable and require an increase in the enrichment of the uranium in order to achieve criticality. Both the effects result in higher power costs.

Plutonium-Aluminum Fuel

The plutonium recycle program being carried out at Hanford[12] has as one of its objectives the development of a suitable plutonium fuel which can be reprocessed and refabricated easily and economically.

In a recent report[13] Hanford has reviewed the various developments on plutonium-aluminum fuels which have been reported by Hanford, Chalk River, Los Alamos, ANL, and ORNL. As a result of experiments conducted at these sites, it was concluded that fuel elements of aluminum-5 and 10 wt.% plutonium irradiated to essentially 100 per cent burn-up of the plutonium atoms would have insignificant radiation damage.

The fuel element proposed for the plutonium recycle reactor by Hanford consists of an aluminum-1.65 wt.% plutonium core in a Zircaloy can. Bonding is to be effected by the dif-

ferential coefficients of expansion of the fuel and can materials. Such a bonding technique would require close tolerances to be held on the fuel and can. This fuel would have to be introduced into the proposed pressurized-tube heavy water moderated and cooled plutonium recycle reactor as spikes; this may not represent the best use of the fuel. (See reference 6 for a discussion of this reactor concept.)

Other fuel materials which can be considered for application to a plutonium recycle reactor are the uranium–20 wt. % plutonium, uranium–20 wt. % plutonium–5 wt. % fissium (references 1, 3b, 6, 14, and 15), and UO_2-PuO_2 (references 16 and 17) fuels which have been reviewed in the past. These fuels were investigated for the fast reactor program.

Aside from the development of a good fuel element for plutonium recycle, the chief problem to be solved for the success of a plutonium recycle system is the development and design of a satisfactory and economic reprocessing facility. Because plutonium constitutes a major health hazard, the handling, reprocessing, and refabrication of plutonium fuel elements will require a major development effort. This will be even more difficult if the reprocessing method chosen does not completely decontaminate the burnt fuel, thus requiring heavily shielded facilities as contemplated in the EBR-II facility.

The efforts being made by both Hanford and ANL[18] on the development of reprocessing and refabricating facilities should contribute much toward the final development of a plutonium recycle system.

In addition to the work described above, a program is under way at MTR[19] to make use of a plutonium core using plutonium-aluminum fuel elements. Reports concerned with the reactor physics aspects of this proposed plutonium core loading are given in references 20 to 23.

Thorium

Irradiation data obtained by Du Pont[24] on 92 extruded thorium slugs, 0.8 in. in diameter and 10 in. long, canned in aluminum and exposed to burn-ups of 800 to 2800 ppm of the Th^{232} atoms, showed excellent dimensional stability. The average changes in dimensions for the 800 ppm burn-up specimens were ±0.005 in. for the length, ±0.002 in. for the diameter, and ±0.002 in. for curvature or warp. Preliminary visual examination of the 2800 ppm burn-up specimens indicate they have good dimensional stability.

Nonmetallic Elements of High Fuel Content

Urania (UO_2)

Because of the great interest in and use of UO_2 as the fuel for power reactors, a review has been made of the UO_2 data available to date, especially as to its performance under long-term irradiation. In general, UO_2 fuel elements have the advantages of being relatively chemically inert and relatively radiation damage resistant. Their primary disadvantages are the brittleness of the UO_2 pellets, relatively low fuel density, and low thermal conductivity. The latter disadvantage is somewhat compensated by the high permissible operating temperature; but, for a given heat flux, oxide fuel elements will probably be thinner than metal elements since the ratio of thermal conductivity for uranium metal to UO_2 is ~18 to 1, whereas for a coolant temperature of 600°F, the ratio of ΔT for uranium metal to UO_2 is ~600/~3600 = 1 to 6. This characteristic, combined with the low fuel density, usually causes a significant loss in neutron economy relative to that which can be attained with metal elements and requires greater subdivision of the oxide fuel, which may result in higher fabrication costs.

In reviewing the data presented below, the reader is referred to the reference reports for more detailed information.

1. General Properties[25,26]

Crystal structure: face centered cubic (CaF_2)
Theoretical density, 10.97 g/cm^3
Theoretical density (fissionable and fertile), 9.7 g/cm^3
Metal atom/cm^3 in oxide, 51.5%
Metal atom/cm^3 in metal
Melting temperature (mean), 2760–5000°F
Linear coefficient of thermal expansion, 11.2×10^{-6}/°C
Specific heat, 0.056 cal/(g)(°C); (0–200°C)
Thermal conductivity coefficient (100% of theoretical density), 0.008 cal/(cm)(sec)(°C); (1000°C)
1.93 Btu/(ft)(sec)(°F); (1000°C)
Tensile strength, ~5000 psi
Modulus of elasticity, 25×10^6 psi
Index of refraction, 2.35

UO_2 fuel pellets can be commercially obtained with bulk densities in the 10.2 to 10.44 g/cm^3 range or 93 to 95 per cent of theoretical density.

2. Melting Temperature. The literature contains various values for the melting point of UO_2. However, the value 2878 ± 22°C (5212 ± 40°F) obtained by Lambertson and Mueller[27] has been generally used. More recent data reported by Wisnyi and Pijanowski[26] indicated the melting point to be 2760 ± 30°C (5000 ± 44°F).

The discrepancy may be accounted for by the possible impurity contamination in the UO_2. Small additions of impurities can vary the melting point radically as indicated on the binary systems diagrams prepared by the National Bureau of Standards.[28]

3. Thermal Conductivity. The generally accepted values of thermal conductivity are those prepared by Kingery and Vasilos.[29] The curve prepared from these values is generally higher than the curve prepared by the Armour Research Foundation (ARF).[30] One explanation of the lower values by ARF lies in the fact that the ARF specimen was found to be badly cracked after the test was completed. This may, however, be more representative of the thermal conductivity of the UO_2 specimens used in reactors which also crack radially under the operating thermal stresses. Table IV-3 is a comparison of the values obtained[31] corrected to 95 per cent dense UO_2.

Table IV-3 UO_2* THERMAL CONDUCTIVITY VS. TEMPERATURE†

Temperature		Thermal conductivity (cal)/(sec)(cm)(°C)		Thermal conductivity (Btu)/(hr)(ft)(°F)	
°C	°F	Kingery‡	ARF	Kingery‡	ARF
200	392	17.7×10^{-3}	12.3×10^{-3}	4.28	2.98
400	752	12.8×10^{-3}	9.4×10^{-3}	3.1	2.27
600	1112	9.9×10^{-3}	7.7×10^{-3}	2.4	1.86
800	1472	8.3×10^{-3}	6.2×10^{-3}	2.01	1.5
1000	1832	7.8×10^{-3}	5.7×10^{-3}	1.89	1.38
1200	2192		5.0×10^{-3}		1.21
1400	2552		4.6×10^{-3}		1.11
1600	2912		4.2×10^{-3}		1.01
§		2.42×10^{-3}		1.0	

*Corrected to 95 per cent of theoretical density.

†Data taken from Report WAPD-184, p. 29.

‡The following information was taken from reference 33: "W. D. Kingery has pointed out that in single-phase ceramics lattice thermal conductivity may, under suitable conditions of elevated temperature or lattice disturbance by irradiation, be reduced to a minimum value set by photon scattering at mean free paths of the order of the lattice spacings; in the case of UO_2, such a minimum value would correspond to about 1 Btu/(hr)(ft)(°F)."

§Data presented by Jakob[32] indicates that the thermal conductivity of powders is independent of density above 1000°C.

4. Irradiation History. Making up for the disadvantage of low density and thermal conductivity, natural UO_2 fuel elements have been irradiated to burn-ups of four and five times that presently achievable with unalloyed natural-uranium metal fuel. This higher burn-up has the effect of reducing both the fabrication and reprocessing costs. Most of the irradiation data previously reviewed[1,6] concerned isolated tests and included only preliminary information. Recently, a more detailed history of the irradiation tests on full-size PWR UO_2 fuel rods has been released.[31,33-35] These rods consist of 10 1/4 in. long Zircaloy-2 tubing (0.359 in. in inside diameter by 0.411 in. in outside diameter) in which 26 UO_2 fuel pellets (0.357 in. in outside diameter) of 93 to 95 per cent of theoretical density are stacked. The heat-transfer bond is helium gas at atmospheric pressure. Because of the number of rods and the large number of UO_2 fuel pellets per rod, these tests are fairly representative of what will result from the use of similar fuel rods in a power reactor.

A summary of the high burn-up data on the PWR blanket fuel rod tests are shown in Tables IV-4 and IV-5. The particular experiments shown are those having the highest burn-ups achieved during the irradiation program. Many more tests are reported in reference 33.

It was reported[33] that no microstructural, dimensional, and property changes have been noted other than those associated with purely thermal effects. Grain growth of the UO_2 specimens occurred at temperatures in pile corresponding to that noted out of pile. The gross radial cracking was anticipated because of the large thermal gradients across the fuel. External dimensional changes were negligible even in the fuel elements irradiated to burn-ups of 10,000 Mwd/ton. Temperatures above melting were achieved in the UO_2 irradiated to 25,000 Mwd/ton without any apparent decrepitation or physical disintegration of the pellets. Some circumferential cracking, which would have an adverse effect on the heat-transfer properties of the pellet, has been noted. However, it was stated that this may be caused by the increased

Table IV-4 DESCRIPTION AND SUMMARY OF AVAILABLE DATA ON UNCYCLED ZIRCALOY-2–CLAD UO_2 FUEL ELEMENTS*

Spec. No.	Heat flux,† Btu/hr/sq ft × 10^{-3}	Burn-up,† Mwd/ton	Calc. central temp., °C	Specimen dimensions: UO_2, diam.	Clearance: Diam.	Clearance: Axial	Tubing, O.D.	Over-all length	Dimensional changes: Diam.	Dimensional changes: Length	Molten zone, diam.	Fission gas release, % Kr^{85}
Experiments 14-12 and 13												
15H	370 (f)	10,900	2650	0.3445	0.0015	0	0.402	5.237	0	0	Not melted	5.0
18H	420 (f)	13,500	>2750	0.3445	0.0015	0	0.400	5.240	0	0	Not melted	8.1
19H	300 (f)	6,900	2200	0.3445	0.0015	0	0.402	5.238	0	0	Not melted	
Experiment 14-14												
82S	330 (e)	14,000	2400	0.3445	0.002	0.080	0.414	5.205	0	0	Not melted	
83S	540 (e)	22,000	>2750	0.3445	0.002	0.080	0.414	5.222	+0.012	0	0.200	
84S	600 (e)	25,000	>2750	0.3445	0.002	0.080	0.414	5.224	+0.015	0	0.230	
85S	300 (e)	12,000	2200	0.3445	0.002	0.080	0.414	5.206	0	0	Not melted	
Experiment 14-18												
9B2	300 (f)	6,430	1400	0.3570	0.002	0	0.413	4.544	0	0	Not melted	0.25
9B3	900 (f)	12,400	>2750	0.3570	0.002	0	0.413	4.560	+0.009	+0.009	0.250	13.6
10B1	890 (f)	12,100	>2750	0.3570	0.002	0	0.413	4.506	+0.008	+0.015	0.275	15.3
10B2	300 (f)	6,100	2200	0.3570	0.002	0	0.413	4.518	0	0	Not melted	
Experiment 14-19												
24B1	340 (f)	6,700	2400	0.3510	0.008	0	0.413		0		Not melted	
24B2	670 (f)	14,400	>2750	0.3510	0.008	0	0.413		+0.002		0.290	
24B3	840 (f)	15,500	>2750	0.3510	0.008	0	0.413		+0.018		0.325	35.6
25B1	340 (f)	7,930	2400	0.3510	0.008	0	0.413		0		Not melted	1.2

Remarks: These two experiments were designed to study the effect of irradiation at high heat fluxes and to high burn-ups on hot-pressed natural UO_2. Sample 15H contained 95 per cent dense hot-pressed UO_2 made from steam oxidized material, whereas samples 18H and 19H contained 91 per cent dense hot-pressed UO_2 made from MCW UO_2. The steam oxidized UO_2 is made by oxidizing uranium in an autoclave at 650°F and saturation pressure. MCW UO_2 is made by reducing UO_3 with cracked ammonia. The results of these experiments indicate that hot-pressed UO_2 is quite stable when irradiated to high burn-ups and high heat fluxes.

Remarks: This experiment was designed to determine the effect of irradiation to extremely high burn-ups on PWR reference rods. The samples contained 93 per cent dense cold-pressed and sintered natural UO_2 and were assembled to reference specifications. The Zircaloy-2 tubing for these rods, however, was machined from bar stock rather than extruded as is the case for the PWR reference rods, and this machined tubing was of somewhat dubious quality. The rods were irradiated in the MTR lattice for 1½ years and achieved an estimated burn-up of 25,000 Mwd/ton. Unfortunately, the cladding split on all the rods, permitting the NaK to attack the UO_2 and also preventing any fission gas studies. In an attempt to determine if the cladding split because of a deterioration in the mechanical properties as a result of the high irradiation exposure, the hardness of the cladding of a high and low flux specimen was measured. Although no control hardness values are available, the hardness of the cladding on both the samples was within the range of as fabricated tubing.

Remarks: This experiment was designed to determine the effect of irradiation to very high burn-ups of 93 per cent dense cold-pressed and sintered UO_2 enriched 6.24 per cent U^{235} in total uranium. The Zircaloy-2 tubing was manufactured by the reference extrusion process. The UO_2 in the two higher exposure rods was molten over a considerable portion of the diameter, yet very little dimensional changes occurred in the samples. The fission gas release values indicate that molten UO_2 retains considerably less of the fission gas than UO_2 irradiated below the melting point.

Remarks: This experiment was designed to determine the effect of large diametral clearances (0.008 in.) on the behavior of reference PWR rods irradiated at high heat fluxes. Although a considerable portion of the UO_2 melted in the two higher exposure samples, the heat fluxes are not known to a sufficient degree of accuracy to ascertain the effect of the 0.008-in. diametral clearance as opposed to the reference 0.002- to 0.004-in. diametral clearance. Again, the effect of melting in the UO_2 can be noted in regard to the amount of fission gas released.

*Data taken from Report WAPD-183, pp. 108, 110, 111, and 115.

†Heat flux, burn-up, and calculated center temperatures are based on estimates of nominal reactor fluxes when indicated by (e) and fission monitor results when indicated by (f). The estimates are good only to ± 50 per cent, whereas the fission monitor data are felt to be somewhat more accurate. The inconsistencies noted between the calculated center temperatures and the observed melting are presumably produced by these inaccuracies.

Table IV-5 DESCRIPTION AND SUMMARY OF AVAILABLE DATA ON IRRADIATION CYCLED ZIRCALOY-2–CLAD UO_2 FUEL ELEMENTS*

Spec. No.	Heat flux,† Btu/hr/sq ft $\times 10^{-3}$	Burn-up† Mwd/ton	UO_2, diam.	Specimen dimensions: Clearance Diam.	Clearance Axial	Tubing, O.D.	Over-all length	Number of cycles	Dimensional changes Diam.	Dimensional changes Length
				Experiment 19-7						
N-5-9-C	450	18,000	0.357	0.002	0.150	0.414	10.298	7,000	0	0
N-5-7-C	450	18,000	0.357	0.002	0.058	0.414	10.302	7,000	0	0
N-5-9-B	450	9,000	0.355	0.004	0.150	0.414	10.303	7,000	0	0
N-5-10-B	450	9,000	0.355	0.004	0.055	0.414	10.297	7,000	0	0

Remarks: This test was designed to determine the effect of irradiation cycling to very high burn-ups on the possible dimensional instability of cycled rods. The rods contained 95 per cent dense cold-pressed and sintered UO_2 enriched 6.2 wt.% U^{235} in total U. No dimensional changes were produced as a result of the irradiation.

*Data taken from Report WAPD-183, p. 117.

†Burn-up and heat flux values are based on estimates of the thermal-neutron flux in the various reactor locations and are considered to be accurate to only ±50 per cent.

densification of the center of compacts at the high operating temperatures and consequent shrinking of the center from the exterior of the pellets. The cracking appears to be independent of burn-up since further cracking with higher burn-up, beyond the initial gross cracking, was not observed.

Metallographic studies on the effect of high burn-up on UO_2 fuel were also made[36] by KAPL. The reader is referred to the reference report for details of the theories proposed on the effects of irradiation on UO_2.

A conclusion which can be drawn from the present irradiation data is that UO_2 fuel elements of the kind typified by the PWR elements do not show an inherent tendency to fail during irradiation exposures up to 10,000 Mwd/ton, and perhaps higher. Gross cracking of the oxide pellets does occur early in their life, the transfer of heat from the interior of the element to the jacket deteriorates slowly with exposure, and there is a release of some gaseous fission products from the oxide which increases with oxide temperature. If the design of the fuel elements makes adequate allowance for these effects, it would appear that the fractional rate of failure of such elements in a reactor, to maximum burn-ups of the order 10,000 Mwd/ton, will be reasonably low; proof that the failure rate is as low as is required for economic reactor performance will require statistical tests involving many elements such as those which would result from actual long-term operation of a reactor using the elements.

5. Bonding Material. The type of material used as the bonding agent in the gap between the fuel pellet and the can will materially affect the heat transfer of the element. A list of the bonding materials which may be used or may contaminate the original material are shown in Table IV-6 along with the temperature drop through a 1-mil bonding gap at a heat flux[33] of 500,000 Btu/hr/sq ft at 400°C.

Table IV-6 UO_2 BONDING MATERIALS*

Material	Temp. drop in a 0.001-in. bonding gap at 400°C, °F
He	288
Xe + Kr	5400
Steam	1490
50% He + 50% (Xe + Kr)	900
Hydrogen	278
Lead	2.1

*Data taken from Report WAPD-183, p. 45.

It should be noted that, since the central temperature of the fuel will be partially dependent on the temperature drop in the heat-transfer bond, a decrease of 286°F in central fuel temperature would occur for a lead bond vs. a helium bond. Also, the mixing of fission-product gases xenon and krypton with the heat-transfer bond, or the mixing or substitution of steam for the heat-transfer bond, will cause a substantial increase in the central fuel temperature of the fuel for the same surface heat flux.

6. Minimum Heat Fluxes for Melting or Grain Growth. Table IV-7, taken from reference 33, lists the experimental observations of the minimum heat fluxes at which melting or grain growth occurred for various conditions.

Table IV-7 MINIMUM HEAT FLUXES FOR MELTING AND GRAIN GROWTH*

	Cold diam. clearance, in.	Btu/hr/sq ft at which observed		GG temp., °C
		Melting	GG	
Defected	0.005–0.008	370,000	340,000	2000
Defected	0.001–0.004	425,000	330,000	2050
Undefected	0.005–0.008	422,000	360,000	2250
Undefected	0.001–0.004	(530,000) est.	430,000	2300

*Data taken from Report WAPD-183, p. 63.

7. Thermal Data Conclusions. As a result of the work described in reference 33, the following empirical conclusions were drawn concerning the thermal behavior of the PWR UO_2 type blanket fuel rods.

1. The thermal capabilities of helium-filled, low-clearance, natural UO_2 PWR fuel elements can be expressed by use of the Kingery-Vasilos UO_2 thermal conductivity values.
2. The thermal performance of helium-filled, low-clearance, enriched fuel elements is described by a thermal conductivity of the oxide of 1 Btu/hr/ft/°F.
3. The thermal capabilities of helium filled, high-clearance natural or enriched UO_2 or steam-filled, low-clearance natural or enriched UO_2 fuel elements are described by a mean UO_2 thermal conductivity of 1 Btu/hr/ft/°F and a gap thermal conductivity of about 0.03 Btu/hr/ft/°F.
4. A steam atmosphere reduces thermal capabilities more than a helium atmosphere at the same initial clearance and with the same atmosphere increases central temperatures.
5. The thermal performance of enriched fuel rods cannot be correlated with available property data.

8. Fission Gas Release. Data on the release of fission gases have been reported previously,[1,6] but a brief summary is made here to complete this review.

The following general conclusions, taken from a study by Bettis Plant,[35] are representative of the data.

1. The release of fission gases from irradiated UO_2 is in all probability controlled by diffusion of the gases from the oxide matrix.
2. The oxide density has a large effect on the gas release because of the variation with density of the diffusion path length to the external surfaces. (Experimental evidence indicates that the fission gas release is reduced considerably with UO_2 specimens which are >90 per cent theoretical density; the gas released for 65 per cent dense packed UO_2 is 40 to 50 per cent,[37] for 91 per cent dense pressed and sintered pellets is 3.1 per cent,[35,38] and for 95 per cent pressed and sintered pellets is ~1 per cent.)
3. Assuming the gas release is due to diffusion, the amounts of gas released can be calculated with a correction being made for the density of the oxide specimen. Calculations agree within a factor of 3 with experimental data on irradiated PWR fuel rods.

It should be noted that, at high burn-ups, the effect of the fission gas released within the clad even with dense 95 per cent UO_2 pellets must be taken into consideration. The two major effects are the increase in pressure due to gas release and the change in thermal conductivity of the helium gas bond. Reference 33 reports that enough xenon and krypton is released in Core-1 PWR reference fuel elements at 1 wt.% burn-up and 1 per cent gas release to dilute the helium by 50 per cent. In such a case, referring to Table IV-6, an increase in the central fuel temperature of 618°F per each 0.001 in. of 50 per cent helium + 50 per cent (xenon + krypton) bonding gap can be expected for the same heat flux generation. With fuel center temperature operation close to the melting point of the UO_2, it is conceivable that such a change would cause the central part of the pellet to melt, releasing much larger percentages of gas. The increase in fission gases released at high burn-ups and on melting are indicated by the data from Experiments 14-12, 14-18, and 14-19 in Table IV-4.

More detailed data on the release of fission products to the coolant water by defected type elements operating in reactor test loops are available in the reference report.[33] The information reported will be useful in evaluating the hazards of a nuclear incident in a UO_2 fueled reactor.

9. Aqueous Corrosion Resistance. As was reported previously,[1] the corrosion of UO_2 specimens in 650°F water and 650–750°F steam is excellent, and tests indicated that UO_2 is essentially inert in water containing any measurable excess of hydrogen. However, because of the thermal fracturing which occurs in the

UO_2, it must be expected that some particles of UO_2 will escape from a defected fuel element. The reference report[33] has elaborated on this mechanism of fission-product release.

10. Fuel-element Failure. Excluding failures due to nuclear excursions, the more common failure to be expected in UO_2 type fuel occurs after the clad has been defected. One failure type has been called "waterlogging" and is caused by water entering the fuel rod in the clearance spaces and fuel pellet voids during a reactor shutdown. On reactor start-up, the trapped water would flash to steam, producing pressures high enough to rupture the clad and possibly fracture the fuel pellets. This was demonstrated by tests made by Bettis Plant and reported in the reference report.[33]

11. Fuel-element Fabrication. The fabrication techniques for the dense, pressed, and sintered type of UO_2 fuel elements have been covered fairly well in the unclassified literature.[39,40]

Hanford[41] has been developing techniques for extruding UO_2 in the shape of rods $\frac{1}{4}$ to $\frac{3}{4}$ in. in diameter and up to 6 ft long for the plutonium recycle program reactor. Both PWR grade and ceramic grade powders were used to achieve densities of 92 per cent of theoretical or greater. The ceramic grade powders were used as received. The PWR grade powders required an activation treatment consisting of either Burudum ball milling or controlled oxidation reduction to achieve high densities.

The development of these techniques combined with possible coextrusion or other cladding methods will be a step toward decreasing the cost of UO_2 type reactor cores.

Thoria-Urania

ANL has fabricated a thoria-urania fuel charge for the BORAX-IV reactor.[42] The fuel is in the form of pressed and sintered pellets, 0.230 in. in diameter and in random lengths of $\frac{1}{4}$ to $\frac{3}{4}$ in. The fuel pellets are jacketed with the aluminum 1 wt. % nickel alloy.

The thoria powder, supplied by National Lead Co., was calcined at 1000°C. The U_3O_8, supplied by Oak Ridge National Laboratory (ORNL), was manufactured by the steam oxidation of enriched metallic chip. Calcining was not necessary. Both powders were received as −325 mesh material.

A mixture of 93.41 wt. % ThO_2 and 6.59 wt. % U_3O_8 in polyvinyl alcohol was ball milled for 3 hr. The ball milling was followed by the addition of water and an aerosol. The wet batch was then granulated and dried to form a free flowing powder. Dry pressing was accomplished in a multiple ram and cavity type press at 13,000 to 15,000 psi. The green pellets were fired, in air, at 1700 to 1750°C. The pellets are inserted in the jackets in the as-fired condition.

The yield of satisfactory pellets made by the process was greater than 95 per cent. Firing shrinkage was found to be about 17 per cent. The apparent fired density, measured by water immersion, was found to be 9.8 g/cm^3, or about 97 per cent of the theoretical density of ThO_2-UO_2 (10.09 g/cm^3). The fired composition of the pellets was calculated to be 93.65 wt. % ThO_2 and 6.35 wt. % UO_2. Irradiation tests on thoria-urania fuel previously reviewed[1,43–45] indicated that this material was dimensionally stable to burn-ups of ~1 per cent of metal atoms with central fuel temperatures of less than 2000°C.

Elements of Low Fuel Content

Uranium-Aluminum

Uranium-aluminum alloys of high uranium content have been difficult to fabricate because of the formation of the intermetallic compound, UAl_4, which makes the alloy very brittle. ORNL has reported that the addition of 3 wt.% silicon to a 48 wt.% uranium-aluminum alloy was sufficient to completely suppress formation of UAl_4, allowing the primary nucleating intermetallic compound, UAl_3, to be retained as the stable phase at low temperatures.[46] Further developments by ORNL indicated that other ternary additives such as zirconium, tin, titanium, and beryllium will also suppress UAl_4 formation. The addition of the silicon also made for easier fabrication of the 48 wt.% uranium–3 wt.% silicon-aluminum alloy.

Fuel plates, having 48 wt.% uranium in aluminum, are being studied by ORNL[47] for application to plate type research reactors using the 20 per cent U^{235} enrichment specified under the Atoms for Peace Plan.

An 18 plate fuel element of 48 wt.% uranium-aluminum alloy, using 20 per cent enriched uranium, containing a total of 190 g of U^{235} and

clad with 6061 type aluminum, has been irradiated in the MTR in a flux of 1.9×10^{14} neutrons/cm^2/sec for 4.5×10^{20} nvt. No significant irradiation damage was observed at the estimated burn-up of 25 per cent of the U^{235} atoms.[47]

Uranium-Zirconium

In a recent report[48] ANL has summarized the results on irradiation of specimens of zirconium-clad, uranium-zirconium fuel plates containing 3, 6, and 14 wt.% highly (93.4 per cent) enriched uranium. The plates were irradiated in open aluminum capsules in a water channel at 70 to 140°F for exposures ranging from 0.69×10^{20} to 16.4×10^{20} nvt thermal and burn-ups varying from 0.03 to 3.3 per cent total atoms. The results are shown in Table IV-8.

Table IV-8 SUMMARY OF IRRADIATION TESTS ON ZIRCONIUM-CLAD URANIUM-ZIRCONIUM FUEL PLATES*

(Plates 17–29, 3% enrichment; plates 30–39, 6% enrichment; plates 41–52, 14% enrichment)

BMI Plate No.	Min. Zr thickness, mil: Plate side	Min. Zr thickness, mil: Plate end	Burn-up, %	Change, %: Density (–)	Change, %: Thickness (+)
Top clad thickness: 20 mil					
18†	120	110	0.350	0.527	1.06
17†	120	80	0.374	0.076	0.841
20	150	200	0.374	0.709	0.839
33	150	320	0.40	0.662	2.22
22	150	210	0.590	0.605	0.0
19†	120	80	0.650	0.360	1.00
31	150	140	0.720	1.02	1.79
32	150	250	0.720	1.44	1.68
29†	140	150	1.10	1.39	1.38
34	150	250	1.10	1.18	1.05
30	150	150	1.20	1.09	1.31
41†	120	150	1.60	0.211	5.32
45	140	210	1.73	2.77	5.23
42†	130	150	2.70	3.19	7.55
43†	140	100	3.0	2.88	8.60
46	140	200	3.0	3.10	8.08
44	150	250	3.3	2.79	8.29
Top clad thickness: 30 mil					
23	150	230	0.480	0.441	0.84
28	130	310	0.480	0.349	1.06
27	130	140	0.590	0.501	
24	140	300	0.650	0.318	1.46
26	130	160	0.715	0.091	0.83
25	130	310	0.715	0.076	0.52
39	140	150	0.92	0.604	1.27
36	150	280	0.92	0.831	1.90
47	150	200	0.96	0.984	1.68
35	140	320	1.20	0.663	1.80
38	140	130	1.37	0.44	1.47
37	150	230	1.37	0.32	1.68
51	120	160	1.73	1.70	3.91
52	130	130	2.2	1.79	5.47
48	140	220	2.2	1.94	3.88
49	140	240	2.7	2.08	2.76
50	140	120	3.3	1.79	4.89

*Data taken from Report ANL-5825, p.5.

†Not cold-pressed before machining; exposed for 387.5 hr to static water at 350°F.

This type of element, although extremely radiation stable, would probably not be as useful as the uranium-aluminum elements previously discussed because of the more expensive fuel and alloying material being used.

References

1. *Power Reactor Technology*, Vol. I, No. 1, December 1957. (Available from Superintendent of Documents, U. S. Government Printing Office, Washington 25, D. C.)
2. J. H. Kittel and S. H. Paine, Effects of High Burnup on Natural Uranium, ANL-5539, May 1957. (Unclassified AEC report.)
3. Papers Prepared for Radiation Effects Review Meeting, Congress Hotel, Chicago, July 31–Aug. 1, 1956, TID-7515(Pt. 2), August 1956. (Confidential AEC report.)
   a. J. E. Minor, High-temperature Irradiation of Unalloyed Uranium. General Electric Company, Richland, Wash.
   b. S. H. Paine and J. H. Kittel, ANL Reactor Materials Irradiation Program. Argonne National Laboratory, Lemont, Ill.
4. Technical Progress Report to the AEC Reactor Division for the Period April 1, 1956, through June 30, 1956, NMI-1175, July 1, 1957. (Confidential AEC report.)
5. J. L. Klein and J. M. Fitzpatrick, Fabrication and Properties of Large Diameter Zirconium-clad Uranium Tubes with Integral Zirconium End Seals, NMI-1179, Sept. 11, 1957. (Secret AEC report.)
6. *Power Reactor Technology*, Vol. I, No. 2, February 1958. (Available from Superintendent of Documents, U. S. Government Printing Office, Washington 25, D. C.)
7. Sherman Greenberg and Joseph E. Draley, Effects of Irradiation on Corrosion Resistance of Some High Uranium Alloys, *Nuclear Science and Engineering*, 3(1): 19 (January 1958).
8. E. Epremian, Nuclear Fuels Newsletter, WASH-702, May 1957. (Confidential AEC report.)
9. E. Epremian, Nuclear Fuels Newsletter, WASH-703, August 1957. (Confidential AEC report.)
10. L. J. Jones, Development and Properties of Uranium-base Alloys Corrosion Resistant in High-temperature Water. Part IV. Radiation Stability of Uranium-base Alloys, WAPD-127, May 1957. (Unclassified AEC report.)

11. E. S. Hodge, W. E. Berry, et al., Effect of Impurities on the Corrosion Behavior of Uranium–10 Wt.% Niobium Alloys in 680°F Water, BMI-1159, Jan. 24, 1957. (Confidential AEC report.)
12. Staff of the Advance Engineering Operation, The Plutonium Recycle Program—A Résumé to the Concept, Program, and Facilities, HW-50700, June 12, 1957. (Unclassified AEC report.)
13. M. D. Freshley, Plutonium-Aluminum Fuel Element Development, HW-52457, Sept. 18, 1957. (Unclassified AEC report.)
14. J. E. Kemme, Irradiation Tests on EBR-II Pin Type Fuel Elements, Metallurgy Information Meeting, Ames Laboratory, Iowa State College, May 2, 3, and 4, 1956, TID-7526(Pt. 2b), March 1957. (Confidential AEC report.)
15. K. F. Smith and L. R. Kelman, Irradiation of Cast Uranium-Plutonium Base Alloys, ANL-5677, May 1957. (Unclassified AEC report.)
16. J. K. Davidson, The Fast Oxide Breeder—A Summary, KAPL-1701, July 1, 1957. (Unclassified AEC report.)
17. W. M. Cashin, The Fast Oxide Breeder—Fuel Irradiation Experiments, KAPL-1784, Aug. 26, 1957. (Unclassified AEC report.)
18. A. S. Shuck, Remote Fuel Fabrication—How It Was Done for EBR-II, *Nucleonics*, 15(12): 50-53 (December 1957).
19. H. L. McMurry and B. W. Johnson, Plutonium Fuel Requirements for Operation of the MTR, IDO-16378, June 11, 1957. (Unclassified AEC report.)
20. B. W. Johnson and H. L. McMurry, Comparison of Flux and Power Distributions and Void and Temperature Coefficients of the MTR with U^{235} and Pu^{239} Fuel, IDO-16384, July 26, 1957. (Unclassified AEC report.)
21. H. L. McMurry and B. W. Johnson, Relative Neutron Lifetimes in the MTR Fueled with U^{235} and Pu^{239}, IDO-16391, Aug. 8, 1957. (Unclassified AEC report.)
22. B. W. Johnson and H. L. McMurry, Reactivity Effects of Xe^{135} and Sm^{149} for the MTR with U^{235} and Pu^{239} Fuels, IDO-16398, Aug. 8, 1957. (Unclassified AEC report.)
23. B. W. Johnson, Nuclear Constants and Technical References Related to Plutonium Fuel Systems, IDO-16403, Sept. 30, 1957. (Unclassified AEC report.)
24. R. P. Marshal, Irradiation of Thorium Slugs, DP-160, May 1956. (Secret AEC report.)
25. J. R. Johnson, L. M. Doney, et al., The Technology of Uranium Oxide—A Reactor Material, ORNL-2011, Feb. 21, 1956. (Unclassified AEC report.)
26. C. A. Bruch and W. M. Cashin, Metallurgy Report of the Research Operation for September, October, and November 1956, KAPL-1658. (Confidential AEC report.)
27. W. A. Lambertson and M. H. Mueller, Uranium Oxide Phase Equilibrium Systems. II. UO_2-MgO, *Journal of the American Ceramic Society*, 36: 332 (1953).
28. S. M. Lang, F. P. Knudsen, et al., High-temperature Reactions of Uranium Dioxide with Various Metal Oxides, NBS Circular 568, National Bureau of Standards, U. S. Department of Commerce, Feb. 20, 1956. (Available from Superintendent of Documents, U. S. Government Printing Office, Washington 25, D. C.)
29. W. D. Kingery, T. Vasilos, et al., Thermal Conductivity—X. Data for Several Pure Oxide Materials Corrected to Zero Porosity, *Journal of the American Ceramic Society*, 37(2): 107-110 (February 1954).
30. J. C. Hedge and I. B. Fieldhouse, Thermal Conductivity of UO_2, ARF GO-22-D3, Sept. 22, 1956. (Unclassified AEC report.)
31. J. Belle and B. Lustman, Properties of UO_2, WAPD-184, September 1957. (Unclassified AEC report.)
32. M. Jakob and G. A. Hawkins, "Elements of Heat Transfer and Insulation," 2nd ed., John Wiley & Sons, New York, 1954.
33. J. D. Eichenberg, P. W. Frank, et al., Effects of Irradiation on Bulk UO_2, WAPD-183, October 1957. (Unclassified AEC report.)
34. J. M. Markowitz, R. C. Koch, and J. A. Roll, Release of Fission Gases from Irradiated Uranium Dioxide, Part I: Apparatus for the Measurement of Fission Gas Release from Fuel Materials During Pile Irradiation, WAPD-180, July 1957. (Unclassified AEC report.)
35. B. Lustman, Release of Fission Gases from UO_2, WAPD-173, March 1957. (Unclassified AEC report.)
36. W. K. Barney and B. D. Wemple, Metallography of Irradiated UO_2-Containing Fuel Elements, KAPL-1836, Jan. 15, 1958. (Unclassified AEC report.)
37. J. F. Eckel, C. A. Bruch, A. Levy, A. H. Willis, and W. E. Seymour, Radiation Effects on Reactor Materials, Papers Prepared for Radiation Effects Review Meeting, Congress Hotel, Chicago, July 31–Aug. 1, 1956, TID-7515(Pt. 2). (Confidential AEC report.)
38. J. Belle and L. J. Jones, Résumé of Uranium Oxide Data. IX. WAPD-TM-44, Mar. 15, 1957. (Unclassified AEC report.)
39. T. J. Burke, J. Glatter, H. R. Hoge, and B. E. Schaner, The Fabrication of High Density UO_2 Fuel Components for the First PWR Core, WAPD-165, May 1, 1956. (Unclassified AEC report.)
40. J. Glatter, H. R. Hoge, and B. E. Schaner, The Fabrication of Dense Uranium Dioxide Cylindrical Compacts by Cold Pressing and Sintering, WAPD-126, Oct. 14, 1955. (Unclassified AEC report.)
41. D. R. Stenquist and R. J. Anicetti, Extrusion of Uranium Dioxide Fuel Cores, HW-51747, Dec. 1, 1957. (Unclassified AEC report.)

42. J. H. Handwerk, C. L. Hoenig, and R. C. Lied, Manufacture of the ThO_2-UO_2 Ceramic Fuel Pellets for BORAX-IV, ANL-5678, August 1957. (Unclassified AEC report.)
43. W. A. Lambertson, M. H. Mueller, and F. H. Gunzel, Jr., Uranium Oxide Phase Equilibrium Systems. IV. UO_2-ThO_2, *Journal of the American Ceramic Society*, 36(12): 397-399 (1953).
44. J. H. Handwerk and R. A. Noland, Oxide Fuel Elements for High Temperatures, *Chemical Engineering Progress*, 53(2): 60F-62F (February 1957).
45. Quarterly Report for April, May, and June 1956, ANL-5623, November 1956. (Confidential AEC report.)
46. Metallurgy Division Annual Progress Report for Period Ending Oct. 10, 1957, ORNL-2422, Dec. 13, 1957. (Secret AEC report.)
47. W. C. Thurber, J. H. Erwin, and R. J. Beaver, The Application of a Nominal 48 Wt. % U-Al Alloy to Plate Type Aluminum Research Reactor Fuel Elements, ORNL-2351, Mar. 11, 1958. (Unclassified AEC report.)
48. R. E. Bailey, Irradiation Effects on Zirconium-clad Uranium-Zirconium Fuel Plates, ANL-5825, February 1958. (Unclassified AEC report.)

Control Materials

Boron-Iron Alloys

In a recent report[1] Bettis Plant has summarized its boron–stainless-steel alloy investigation program. Austenitic stainless-steel alloys containing boron in amounts up to 3 per cent were investigated for possible use as control-rod materials. Irradiation of the boron–stainless-steel alloys studied produced a severe decrease in the impact strength, making them unusable for the contemplated purpose.

Further developments by the British on the production of high boron-iron alloys have recently been reported in a British journal.[2] The article indicated that, by the addition of aluminum, alloys containing up to 4.75 per cent boron were successfully forged, rolled, and extruded and that boron-iron alloys containing up to 6 per cent boron were successfully cast. Iron-boron-aluminum control rods produced in the form of extruded tubes containing up to 3.8 per cent boron and cast tubes containing up to 5 per cent boron are presently being used in the Calder Hall reactors. However, unconventional techniques are required during forging, rolling, and extruding of these high boron-iron-aluminum alloys.

With boron contents of the order of 3 per cent instead of 1 per cent, boron-iron control rods would become more attractive relative to those made of hafnium since the problem of burn-out of B^{10} will be much reduced.

Some of the problems not covered in the article were the corrosion resistance of the alloys in high temperature water and the dimensional stability of the alloys under irradiation.

Moderator, Shielding, and Structural Materials

Zirconium Hydride

Further studies by BMI[3] on the fabrication of delta phase zirconium hydride for possible use as a moderator or radiation shield have yielded the following properties data:*

1. Mean coefficient of thermal expansion for $ZrH_{1.82}$ (68 to 1337°F) is 6.5×10^{-6}/°F.
2. Thermal conductivity of a $ZrH_{1.63}$ specimen varied between 5.7 Btu/hr/ft/°F at 300°F to 5.1 Btu/hr/ft/°F at 1300°F.
3. The hot hardness of $ZrH_{1.60}$ specimens varied between 164 kg/mm^2 at room temperature to 42.5 kg/mm^2 at 1490°F.
4. The tensile strengths of $ZrH_{1.80}$, previously reported,[4,5] are 9700 psi at 1130°F and 4060 psi at 1275°F.

A disadvantage of the use of zirconium hydride at high temperatures as a moderator is the canning required to retain the hydrogen released under irradiation. BMI has directly bonded satisfactorily specimens of delta phase zirconium hydride to 304 and 347 stainless-steel cladding.[6]

Aluminum-Nickel Alloys

The use of aluminum alloys in water-cooled power reactors has been limited by the low structural strength and poor corrosion resistance of the alloys at elevated temperatures. Recently, some alloys of aluminum have been investigated which show potential application to power reactors.

Tests were conducted by Draley and Ruther at ANL on an alloy of aluminum M-388, which contains 1 per cent nickel in type 1100 aluminum.[7] These static tests[7,8] showed a corrosion rate of M-388 alloy in 500°F distilled water of ~2.3 to 3.3 mdd.† This would be equal to a corrosion rate of ~1.2 to 1.7 mils per year. In a more recent report by Martinec, specimens of M-388 alloys showed a corrosion rate of ~15.8 to 17.4 mils/year.[9] These high corrosion rates were obtained in in-pile and out-of-pile

*Delta phase is defined as all material having a hydrogen-to-zirconium atomic ratio between 1.5 and 2.0 or an N_H (number of hydrogen atomic $\times 10^{-22}$ per cm^3 of sample) between 5.5 and 7.3.

†mdd = milligrams per square decimeter per day.

dynamic (16 ft/sec water) corrosion tests of M-388 alloy in 1 megohm-cm, ~480°F water of approximately neutral pH for a period of 2500 hr. The results of the tests indicated that there was essentially no difference in corrosion rate of this alloy in pile or out of pile. However, the high corrosion rate obtained under the dynamic conditions as compared to the low corrosion under static conditions would make this material useless in power reactors. Erosion under the dynamic operating condition was one explanation of the higher corrosion rate offered by the author. A more comprehensive analysis of the higher rate, taking into consideration the effects of the specimen surface area to water volume ratio (contamination factor) and the pH of the water, would be of interest. Draley has pointed out that the above conditions can have a material effect on the corrosion rate. Data on the effect of pH on corrosion of aluminum alloys indicated a major reduction in the equilibrium corrosion rate at a pH of ~3 to 3.5 and a major increase in corrosion rate at a pH above 8 (references 7 and 10). In fact, a 30-day corrosion test of M-388 alloy in 550°F phosphoric acid of pH 3.5 (measured at room temperature) resulted in a corrosion rate of less than 0.1 mdd (0.5 mil/year).[7]

ANL has also been studying an improved aluminum-nickel alloy of near-eutectic composition known as A-203 (5.6 wt. % nickel – 0.3 wt.% iron – 0.2 wt. % titanium – <0.02 wt.% silicon). Tests conducted in superheated steam at 300 psi and 840°F indicated this material was far superior to M-388 alloy.[7] The A-203 specimen, after 14 days of test under the above conditions, showed very little corrosion, whereas the M-388 alloy being used as a reference was completely oxidized. A disadvantage of this A-203 alloy is the higher macroscopic absorption cross section resulting from the increased nickel content (0.0217 cm^{-1} for A-203, 0.0151 cm^{-1} for M-388, 0.013 cm^{-1} for aluminum, 0.0076 cm^{-1} for zirconium, and 0.267 cm^{-1} for 304-L stainless steel). However, the absorption cross section is still low compared to stainless steel.

A Hanford report[11] has reviewed much of the data on the corrosion of aluminum and has presented a method of predicting corrosion rates for several aluminum alloys when used as canning materials for fuel elements. Rates were predicted for several geometric arrangements with water having different inhibitor concentrations and pH. It was concluded in this report that, from a corrosion standpoint, aluminum may potentially be used in a reactor with water having outlet temperatures as high as 350°C.

Further studies have been made by Hanford to determine the cause of the change from uniform corrosion of aluminum in water above 100°C to the rapid integranular corrosion[12] above ~250°C. The aluminum corrosion films formed in 310°C water on type 1245 and M-388 aluminum alloys were examined by X-ray diffraction, electron microscopy, and optical microscopy, but no theory was proposed as to the mechanism causing the change.

Because of the excellent potentials of some of the aluminum-nickel alloys, it would appear that further development may produce an extrudable material which is corrosion resistant at elevated temperatures and useful for power reactors. Very little data is available on the strength properties of these alloys at elevated temperature, although Hanford has published some room temperature data on M-388 alloy.[13] However, to be useful in power reactors and to decrease the cost of reactor core fabrication, an aluminum alloy would be required to have adequate strength as well as corrosion resistance at the elevated temperature.

Ceramic Glazes

Because of the high corrosion of metallic uranium in water, cladding of some type is normally used on these elements. Hanford has recently reported[14] on some of the techniques being used to apply ceramic glazes to uranium metal and the corrosion resistance of the ceramic glaze to boiling water and 130°C water and steam. One-mil-thick coatings of the glaze were resistant to shock and abrasion. However, in 130°C water, the particular glaze used dissolved rapidly, and in 8 hr the coating was completely removed. The glaze-uranium interface, about 0.1 mil thick, required an additional 24 hr before it was completely dissolved.

It appears that a potential use exists for these ceramic coatings as a secondary barrier to corrosion in the event of a clad failure and as a possible primary corrosion barrier in the case of compatible coolants such as the organics. Although the preliminary results appear to be relatively poor, further work on various

glazes may lead to a type which will be suitable for fuel elements.

Stainless-steel Fuel-element Cladding

Design changes have been proposed for the APPR fuel elements on the basis of findings of the sensitizing of the type 304-L stainless-steel clad when subjected to reducing and descaling as part of the fabrication procedure.[15] These elements are made up of fuel plates containing a powder-metallurgy-prepared fuel core consisting of 0.14 wt. % boron carbide and 26 wt. % uranium dioxide in a type 304-B stainless-steel matrix which is clad with type 304-L stainless steel. The reason for the clad material, which normally contains only 0.03 per cent carbon, becoming highly sensitive to intergranular attack is due to the diffusion of carbon from the type 304-B stainless-steel matrix (containing 0.07 per cent carbon) resulting from the hot rolling (1150°C), annealing (1125°C), and brazing (1135°C) operations during manufacture of the fuel elements. The carbon content of the clad material after these hot forming and annealing steps was essentially the same (0.07 to 0.08 per cent) as type 304 stainless steel.

Acid cleaning with 15 per cent HNO_3 – 5 per cent HF in an aqueous solution after the flatten anneal-operation, to remove any oxide, resulted in intergranular attack of the carbides precipitated in the grain boundaries. In most cases tested and observed, penetration was complete through the clad and frame of the fuel elements. Fuel elements with the resulting sensitized type 304 clad, if not cleaned with a reducing acid, are suitable for operating in 500°F water with an acceptable corrosion rate.

To eliminate the intergranular corrosion due to cleaning acid attack, it is proposed to substitute type 347 stainless steel, stabilized with niobium, for either or both the compact and clad materials.

Corrosion-resistant Materials for Molten Fluoride Salt Fuel Systems

In a recent article on the Aircraft Reactor Experiment (ARE),[16] the potential of molten fluorides of uranium, thorium, and plutonium as power reactor fuels was reviewed. One of the primary problems which must be solved before these fluoride fuels can be applied to large central power plants is that of corrosion. The materials which appear to be best suited for containing these fuels are the high nickel content alloys such as the Inconels and Hastelloys.

Hastelloy B, a nickel alloy having a nominal composition (nickel – 28 per cent molybdenum – 5 per cent iron), has good creep behavior and is very resistant to corrosion in various nonaqueous environments at elevated temperatures. ORNL[17] has recently reported on the effect of aging of Hastelloy B after 100, 500, and 1000 hr at various temperatures — 1100, 1300, 1500, and 1600°F. The results of these tests showed that aging results in a small improvement in the room and elevated temperature tensile strength, accompanied by a marked reduction in room and elevated temperature ductility. The most prominent loss in ductility occurs with aging at 1300°F.

Battelle Memorial Institute (BMI) conducted a series of experiments on the behavior of five commercial high-temperature alloys (Inconel, Inconel X, Hastelloy B, Hastelloy W, and Hastelloy X) to corrosion by 1500 to 1650°F peak temperature fluoride fuel salts.[18] It was stated that, in general, the corrosion results were in accord with the known chemistry of fluoride-salt corrosion processes. An increase in peak salt temperature increased the degree of attack in the salt heating region of the loops, and the increase in corrosion had a direct effect on the rate at which the corrosion products were deposited on the cooled walls. Chromium was shown to be a major corrosion product, as evidenced by the most extensive attack on components from Hastelloy X, an alloy which contains the highest percentage of chromium of the materials investigated. Experimental studies on the mass transport of chromium in Inconel–fluoride fuel systems were also made using radioactive Cr^{51} as a tracer material. Isothermal and polythermal experiments were conducted, and rates of diffusion of chromium in Inconel at 600, 700, 800, and 900°C were determined.[19]

ORNL has been conducting an investigation of the effects of radiation on the corrosion of Inconel exposed to fluoride fuel mixtures, as well as the effect of radiation on the physical and chemical stability of fuel mixtures.[20] Static and in-pile forced-circulation loop tests were conducted. In all the tests no major changes, other than normal fuel burn-up, occurred in the fuel

mixtures as a result of irradiation. Examination of the Inconel capsules and tubing also showed no corrosion as a result of the irradiation; the normal corrosion was kept low by careful control of the salt-metal interface temperature and by limiting the maximum wall temperature to 1500°F.

Briefly Noted Reports

Irradiation Effects on Electronic Components and Systems

A tabular summary[21] has been prepared by the Radiation Effects Information Center of the effects of nuclear radiation on electronic systems and components such as resistors, capacitors, vacuum tubes, batteries, printed-circuit boards, thermocouples, diodes, transistors, and strain gauges.

A memorandum report[22] has also been prepared by the Radiation Effects Center on the electrical leakage in insulators exposed to nuclear radiation. The insulators checked were polyethylene terephthalate, amber, polystyrene, perspex, polytetrafluorethylene, and polythene.

Specification for the Army Package Power Reactor (APPR-1)

The final specifications for the fuel elements and control-rod elements of the APPR have been released in a recent report by ORNL.[23] The specifications included in this report cover design, material requirements, and fabrication procedures developed.

References

1. L. B. Prus, E. S. Byron, and J. F. Thompson, A Summary of the Bettis Boron–Stainless Steel Alloy Investigation, WAPD-TM-61, May 1957. (Confidential AEC report.)
2. T. H. Middleham, J. R. Rait, and E. W. Colbeck, High-Boron Alloy Steels, *Journal of the Iron and Steel Institute*, 187: 1–14 (September 1957).
3. J. B. Vetrano, Delta-Phase Zirconium Hydride as a Solid Moderator, BMI-1243, Dec. 18, 1957. (Confidential AEC report.)
4. *Power Reactor Technology*, Vol. I, No. 2, February 1958. (Available from Superintendent of Documents, U. S. Government Printing Office, Washington 25, D. C.)
5. D. L. Keller, Evaluation of Reactor Core Materials for a Gas-cooled Reactor Experiment, BMI-1208, July 11, 1957. (Confidential AEC report.)
6. S. J. Paprocki, E. S. Hodge, and C. B. Boyer, The Cladding of Delta-Phase Zirconium Hydride, BMI-1244, Dec. 27, 1957. (Unclassified AEC report.)
7. J. E. Draley and W. E. Ruther, Experiments in Corrosion Mechanism: Aluminum at High Temperatures, ANL-5658, April 1957. (Unclassified AEC report.)
8. Metallurgy Division Quarterly Report for January, February, and March, 1956, ANL-5563, June 1956. (Secret AEC report.)
9. E. L. Martinec, Corrosion of an Aluminum-Nickel Alloy in a Reactor Test Loop, ANL-5783, September 1957. (Unclassified AEC report.)
10. W. E. Ruther, Corrosion Experiments with 2S Aluminum at 200°C, ANL-5500, March 1956. (Unclassified AEC report.)
11. J. A. Ayres, Corrosion Rates of Aluminum in Nuclear Reactors Cooled by High Temperature Water, HW-52844, Oct. 4, 1957. (Secret AEC report.)
12. V. H. Troutner, High Temperature Aqueous Corrosion Product Films on Aluminum, HW-53389, Nov. 15, 1957. (Unclassified AEC report.)
13. R. S. Kemper and K. F. Powell, Mechanical Properties of Aluminum Alloy M-388: Effect of Fabrication Variables, HW-54364, Jan. 6, 1958. (Unclassified AEC report.)
14. D. W. Shannon, Ceramic Coatings on Uranium, HW-53666, Jan. 13, 1958. (Confidential AEC report.)
15. R. J. Beaver, R. C. Waugh, et al., Investigation of the Factors Affecting Sensitization of Army Package Power Reactor (APPR-1) Fuel Elements, ORNL-2312, Oct. 8, 1957. (Unclassified AEC report.)
16. R. C. Briant and A. M. Weinberg, Molten Fluorides As Power Reactor Fuels, *Nuclear Science and Engineering*, 2(6): 797–803 (November 1957).
17. R. E. Clausing, P. Patriarca, and W. D. Manly, Aging Characteristics of Hastelloy B, ORNL-2314, Aug. 12, 1957. (Unclassified AEC report.)
18. J. H. Stang and J. F. Lagedrost, Pumping-loop Corrosion Studies of Fused-Salt-Reactor Structural Materials, BMI-1191, June 3, 1957. (Secret AEC report.)
19. R. B. Price, D. N. Sunderman, et al., A Tracer Study of the Transport of Chromium in Fluoride Fuel Systems, BMI-1194, June 18, 1957. (Secret AEC report.)
20. G. W. Keilholtz, J. G. Morgan, and W. E. Browning, Effect of Radiation on Corrosion of Structural Materials by Molten Fluorides, ORNL-2373, Aug. 28, 1957. (Secret AEC report.)
21. J. F. Hanse, S. E. Harrison, and W. L. Hood, The Effect of Nuclear Radiation on Electronic Compo-

nents and Systems, REIC-2, The Radiation Effects Information Center, Dec. 31, 1957. (Unclassified U. S. Air Force report.)
22. G. E. Lamale and P. Schall, Memorandum on Electrical Leakage in Insulators Exposed to a Nuclear Environment, The Radiation Effects Information Center, Jan. 15, 1958. (Unclassified U. S. Air Force report.)
23. R. J. Beaver, R. C. Waugh, and C. F. Leitten, Specifications for Army Package Power Reactor (APPR-1) Fuel and Control Rod Components, ORNL-2225, Aug. 7, 1957. (Unclassified AEC report.)
24. W. E. Bost and T. F. Davis, comps., Technical Information Service Extension, December 1957. (Unpublished.)
25. S. F. Lanier, comp., Technical Information Service Extension, July 1957. (Unpublished.)
26. W. E. Bost, comp., Technical Information Service Extension, August 1957. (Unpublished.)

PROGRESS ON SPECIFIC REACTOR TYPES

LIQUID METAL FUEL REACTORS

[*Editor's Note:* Since the time this information was compiled, the LMFRE program has been revised so that a 5-Mw (heat) reactor is now planned for completion in 1961. It will be a single-region reactor employing bismuth as the intermediate coolant.]

Introduction and Summary

Since 1947, the Brookhaven National Laboratory (BNL) has been developing a nuclear power plant which would use a solution of uranium in molten bismuth as the reactor fuel. By 1950, the initial solubility studies had been completed and work was begun on fuel processing. By 1954, the research and development had reached a stage at which an evaluation of the system by an outside contractual firm was sponsored by the Atomic Energy Commission. A group, headed by The Babcock and Wilcox Co., consisting of 17 companies and two national laboratories was awarded a contract for a formal evaluation study in November 1954. The results[1] of this evaluation (BAW-2) were sufficiently encouraging to warrant the development and construction of an experimental liquid metal fuel reactor. The Liquid Metal Fuel Reactor Experiment (LMFRE), to be designed and built by Babcock and Wilcox Co., is expected to be completed in 1959. The present concept is for a 20-Mw (heat) reactor initially, with provision for later increases to 33 Mw (heat). In the meantime BNL is continuing supporting research and development work and has begun some preliminary work on the possible development of an LMFR system using plutonium as the fuel.

A number of reports related to liquid metal fuel reactors have been issued in the last few months,[2–6] most of them dealing with the LMFRE. It therefore seems appropriate to review briefly the general status of development of the reactor type.

In this review the essential characteristic of the liquid metal fuel reactor is considered to be the use of a fissionable material dissolved or suspended in a nonfissionable liquid metal as fuel. A number of different systems are possible within the scope of this definition. The one which has had the most development and which is to be built as the LMFRE uses a solution of uranium in molten bismuth as fuel. Those proposed liquid metal fuel concepts which differ widely from this one involve the use of fuel slurries; the use of slurries extends the range of possible carrier fluids and increases the range of possible design variables. Even the solution reactor concept involves the use of slurries of fertile material in a blanket if significant conversion ratios are to be obtained. Since liquid metal slurry technology is not well developed, it would seem probable that the course of development of the liquid metal fuel reactor will involve first the development of the solution-fueled type, that the slurry development will be directed first toward blankets for this reactor type, and that if the liquid metal fuel concept continues to be an attractive one the use of slurries may extend to the reactor fuel at a later date.

Many of the characteristics of the solution reactor are determined by the solubility limits of uranium in bismuth. At temperatures corresponding to the minimum temperatures in presently contemplated systems, the solubility ranges from 1000 to 2000 ppm. With such a dilute solution, the reactor must operate in the thermal- or near thermal-neutron energy range, and the preferred system of conversion, if not the only practical one, is by leakage neutrons in an external blanket. A moderator is necessary in the core (or possibly surrounding the core) and in the blanket. Graphite is favored as the moderator material. Because of the low absorption cross sections of bismuth and graph-

ite, the conversion ratio is potentially high, and breeding ratios slightly greater than 1 are hoped for on the U^{233}-thorium cycle. To achieve this goal, continuous or nearly continuous chemical processing is required to keep the fission-product content low, a core container of low absorption must be developed, and an efficient blanket must be provided. The present hope is to make the core container of graphite, and the LMFR project is proceeding along this path.

Although rather high power densities and specific powers are attainable in the reactor proper, the over-all specific power is much lower because of the extra inventory in the circulating system, at least in the externally cooled "open" systems which are presently receiving most attention. It appears reasonable, however, to expect specific powers of 20 kw (heat) per liter of bismuth, or perhaps considerably higher, in practical reactors of this type. At such values of specific power, inventory charges do not appear to be excessively large.

The materials problems of the liquid metal fuel reactor cannot be considered solved. However, most of the uncertainties are related either to radiation effects or to the effects of practical long-term large-scale use, and a reactor experiment such as the LMFRE is probably the logical next step in the materials development. Aside from graphite, the materials for the primary loop are expected to be low chrome steels (croloy). Mass transfer appears to be a problem with any metals in the primary system, but it is thought to be controllable by additives to the fuel solution if croloy is the material used and if temperature differences in the system are not too high.

As in other fluid fuel reactors, the problems of maintenance and of the containment of fuel in case of a breach of the primary system are major ones. They are accentuated in reactors using bismuth as the fuel carrier by the production of Po^{210} in the fuel solution. On the other hand the prompt negative power coefficient of reactivity of the reactor, the absence of stored mechanical energy in the primary circuit, and the apparent absence of possibilities for rapid chemical reactions favor solution of the containment problems.

It is not profitable to attempt cost estimates on plants which still require major research and development. It can be said of the liquid metal fuel reactor that its hope for economic power lies in low fuel cost, which may come from high neutron economy, the absence of fuel fabrication cost, and high thermal efficiency. Whether a low fuel cost can actually be attained will depend on the cost of chemical reprocessing, which is generally considered to take place in a facility integral with the liquid metal fuel power plant. Whether other operating costs and capital costs can be made low enough to achieve a low total power cost will probably be determined only from further research and development and from reactor experience.

For special purposes the liquid metal fuel "burner" reactor (without conversion) may prove to be attractive. Estimates indicate that fuel costs in the range 2.5 to 3 mills/kw-hr may be possible with such reactors.

More detailed discussion of the above points will be found in the following sections.

Fundamental Characteristics

Reactor Concepts

In the following discussion the essential characteristic of the liquid metal fuel reactor is considered to be the use, as fuel, of a fissionable material dissolved or suspended in a nonfissionable liquid metal. This definition is an arbitrary one, adopted to restrict the scope of the discussion to reactors which have reasonably closely related characteristics. A number of reactor arrangements may be imagined within the scope of the definition. The original LMFR concept employed a solution of uranium in molten bismuth. This fuel solution was circulated in a primary circuit which contained a reactor vessel and a heat exchanger. The fuel solution became critical and generated fission heat in the reactor vessel, which contained graphite as a moderator; the heat was extracted from the hot circulating fuel in the heat exchanger and was then available for power generation. A further characteristic feature was the circulation of a side stream of fuel to an integral chemical processing plant.

A number of variations on the basic LMFR concept have been considered. These variations arise from considerations of different fuel types (e.g., solution or slurry), different methods of providing moderation in the reactor vessel, and different methods of incorporating fertile material. These questions are considered specifically in the following sections. In addition,

variations arise from two possible ways of cooling the fuel (externally or internally) and from two possible types of arrangement of the primary loop components (compact or open).

In an externally cooled LMFR the fuel is pumped through the core to an external heat exchanger. This method allows the simplest core design and heat exchanger maintenance but requires the largest inventory of expensive fuel solution (assuming bismuth to cost $2.25/lb, a 700 ppm solution of uranium in bismuth would cost $4785/cu ft). The principal advantage of the internally cooled LMFR is the reduced fuel inventory required. In this concept a coolant is circulated through the core, where it picks up heat from the stagnant core fluids. However, the core must be designed to contain two fluids. The increased structural material required in the core structure increases the complexity as well as the parasitic absorbing material and hence would require an increase in U^{235} concentration. An interesting modification of the internally cooled concept is one in which the blanket slurry is circulated through the core as both breeder matrix and coolant. The blanket slurry is then pumped to an external heat exchanger for steam production.

The compact arrangement of the primary system, also known as the "pot type" design, contains the entire reactor, primary heat exchanger, and pumps within the reactor vessel or "pot." The compacting of all the equipment into a single vessel reduces the flexibility of design and increases the difficulty of maintenance, but it does provide for the minimum inventory of fuel consistent with an "external" heat exchanger and for good containment of the fuel circuits. In the open arrangement, which is the type receiving the most consideration at present, the heat exchangers, pump, and auxiliary equipment are located outside the main reactor vessel. This arrangement allows the greatest freedom of choice in fixing the design variables, improves accessibility of components, and simplifies maintenance procedures.

Table VI-1 CHARACTERISTICS OF PROPOSED LMFR TYPE REACTORS

	B&W		BNL	B&W	KAPL
	LMFRE (Initial operation)	LMFRE (Later operation)	LMFRE	Full-scale LMFR	UO_2-LMFR
Power, Mw (heat)	20	33⅓	5	550	
Power, Mw (elec.)				226	
Fuel	U in molten Bi		U in molten Bi	U^{233} in Bi	UO_2 slurry
Blanket	Th_3Bi_5 slurry in Bi (experimental loops only)		Th_3Bi_5 slurry in Bi	Th_3Bi_5 slurry in Bi	None
Core inlet temp., °F	750	750	752	752	650
Core outlet temp., °F	885	975	1022	1022	1000
Control	Tantalum rods		Cr-Mo steel rods		
Intermediate coolant	Na		Air	Pb-Bi eutectic	None
Steam, °F/psi	800/600			975/2000	
Moderator	Graphite		Graphite	Graphite	Graphite and Be
Primary heat exchanger	External		External	External	External

A summary of the main features of several LMFR reactors which have been proposed is given in Table VI-1. The open arrangement, with external heat exchangers, has been specified for the LMFRE despite the accompanying penalty of high fuel solution inventory.

Chemical Form of Fuel and Fertile Material

1. Core Material. The principal chemical form of fuel presently being considered is a solution of uranium metal in liquid bismuth. At the anticipated reactor operating temperature,

uranium is soluble in bismuth in more than sufficient concentration to meet criticality requirements but not in sufficient concentration to allow the use of dissolved U^{238} as a fertile material. Some physical properties of bismuth are shown in Table VI-2. In general, the physical properties of the uranium-bismuth fuel solution are similar to those of pure bismuth, although the presence of uranium metal alters the chemical reactivity of the mixture slightly. Care must be exercised to prevent the loss of uranium by oxidation. Single-phase fuel solutions usually contain some zirconium and/or magnesium as corrosion inhibitors. Although the addition of lead to bismuth will lower the melting point of the liquid, lead also decreases the solubility of uranium to a point where the concentration would be below that required for criticality.

Table VI-2 PHYSICAL PROPERTIES OF BISMUTH*

(atomic weight, 209; melting point, 271.0°C (520°F); boiling point, 1477°C (2691°F); volume change on fusion, −3.32 per cent)

Temp., °C	300	400	500	600
Temp., °F	572	752	932	1112
Vapor pressure, mm Hg	10^{-9}†	3.5×10^{-5}†	2.3×10^{-4}	6.3×10^{-4}
Density, g/cm³	10.03	9.91	9.79	9.66
Specific heat, cal/(g)(°C)	0.0343	0.0354	0.0365	0.0376
Viscosity, centipoises	1.66	1.37	1.16	1.00
Thermal conductivity, Btu/(hr)(ft)(°F)	9.9	9.0	9.0	9.0
Electrical resistivity, ohms	128.9	134.2	139.8	145.2
U solubility, ppm	530	2150	6300	15000
Pu solubility, ppm‡		5000	15000	38000

* Reproduced from Table 18.11 in reference 7.
† Extrapolated results.
‡ From reference 8.

For two-phase slurry types of liquid fuels, a number of possible combinations exist. Intermetallic compounds, such as UBi, U_3Bi_5, and USn_3, form finely divided dispersions in various alloys of lead, bismuth, and tin. The alloys would have two advantages: (1) a lower melting point than pure bismuth and (2) a density which may be adjusted very closely to that of the uranium intermetallic compound and thus yield a slurry with very low settling rates. Although potentially useful, these types of slurries have not been proposed for use in the reactors presently being considered.

A third type of liquid fuel which has been proposed for use in a reactor system is a uranium oxide slurry in molten bismuth. Slurries of UO_2, UC, and USi_2 in bismuth, lead, or Li[7] have also been considered and are still of interest. Experiments on a UO_2-NaK slurry have been reported recently.[9] A slurry of UO_2 in molten bismuth would have a considerably lower settling velocity than many of the other slurry systems because of the small density difference between the two phases. Lead, although it has a higher absorption cross section than bismuth, would avoid the Po^{210} problem. The preparation and wetting of UO_2 has been accomplished[10] in liquid bismuth with magnesium additive, but it has not yet been demonstrated that a slurry of UO_2 in lead can be prepared.

2. Fertile Material. Although burner reactors of the LMFR type may prove attractive for some purposes, the economic advantage that may be gained from breeding or conversion is generally considered to justify the increased size and complexity of a breeder reactor. The most commonly considered form of the fertile material in the reactor blanket is a slurry of fine particles of thorium bismuthide (Th_3Bi_5) in molten bismuth. A slurry containing not more than ~10 wt. % thorium is expected to have a sufficiently low viscosity to permit handling and pumping the blanket slurry through the external heat exchanger. The possibility of reducing the fuel requirements by using a stagnant liquid metal fuel with a circulating fertile slurry as coolant has been suggested[9] although not as yet incorporated into any existing designs.

Moderators

Although the possibility of an unmoderated liquid metal fuel reactor has been mentioned,[8] present development is directed toward reactors operating primarily in the thermal-neutron energy range. The solubility limits of uranium in bismuth are so low that moderation seems to be a necessity for a practical reactor of the solution type. The main development effort is presently directed toward reactors of this type in which the moderator is distributed through the core volume in the form of some fixed structure. Chernick[8] has pointed out, however, that the use of an external moderator, i.e., a moderator which surrounds the core and is in effect a reflector as well as the moderator, is rather attractive because of the resulting simplicity of the reactor. The moderating materials that have been principally considered for use in liquid metal fuel reactors are graphite and beryllium. The possibility of beryllium oxide has also been mentioned.[10]

1. Graphite. At the present time graphite is the preferred moderating material because of its availability, its lower cost, and the greater existing knowledge of its characteristics. There are, however, several unique requirements for the graphite to be used in LMFR systems. The graphite must be able to resist the penetration of the liquid metal fuel at the reactor operating conditions of temperature and pressure. Impervious graphite in small pieces has been obtained, and industry is reported to be developing impervious graphite in sizes which would be useful in the LMFR. A further requirement is that the graphite be able to withstand both corrosion and erosion by the fuel solution and by the blanket slurry if one is used. Investigations to date indicate that graphite of impervious reactor grade does not suffer any appreciable corrosion at reactor temperature and pressure.[7,11] Data on the effects of radiation on the corrosion and erosion of graphite by the fuel solution are not presently available. Indications[7,11] are that the graphite is protected by a layer of ZrC and ZrN (nitrogen arises from gases trapped in the steel piping external to the core). This protective layer could conceivably be removed by fission recoils, or the fission recoils could be driven behind the protective layer and build up a high poison level in the graphite core.

2. Beryllium. The second most commonly considered moderator material is beryllium. Beryllium has been reported[7] to have good resistance to chemical attack and to mass transfer in liquid bismuth at the proposed reactor operating temperatures. The solubility of beryllium in molten bismuth at 572°C has been reported[7] to be 0.001 per cent. In view of the reportedly good characteristics in a dynamic system, this rather high solubility, if true, may mean that the rate of solubility is quite low. No data have been reported on possible reactions between beryllium and uranium, the zirconium and magnesium additives, and fission products in liquid bismuth. In a recent proposal[10] for a UO_2-Bi slurry LMFR, beryllium tubes, carrying the liquid fuel and inserted in holes in the bulk graphite moderator, were considered since it was felt that beryllium metal would be more resistant than graphite to abrasion by the UO_2 slurry.

Although recent advances in the technology of beryllium have reportedly improved its mechanical properties, there remains some question as to the effects of high thermal stresses resulting from transient temperatures in the reactor.[7,12]

Neutron Economy

The macroscopic absorption cross section of liquid bismuth is only about twice that of reactor grade graphite. Consequently, if the reactor core contains no other materials than uranium, bismuth, and graphite (or beryllium), the parasitic absorption of neutrons will be quite small, even at the rather low ratios of uranium to bismuth which are dictated by the solubility limitations. The potential conversion ratio in such a reactor using U^{233} as fuel could be well above unity. Because of the solubility limits, however, it does not appear to be feasible to provide for a large degree of internal conversion in a solution type reactor. The efficient capture of the excess neutrons in an external blanket poses three problems: the provision of a core container of low neutron absorption, the incorporation of sufficiently high densities of fertile material in the blanket, and the efficient blanketing of the inlet and outlet ducts. The preferred solution to the first of these problems would be a core vessel composed of a low cross-section material. Vessels composed of graphite are seriously considered, although they have

obvious problems. An alternative which is less attractive from the standpoint of neutron economy is the use of a more highly absorbing material (e.g., croloy) which is "shielded" from the thermal neutron flux by adjacent layers of fuel and blanket fluid which do not contain moderator. This principle of "immoderation" has also been considered as a method of reducing leakage around the inlet and outlet ducts. The proposed solution for the problem of providing a sufficiently high concentration of fertile material in the blanket is the use of a slurry. Of course it would be possible to provide for internal conversion if a slurry of fertile plus fissionable material were used in the reactor core, and this system has been considered in reference 10 and elsewhere. Most of the current development, however, is directed toward the use of a solution in the core and a slurry in the blanket.

It may be said in summary that, although the liquid metal fuel reactor has potentially a conversion ratio which is quite high because of the low neutron-absorption cross sections of the proposed materials of construction, and because of the possibility of continuous or semicontinuous removal of fission products, the practical attainment of a very high conversion ratio involves the solution of a number of rather fundamental problems.

Fuel Cycles

Two methods of operation of LMFR type reactors have been proposed — burner and breeder (or converter) reactors. The burner reactor concept is a very simple one, in which U^{235} is burned to produce power without the production of new fissionable material. The simplicity of this concept results from the absence of a blanket and a blanket handling system, the absence of a chemical reprocessing system (except for gaseous fission-product separation), and the absence of a radioactive fuel handling system. Fresh U^{235} is continuously fed into the reactor to overcome fission-product poisons and higher isotope build-up. The end of a fuel loading[4] (estimated to be 6 to 12 years) occurs when the maximum solubility of uranium in liquid bismuth is reached. At the end of fuel life the entire inventory of fuel solution is removed for chemical processing and recovery of the bismuth and U^{235} remaining. Any economic advantage which this concept may have is expected to be in the lower capital cost and in lower chemical processing costs. The latter costs, for processing enriched U^{235}, especially in a bismuth matrix, are still uncertain.

The second concept, that of a breeder (or converter), is the type currently receiving the most attention. Its principal advantage is expected to lie in the low fuel cost resulting from the high conversion ratio theoretically attainable. With the continuous or semicontinuous removal of fission-product poisons, the core fluid lifetime would be expected to be limited only by the build-up of the higher isotopes of uranium. Although ~100 years[4] would be required to build up sufficient higher isotope concentration to reach the solubility limit of uranium in bismuth, a core reprocessing cycle of ~30 years is generally assumed for economic studies.

Operating Temperatures

The maximum allowable fuel temperature is determined by the limitations of the materials of construction. The low chrome steels, which are presently considered as the primary materials (other than graphite), are thought to be usable to temperatures of about 550°C with bismuth.[7] At temperatures in this range the vapor pressure of bismuth is quite low (< 1 μ Hg at 500°C); consequently, the primary system requires no pressurization.

Power Density and Heat Transfer

Since the fission heat is generated directly within the heat transport fluid, considerations of heat transfer do not limit the power density in the liquid metal fuel reactor proper. The limiting factors appear to be the permissible temperature rise of the fuel in passing through the core and the permissible flow velocity. The flow velocity limit is based on considerations of erosion and has been taken as ~10 ft/sec, although this limit has not been definitely established by experiment. The permissible temperature rise is determined by considerations of maximum permissible fuel temperature, as limited by corrosion; minimum permissible fuel temperature as determined by uranium solubility limits and power cycle considerations; and possibly by considerations of thermal shock and mass transfer of materials. Temperature rises of ~200°C are thought to be feasible.[8] With a temperature rise of this mag-

nitude, each cubic foot of bismuth-uranium fuel solution would transport $\sim 2 \times 10^6$ calories of heat from the reactor core to the heat exchanger. At a flow velocity of 10 ft/sec, in a reactor 12 ft long, such a temperature rise would correspond to a power density of ~ 6.7 Mw per cubic foot of bismuth in the core, or 240 kw per liter of bismuth in the core.

pressure steam into it is eliminated. Possible fluids for the intermediate exchanger are sodium, bismuth, and lead-bismuth eutectic. Fused salts and gases have also been mentioned.

In Table VI-3 the physical properties important to heat transfer for bismuth and sodium are compared with those of ordinary water. A fused salt mixture is also included for comparison. Of these coolants, liquid bismuth requires the largest pumping power for a given heat transfer, but it has the smallest neutron-absorption cross section. Liquid metals, unlike water or fused salts, should be completely free of radiation damage.

Table VI-3 PHYSICAL PROPERTIES OF SOME LIQUID COOLANTS*

Property	Bi, 450°C	Na, 450°C	KCl-LiCl, 450°C	H_2O, 250°C
Melting point, °F	520	208	664	32
Boiling point, °F	2691	1621		212
Density, lb/ft^3	613	52.5	103	50.0
Specific heat, Btu/(lb)(°F)	0.036	0.304	0.31	1.16
Heat capacity, Btu/(ft)^3(°F)	22.1	15.95	31.9	57.8
Thermal conductivity, Btu/(hr)(ft)(°F)	8.95	39.5	1.47	0.357
Viscosity, cp	1.28	0.245	3.4	0.110
Prandtl number, $C_p\mu/k$	0.0125	0.00454	1.7	0.863

* Reproduced from Table 18.15 in reference 7.

The specific power based on the total amount of fuel solution in the system is considerably lower than that based on the fuel in the core and is affected by the heat-transfer properties of the fuel solution since the heat must be extracted in a heat exchanger. The large liquid metal fuel reactor design described at Geneva attained an over-all specific power of ~ 0.58 Mw per cubic foot of fuel solution (20 kw/liter.)[13] The studies of Dwyer[14] indicate that specific powers several times as large might be reached in such externally cooled liquid metal systems. The specific powers attainable with internally cooled reactors might be considerably higher; studies of this reactor type have not been sufficiently extensive to indicate clearly the practical limits on specific power.

In the externally cooled liquid metal fuel system, the fission heat may be transferred directly from the metal fuel to steam, or an intermediate coolant may be used. Although the direct transfer represents the system which is conceptually the simpler, there are a number of advantages in the use of the intermediate coolant. Some of these are: a smaller heat exchanger can be used with the intermediate coolant, thus reducing the fuel inventory; thermal stress problems are reduced; the decomposition of water by gamma radiation from the highly radioactive fuel solution is avoided; the possibility of rupture of the primary system by leakage of high-

Reactor Stability and Control

The negative temperature coefficient of reactivity of the fluid fuel is such that the liquid metal fuel reactor is expected to be inherently self-regulating with load demands. Although the average temperature of the reactor will remain nearly constant, the inlet and exit temperatures will adjust to the heat removal (equivalent to load demand) in the heat exchangers.

The temperature coefficient of reactivity of the liquid metal fuel reactor type has two principal components: (1) the prompt temperature coefficient ($\sim -5 \times 10^{-5}$/°C in the LMFRE) results from the rapid thermal expansion of the fluid fuel; (2) the delayed temperature coefficient ($\sim -1.3 \times 10^{-4}$/°C in the LMFRE) depends on the slower heating of the graphite matrix and other structural members.

The relatively large prompt negative coefficient should give a high degree of inherent protection against the effects of reactivity accidents. The limitation on this self-protection is thought to be the pressure built up by the rapid expansion of the fuel solution during the

power transient. The pressure rise could be increased by the boiling of the bismuth (boiling point 1477°C at atmospheric pressure) under the influence of a sufficiently energetic transient. Calculation indicates that the LMFRE could tolerate a reactivity excess of 3.2 per cent k_{eff}, added at a ramp rate of 2 per cent per second, without generating a pressure peak of more than a few psi.[5]

Despite the fact that the reactor is expected to be self-regulating and to require no control rods, the LMFRE will incorporate control rods to ensure the safety of the experiment and to establish the feasibility of operation without control rods.

Chemical Processing

One of the principal advantages claimed for the LMFRE concept is the possibility of maintaining the fission-product poisons at a low level and, hence, the breeding ratio at a high value. A major portion of the LMFR program at BNL has been directed toward the development of processing schemes applicable to the three types of chemical separations required: (1) volatile fission-product removal, (2) nonvolatile fission-product removal, and (3) blanket processing.

The first type of processing, the removal of volatile fission products (which represent about 25 wt.% of the total),[1] is common to all types of LMFR reactors. Volatile fission products such as xenon and iodine may be continuously removed by passing the uranium-bismuth stream through a degasser, whose function is to expose a large surface area of liquid metal and hence allow the insoluble gases to escape.[15] If necessary, an inert sparge gas may be used. Bismuth and polonium vapors may be removed by passing the gas through a cold trap. Although an in-pile loop, operating at low neutron flux, has demonstrated that xenon may be easily removed from a solution of uranium in bismuth,[15] the rate of removal, and hence the degasser efficiency in a full-scale reactor at high flux, is not yet known. Operation of the LMFRE is expected to yield some answers on the efficiency of degasser operation, the solubility in bismuth, and the adsorption of volatile fission products on graphite under reactor operating conditions.

For slurry fuels or blankets it is felt that if the particle diameter is less than the fission fragment recoil distance a considerable fraction of the fission products will be removed from the solid phase.[10] There has as yet been no experimental verification of this fact nor any study of the adsorption of fission-product atoms on the solid material.

The second type of chemical process requirement actually covers two groups of nonvolatile fission products. The first of these groups, representing ~40 per cent of the total fission products,[1] are those which are soluble in fused salt and may be removed in an extraction process, either continuously or semicontinuously (batchwise operation). Since it is important to have the uranium stay in the liquid bismuth stream, only those fission products which form chlorides that are more stable than UCl_3 may be removed by this extraction process.[1] A semicontinuous or batchwise type of operation has the advantage that, being separate from the main reactor circuit, a failure or breakdown in the processing stages will not interrupt normal reactor operation, and the potential hazard of slugging the reactor with extra-rich fuel solution is minimized. Although the experimental partition coefficients are lower than the predicted values, the evidence indicates that usable separation factors are obtained. The separation may be carried out by either the "buffer" or "stoichiometric" methods.[1,15] In the former the metal phase (Be-U-Mg-Zr) would be contacted with a KCl-NaCl-MgCl eutectic. In the latter $BiCl_3$ would be added to the salt and calcium to the metal. Careful control of concentration must be maintained to effect a useful separation with minimum loss of uranium.

The second group of nonvolatile fission products are those whose chlorides are less stable than UCl_3. These cannot be transferred to the salt phase without also transferring uranium from the bismuth to the salt.[1] Since these represent a fairly small portion of the fission products (~35 per cent), they may be removed by ordinary wet chemical methods in a batchwise operation scheme at fairly long time intervals.[1]

An alternative chemical processing scheme for uranium-bismuth fuel solutions is the oxide slagging method.[6] In this method all the nonvolatile fission products are treated as a single group. All the components (including the ura-

nium) except bismuth and the noble elements are removed as an oxide slag and are sent to a conventional wet chemical processing plant for recovery of the uranium. The bismuth may be recovered by vacuum distillation, although considerable development work remains before the oxide slagging method is commercially acceptable.

In addition to the above processes, the fluoride volatility process is now being investigated in connection with liquid metal fuel.

Basically the economics of fission-product separation will be the factor which determines the optimum degree of fission-product separation. It may be that the most economic system is one which tolerates a fairly large average fission-product level with a corresponding sacrifice of breeding ratio.

Before the UO_2 slurry can be used as a fuel in a power reactor, a satisfactory chemical processing scheme must be developed. Centrifugation and shipment to a central wet chemical processing plant may prove to be an economic possibility, although it is hoped that the PuO_2-UO_2 slurry may be physically separated by centrifugation from the majority of the fission-product poisons and immediately returned to the reactor.[10] This simple processing scheme could be economic if the residual poison level is sufficiently low.

The three principal blanket systems which have been considered for the LMFR are (1) a fluidized bed of thorium fluoride, (2) a slurry of thorium bismuthide in molten bismuth,[1,16] and (3) thorium oxide in molten bismuth. The first of these consists of a fluidized bed of ThF_4 in a gas which can be circulated through heat exchangers. A small bypass stream removed for chemical processing is passed into a flame of hydrogen, burning in excess fluorine. The high temperature of this flame will melt the ThF_4, allowing the uranium and protactinium to escape into the fluorine atmosphere where volatile UF_6 and PaF_5 are formed. The ThF_4 quickly resolidifies and may be readily separated from the gaseous UF_6 and PaF_5 by physical means.[16] Although the process showed promise in preliminary tests, heat exchanger and corrosion problems have virtually postponed the fluidized bed separation process for future development.

The second and third processes involve the extraction of the bred U^{233} and protactinium from a thorium bismuthide or oxide slurry in liquid bismuth. A portion of the slurry flows continuously through the chemical processing stages. This method requires that the U^{233} and protactinium be transferred from the solid Th_3Bi_5 or ThO_2 particles into solution in the liquid bismuth. Since Th_3Bi_5 is partially soluble at elevated temperatures, cycling the molten bismuth slurry between 850 and 350°C will consecutively dissolve and reform the Th_3Bi_5 particles, releasing the majority of the uranium and protactinium in the process.[1] The solution of uranium and protactinium may be separated from the solid Th_3Bi_5 particles either by centrifugation, leaving the uranium and protactinium in solution, or by fused salt extraction of the uranium and protactinium. The solid Th_3Bi_5 may be returned to the blanket, reconstituted in fresh bismuth if necessary.

The ThO_2 slurry could be processed by mechanically separating the ThO_2 from the bismuth and processing it by the existing Thorex process.

Corrosion and Materials Problems

One of the major problems remaining in the development of an LMFR type reactor is the development of container materials suitable for use at high temperatures. In addition to uranium there are a number of metals which are soluble in molten bismuth. These range from iron at a few ppm to nickel, copper, aluminum, and magnesium at several per cent. So far only molybdenum, niobium, tantalum, and tungsten appear to be essentially insoluble.

In the primary circuit of the LMFR type reactors, there is a temperature differential between the hot liquid fuel leaving the core and the cooler fuel from the heat exchanger. Owing to the difference in solubility of container materials with temperature, a phenomenon known as mass transfer can occur. This is caused by material dissolving in the fluid in the hotter regions of the fuel and precipitating in the colder regions where the solubility is lower. Mass transfer not only causes corrosion in the hotter regions of the fuel circuit but can lead to plugging in the cooler regions.

It has been found experimentally[7,11,16] that the addition of certain soluble materials, such as magnesium, titanium, and zirconium, to the

liquid bismuth will greatly reduce the mass transfer in certain types of steel alloys. The current thinking is that the presence of an inhibitor, such as zirconium, forms an inert adherent layer of ZrN (from nitrogen trapped in the steel) which forms a barrier to solution of iron in the hot zone and apparently retards the precipitation in the cold zone, especially if the temperature difference (and hence solubility difference) is low. The presence of zirconium in molten bismuth apparently increases the amount of iron which may be held in a stable supersaturated solution. However, if the temperature difference becomes too great, mass transfer may again appear. The additional presence of magnesium in the molten fuel is necessary as an oxygen "getter" to prevent the formation of insoluble UO_2. Low alloy chromium steels have been selected for use as container materials in the LMFRE. Table VI-4 shows the observed mass transfer for a number of alloys, operating under several different conditions.[7] Initially the LMFRE is expected to operate at 400 to 475°C (750 to 885°F), a temperature differential of 75°C (135°F). If conditions warrant, the temperature differential will later be increased to 125°C (225°F) by increasing the total power to 33⅓ Mw.

The same type of phenomenon is thought to be responsible for the prevention of the known reaction between graphite and uranium to form UC. A thin layer of ZrC (containing some ZrN), preferentially formed on the surface of the graphite, appears to inhibit the corrosion of the core graphite by bismuth, uranium, or fission products.

Table VI-4 SUMMARY OF THERMAL CONVECTION LOOP DATA[7]

Material, wt. %	I.D., in.	Liquid metal constituents, Bi plus metals in ppm	Temp. gradient, °C	Time of operation, hr	Condition at end of operating time
2¼ Cr–1 Mo	0.622	U, 1000	550–510	310	Completely plugged
2¼ Cr–1 Mo	0.622	U, 1000 Zr, 250 Mg, 350	550–510	13,600	Shutdown due to mechanical failure
5 Cr–1½ Si	1.70	U, 450 Zr, 180 Mg, 200	550–520	30,000	Still operating
2¼ Cr–1 Mo	0.622	U, 1000 Zr, 200 Mg, 350	550–415	8,000	Still operating; graphite cylinder in loop; slight pptn. present in cold leg; pitting in hot leg
2¼ Cr–1 Mo	0.622	U, 1000 Ti, 150 Mg, 350	550–445	3,000	Plugged
Bessemer steel	0.622	U, 1000 Zr, 270 Mg, 350	550–415	7,000	Still operating; slight pptn. in cold leg
2¼ Cr–1 Mo	0.622	U, 1000 Zr, 250 Mg, 350	550–460	10,000	Slight pptn. in cold leg; shutdown for metallographic examination
9 Cr–1 Mo	0.622	U, 1000 Zr, 250 Mg, 350	550–400	4,000	Still operating; appreciable pptn. in cold leg; pitting in hot leg

The addition of uranium to liquid bismuth in metal systems is accompanied by a large initial loss of uranium unless the system is first "conditioned" with zirconium and magnesium. The system is conditioned when the zirconium and magnesium concentrations remain constant. In any subsequent losses, magnesium or zirconium will be lost in preference to uranium.

Radiation Effects

The effects of radiation on corrosion rates, on chemical reactions between the uranium-

bismuth fuel and materials of construction, and on the physical properties of the moderator and construction materials are not yet known with reliability. Indications are that the physical characteristics of the graphite to be used as moderator in the LMFRE improve with increased temperature, and the growth problem associated with graphite in low temperature reactors is not expected to exist to any troublesome degree. The remainder of the structural materials are outside the region of highest flux, and the damage they may suffer from radiation is expected to be negligible.

The greatest concern about radiation is its effect on fission-product absorption and uranium holdup in the graphite of the LMFRE core. These are problems that can be answered only by actual operation of a reactor under conditions that will exist in a power reactor station of the LMFR type.

Containment and Maintenance

In common with other fluid fuel type reactors, the LMFR concept faces two major classes of problems connected with the use of highly radioactive materials in a liquid state: containment problems and maintenance problems. These problems in the LMFR are further complicated by the presence of Po^{210}, formed from neutron capture in the bismuth fuel carrier. Po^{210} constitutes a hazard since it is toxic and difficult to contain. The LMFRE, after two years operation at full power, would contain about 5.8×10^5 curies of Po^{210} activity.[12] Provision must be made to contain the liquid fuel in the event of a leak or a disastrous reactor excursion. The polonium also constitutes a potential health hazard during maintenance operations on the primary system. Maintenance problems are further complicated by the fact that pumps, piping, and heat exchangers become radioactive from the absorption of delayed neutrons emitted by the circulating fuel.

The tolerance levels for Po^{210} are comparable to those for Pu^{239} in terms of microcuries. However, since Po^{210}, with a much shorter half life, has a higher specific activity, the tolerance of Po^{210} in terms of micrograms is much smaller than for Pu^{239}. Table VI-5 summarizes the published tolerance levels[17] of Po^{210} and Pu^{239}.

The LMFRE is an example of one approach to containment and maintenance problems. The preliminary plans provide for isolation of the components of the primary circuit in concrete cells lined with stainless steel. The latter provision is to prevent contact of molten bismuth with concrete and to ensure containment of the radioactivity. The cell openings, to be sealed during operation with a low-melting alloy, will be all of the same size to permit installation of a special maintenance plug. All maintenance on the primary circuit will be done remotely, using a large hoist to handle heavy equipment and television cameras to observe the work. The large number of special tools and procedures which will be required remain to be developed and tested. It will also be necessary to develop special tools and handling techniques for the chemical processing stages.

Table VI-5 TOLERANCE LEVELS FOR Po^{210} AND Pu^{239}

Isotope	Maximum permissible concentrations for continuous-exposure in air		Maximum permissible level in total body	
	$\mu c/ml$	$\mu g/ml$	μc	μg
Po^{210} (sol.)	2×10^{-10}	4.4×10^{-14}	0.02	4.4×10^{-6}
Po^{210} (insol.)	7×10^{-11}	1.6×10^{-14}	0.007	1.6×10^{-6}
Pu^{239} (sol.)	2×10^{-12}	3.2×10^{-11}	0.04	6.5×10^{-1}
Pu^{239} (insol.)	2×10^{-12}	3.2×10^{-11}	0.008	1.3×10^{-1}

Maintenance of the secondary circuits, the intermediate sodium system, and the steam system will be accomplished directly, after drainage and storage of the sodium.

Components

The principal components of a specialized nature required for the LMFR concept are pumps, core tank, and heat exchangers, capable of operating with molten bismuth at the expected operating temperatures of the reactor and under intense gamma-ray irradiation.

Pumps

In LMFR systems a typical operating temperature range as presently established by metallurgical and solubility limitations is ~750 to 1020°F. With this temperature differential, a pumping rate of ~72 gal/min/Mw (heat) would be required (36,000 gal/min at 500 Mw (heat). The pumps must be completely leaktight since no oxygen can be permitted in the system

and none of the highly radioactive fluid can be permitted to escape. Since bismuth expands upon solidification, the pumps must be drainable.

Both electromagnetic and mechanical pumps have been considered for use in LMFR systems. Although electromagnetic pumps have the advantage of being completely sealed and of providing easy stable control of flow and easy drainability, they have rather poor efficiency and have not been tested for liquid metal fuels except on a very small uranium-bismuth system at low flow rates.

For the large pumping rates required, centrifugal pumps are the only type of mechanical pump presently being considered. There are several types of centrifugal pumps being considered, including the gas-filled sump type and the flooded canned rotor type. The LMFRE, to be built by Babcock and Wilcox Co., will be provided with two 2680 gal/min centrifugal sump pumps,[5] with variable speed drive, one operating and one serving as a stand-by in case of a pump failure.

Core Tank

In breeder reactors the attainment of a positive breeding ratio requires the use of a core tank whose neutron absorption is low. The separating vessel might be graphite or beryllium, although the use of either requires development of fabricating techniques and means of making a satisfactory joint between the separating vessel and the main reactor vessel. Present concepts of large reactors consider the use of croloy steel as the core tank to separate the core fluid and blanket slurry, although the high absorption of the croloy steel yields a conversion ratio less than 1.

The LMFRE will avoid part of the problem of the core tank material by using beryllium sheathed experimental loops in the reflector. Hence leaks between the core fluid and reflector coolant through the graphite core pressure seal are not expected to be serious.

Heat Exchangers

The concensus of present opinion seems to be that an intermediate heat exchange medium, usually sodium, should be used in LMFR designs. This then requires two heat exchange systems, one between the uranium-bismuth fuel and sodium and one between the sodium intermediate coolant and water. Since the achievement of high specific power in the LMFR is highly desirable to reduce fuel inventory, there is a premium on minimum heat exchanger size. The problems of corrosion and thermal stresses at the LMFR operating temperature are expected to be answered by the operation of LMFRE. The LMFRE heat exchanger[15] will be a U-shaped two-pass tube-and-shell type, constructed of welded chromium-molybdenum steel. Future developments are expected to improve the characteristics of heat exchangers[1] for bismuth-sodium systems.

Costs

The principal cost advantage of the LMFR concept lies in the low fuel fabrication costs and in the high thermal efficiencies made possible by the high operating temperature. A further advantage may lie in the attainment of a high conversion ratio. Exploitation of this possibility requires the development of chemical processing, either continuous or semicontinuous, to maintain a low level of parasitic absorbing material, and solution of the problems of an efficient breeder blanket. Three existing concepts take different approaches to the problem of achieving low total power cost. These are: (1) the burner reactor, in which the breeding characteristics are sacrificed in favor of lower chemical processing costs and lower capital costs; (2) the breeder reactor, in which maximum advantage is taken of the attainable conversion ratio despite the chemical processing and capital costs; and (3) the converter reactor which attempts to compromise between the breeding advantage and processing costs. Since rather extensive research and development are still necessary on the three types of proposed reactors, it is hardly possible at this time to make a reliable cost comparison, which involves the balancing of fuel costs, operating costs, and capital costs, or to arrive at an absolute estimate of the total power cost for any of the three types. It is worth while, however, to consider some of the estimates of fuel costs which have been made in the past. Power costs were estimated in reference 4 for breeder and burner reactor types. The burner reactor plant assumed was the simplest conceivable on the basis of present technology, incorporating a chemical plant only for degassing, for fuel make-up and removal, and for bismuth cleanup.

The limit of core lifetime determined by the build-up of fission-product poisons and the maximum solubility of uranium in bismuth was estimated to be between 6 and 12 full power years. At the end of life the entire core was processed to recover the residual fissionable material. The estimates for the breeder reactor were based on a breeding ratio of 1.00, an assumed core lifetime of 30 years, and continuous chemical processing which included estimated improvements in the processing scheme expected within the next 5 to 10 years. Table VI-6 gives the estimated fuel costs from this comparison, as well as the estimated fuel costs for an oxide slurry converter reactor.[10] The converter is assumed to operate at conversion ratios between 0.5 and 0.8. The fuel, a low enrichment UO_2 slurry in liquid bismuth, is to be shipped to a central chemical processing station or processed in a small on-site processing plant. It is estimated that the reactor could be designed to operate on natural UO_2 feed, although the effective enrichment of the reactor would be higher because of the presence of converted plutonium. A processing cost of $25 per kilogram ($22,680 per ton) of uranium, based on central processing plant costs, was assumed. Should the simple oxide centrifugation separation scheme, which is visualized as a possibility, prove to be effective, the reprocessing costs could conceivably be quite low.

Table VI-6 FUEL COSTS IN LMFR POWER STATIONS

(Mills per kilowatt hour)

	Burner		Converter		
	6-year life	12-year life	Natural U feed*	3% enriched U†	Breeder‡
U inventory	0.330	0.240	0.24	0.33	0.290
U consumption	1.985	1.985	1.24	0.83	
Reprocessing, including Bi make-up	0.373	0.294	1.03	0.21	0.972
Total fuel cost	2.69	2.52	2.51	1.37	1.26

* Conversion ratio of ~0.78.
† Conversion ratio of ~0.53.
‡ Conversion ratio of 1.00 assumed.

In Table VI-6 the fixed capital charges for reprocessing equipment (for the cases in which on-site processing is done) are considered to be included in the plant capital investment and do not appear in the fuel cost estimate. Furthermore, although fuel fabrication costs in an LMFR reactor would be small, there still remains some cost connected with the fabrication of the suitable fuel solution or slurry. For example, the costs of conversion from UF_6 (as obtained from the AEC) to either metal or oxide form and preparation of the final solution or slurry are not negligible.

LMFRE Characteristics

The experimental liquid metal reactor,[3,5,12] presently being designed and scheduled to be built by the Babcock and Wilcox Co., is an externally cooled reactor, with a liquid sodium intermediate coolant loop, in an open arrangement. It is designed primarily as a "burner" type reactor, i.e., it will burn enriched U^{235} with no attempt at breeding, although the design provides for two experimental "breeder" loops in the reflector to test the feasibility of using a blanket in a full-scale LMFR breeder reactor.

The core of the LMFRE will be a cylinder of high density graphite, with holes drilled in a vertical direction for fuel passage. Holes are also provided in the core for four control rods and one central test thimble. Surrounding the core will be a 5-in. annulus of graphite, to serve as an additional barrier between the core fuel solution and the reflector coolant which will be pure liquid bismuth. Pressure seals at the top and bottom are expected to provide a minimum leakage of the reflector coolant, which will be at a slightly greater pressure, into the core fluid fuel solution. The reflector consists of blocks of graphite machined and arranged to form an annular reflector 2 ft 3 in. thick. An annular gap between the core and reflector and

between the reflector and pressure vessel provides passages for the reflector coolant.

The core is to be assembled from graphite pieces, machined to fit together in a tongue and groove arrangement to provide mechanical strength. Joints between the pieces will be cemented, impregnated, and baked prior to installation. The reflector will be machined with offsets to prevent neutron streaming but will not be cemented in the vertical direction in order to allow for thermal expansion. Specially machined key blocks will be used to hold the reflector and core together. Additional support is provided by a steel base plate, supported by molybdenum rods passing through the outer region of the reflector to serve as a clamp.

Five beryllium-lined experimental holes are to be provided, one in the core and four penetrating the reflector region. The central core hole will be used for materials study under intense neutron irradiation. Two of the reflector holes will be used for corrosion studies under conditions of high temperature differential; the remaining two holes will be used for breeder blanket-slurry studies.

In addition to concentration control, the reactor will have four hollow tantalum control rods, housed in beryllium sheaths, within the core region. Three of these rods will be shim safety rods, and the fourth will be a servo-controlled regulator.

The reactor vessel is divided into two major regions, with a flange and bolted joint. The lower portion will house the core, reflector, and piping connections, whereas the upper vessel serves as the control-rod housing and drive mounting.

Operating characteristics of the LMFRE are shown in Table VI-1.

References

1. Liquid Metal Fuel Reactor, Technical Feasibility Report, BAW-2(Del.), June 30, 1955. (Unclassified AEC report.)
2. Liquid Metal Fuel Reactor Experiment, Test Program Report, BAW-1009, April 1957. (Unclassified AEC report.)
3. Liquid Metal Fuel Reactor Experiment, Objectives and Design Parameters, BAW-1011, May 1957. (Unclassified AEC report.)
4. Liquid Metal Fuel Reactor Experiment, The Economic Comparison of a Large-scale LMFR Breeder and Burner, BAW-1012, May 1957. (Unclassified AEC report.)
5. Liquid Metal Fuel Reactor Experiment, Preliminary Hazards Evaluation, BAW-1017, July 1957. (Unclassified AEC report.)
6. D. Mars, J. N. Inglima, and R. T. Schomer, Preliminary Design of an LMFR Power Plant, *Nuclear Science and Engineering*, 2(5): 582 (September 1957).
7. Reactor Handbook, 2d ed. (Unpublished).
8. J. Chernick, The Small LMFR for Research and Special Power Applications, BNL-2618. (Unclassified AEC report.)
9. B. M. Abraham, H. E. Flotow, and R. D. Carlson, UO_2-NaK Slurry Studies in Loops to 600°C, *Nuclear Science and Engineering*, 2(4): 501 (July 1957).
10. J. K. Davidson, W. L. Robb, et al., A UO_2-Liquid Metal Slurry Reactor for Economic Power, KAPL-1686, Dec. 15, 1956. (Unclassified AEC report.)
11. J. R. Weeks, C. J. Klamut, et al., Corrosion Problems with Bismuth Uranium Fuels, Paper P/118, Volume 9, pp. 341–355, Proceedings of the International Conference in Geneva, August 1955. (Available from the International Documents Service, Columbia University Press, 2960 Broadway, New York 27, N. Y.)
12. Liquid Metal Fuel Reactor Experiment, Quarterly Progress Report, November 1956–February 1957, BAW-1004, 1957. (Unclassified AEC report.)
13. F. T. Miles and C. Williams, Liquid Metal Fuel Reactor, P/494, Volume 3, pp. 125–133, Proceedings of the International Conference in Geneva, August 1955. (Available from the International Documents Service, Columbia University Press, 2960 Broadway, New York 27, N. Y.)
14. O. E. Dwyer, Heat Exchange in LMF Power Reactors, *Nucleonics*, 12(7): 30 (1954).
15. The Preliminary Design of the Liquid Metal Fuel Reactor Experiment, BNL-3247, Apr. 30, 1956. (Unclassified AEC report.)
16. Liquid Metal Fuel Reactors, *Nucleonics*, 12(7): 11 (July 1954).
17. Maximum Permissible Amounts of Radioisotopes in the Human Body and Maximum Permissible Concentrations in Air and Water, Handbook 52, U. S. Department of Commerce, National Bureau of Standards, 1953.
18. Nuclear Problems of Non-Aqueous Fluid-fuel Reactors, MIT-5000, Oct. 15, 1952. (Unclassified AEC report.)

The recently issued hazard summary report[1] for the Experimental Breeder Reactor II (EBR-II) is of interest as a discussion of the hazards characteristic of fast-neutron reactors and as a report on the present status of the EBR-II design.

EBR-II is an unmoderated, heterogeneous, sodium-cooled reactor and power plant with a power output of 62.5 Mw of heat. The energy produced in the reactor is converted to 20 Mw of electricity through a conventional steam cycle. The reactor may be fueled with U^{235} or plutonium, and the plant includes an integral fuel processing facility where the irradiated fuel is processed, fabricated, and assembled for return to the reactor. Although provisions are being made for subsequent loading of the reactor with uranium-plutonium fuel, the descriptions and analyses presented in the current hazards summary report pertain only to an enriched-uranium loading.

The EBR-II is primarily an engineering facility to determine the feasibility of this type of reactor for central-station power-plant application. Major emphasis has been placed on achieving high thermal performance at high temperatures and high fuel burn-up with a fast and economical fuel processing system. The thermal performance of the reactor and the size of the system components are such as to permit direct extrapolation to central-station application. The design objective has been to permit a maximum of experimental operational flexibility by separation of the plant systems and yet to permit extrapolation to a commercial plant which would not require the same degree of separation.

The plant will be located at the National Reactor Testing Station (NRTS) because the maximum operational flexibility of the reactor system is desired and because of the limited information available pertaining to power reactor operation with plutonium fuel.

The reactor consists of an enriched core surrounded on all sides by a fertile blanket of depleted uranium. The fuel elements which comprise the core section of the reactor consist of small diameter cylindrical pin assemblies. The design of the fuel element is influenced by the desire for high thermal performance, high burn-up, and simplicity of construction. The fuel pin is a loose fit in a thin-walled tube which provides a clearance annulus between the pin and the tube wall. This annulus is filled with static sodium to provide a heat-transfer bond between the fuel and fuel tube. Heat is removed from the fuel element by the primary sodium flowing along the outside of the fuel tube.

The reactor operates with a maximum power density in the core of ~1370 kw/liter, with a maximum coolant velocity of 26 fps, and with reactor coolant temperatures of 700°F inlet and 900°F outlet. Reactor control is effected by the movement of fuel into and out of the reactor core. This is accomplished by 12 modified movable fuel subassemblies, which move vertically, and are located at the outer edge of the core.

Heat is removed from the reactor by the primary sodium coolant system and transferred to the secondary sodium system in a shell-and-tube heat exchanger. The secondary system transfers the heat to the steam generator where superheated steam is produced to drive a conventional turbine generator.

The relation between EBR-II and the Enrico Fermi Plant of the Power Reactor Development Company (PRDC), the other fast-reactor project presently under way in the United States, is defined in reference 2: "... the PRDC reactor is designed to demonstrate the feasibility of utilizing a fast breeder reactor in the day-to-day production of electric power on a substantial scale. EBR-II, on the other hand, is an advanced reactor experiment which will test further steps in sodium-cooled fast-reactor technology and will go forward with the full plutonium fuel cycle, including pyrometallurgical reprocessing." Some of the important characteristics of EBR-II are compared in Table VII-1 with those of the Enrico Fermi reactor and with those of the British Dounreay reactor.

The EBR-II reactor is provided with a pressure vessel type secondary containment struc-

ture 80 ft in diameter and 146 ft high, designed for an internal pressure of 24 psig.

Characteristic features of the hazard considerations for the reactor are summarized below:

effort has been made to achieve a very rigid close-packed arrangement of the fuel and, in addition, to produce preferential bowing such as to effect a probable bowing coefficient which is essentially zero or negative. To the best of

Table VII-1 COMPARISON OF FAST-NEUTRON REACTOR AND PLANT CHARACTERISTICS: EBR-II, EBR-I, EFFBR (ENRICO FERMI), AND DFR (DOUNREAY) PLANTS

	EBR-II[1]	EBR-I[3]	EFFBR[4]	DFR[5,6]
General characteristics:				
Reactor thermal power, Mw	62.5	1.4	300	~60
Gross electrical power, Mw	20.0	0.2	100	15
Reactor coolant type	Na	NaK	Na	Na*
Coolant temperature to reactor, °F	700	442	550	~390
Coolant temperature from reactor, °F	900	600	800	~650
Coolant flow rate through reactor, gpm	8,200	292	30,400	~10,000
Feed-water temperature to steam generator, °F	550	446	400	
Steam temperature, °F	850	529	755	622†
Steam pressure, psig	1,300	390	600	200†
Steam flow rate, lb/hr	0.248×10^6	3,630	1.02×10^6	
Reactor data:				
Core dimensions				
Equivalent diameter, in.	19.04	7.9	30.5	22
Height, in.	14.22	8.5	31.2	21
Volume, liters	66.3	22.5	330	~178
Fuel alloy type	Fissium	Uranium	U-Mo alloy	Uranium
Fuel alloy composition, wt.%				
Uranium	95.0	100	90.0	100
Molybdenum	2.5		10.0	
Zirconium	0.2			
Ruthenium	1.5			
Rhodium	0.3			
Palladium	0.5			
Enrichment, U^{235}, %	49	93.5	27	~40
Critical mass, U^{235}, kg	170	48.2	485	
Specific power, kw/kg of total uranium	154	16.7	~149	
Pumps, primary sodium loops				
Pump type	d-c electro-magnetic‡	d-c electro-magnetic and centrifugal	centrifugal	a-c linear§ induction
Capacity, gpm	10,000‡	500	11,800	400
Head, psi	75‡	25	110	16
No. of pumps	2	2¶	3	24
Pumps, secondary sodium loops				
Pump type	a-c linear induction	centrifugal	centrifugal	a-c linear§ induction
Capacity, gpm	6,500	500	11,800	400
Head, psi	65	30	22	16
No. of pumps	1	1	3	24

*Initial loading, NaK.
†518°F and 150 psig initially.
‡Recent plans call for use of two centrifugal pumps each delivering 4250 gpm at a head of 60 psi.
§NaK pumps.
¶Either pump carries the full load.

1. The operational instabilities which were exhibited in the past by the EBR-I reactor have not as yet been completely explained. It is believed that these were, at least in part, due to mechanical instability in the reactor, notably bowing of the fuel elements. In EBR-II every

current knowledge, the reactor will have negative reactivity coefficients—prompt, slow, power, and isothermal.

2. The fast reactor differs from most thermal reactors in that the possibility of a very substantial increase of reactivity following a hypo-

thetical fuel melt-down is difficult to disprove. The report states that, although there is no indication that fuel alloy melting would definitely result in a prompt critical assembly in EBR-II, pessimistic assumptions on a gravity-induced accident of this nature suggest the equivalent of 300 lb of TNT as a reasonable upper limit for the energy release. It is estimated that the primary containment system of the reactor would easily contain a nuclear accident equivalent to the detonation of 300 lb of TNT at the center of the reactor.

3. The chemical reaction between sodium and air would represent a relatively large energy release if a major fraction of the air in the containment building were to react. A rapid reaction of this kind could occur only if large masses of sodium in dispersed form were ejected from the reactor system into the air; this could presumably be caused only by a rather violent nuclear energy release. The secondary containment is estimated to be adequate to contain such a chemical reaction.

4. Because of the very high power density which is characteristic of fast-reactor designs, the loss of coolant accident is one which must receive careful attention. Features of the EBR-II design which minimize the probability of such a failure are: the pool type arrangement of the primary system makes the loss of coolant extremely improbable; either one of three pumps—two main pumps and one auxiliary—are sufficient for shutdown cooling; in the event of failure of all three pumps, the shutdown reactor will cool by natural convection; the large mass of sodium in the primary reactor tank has a very large heat capacity which prevents rapid temperature rise in the primary system; the heat will be dissipated from the primary system to the atmosphere by natural-convection shutdown coolers in the event of failure of the secondary coolant system.

References

1. L. J. Koch, H. O. Monson, D. Okrent, M. Levenson, W. R. Simmons, J. R. Humphreys, J, Haugsnes, and V. C. Jankus, Hazard Summary Report Experimental Breeder Reactor II (EBR-II), ANL-5719, May 1957. (Unclassified AEC report.)
2. Robert W. Hartwell, Design and Construction of the Enrico Fermi Atomic Power Plant, 1958 Nuclear Engineering and Science Conference, Chicago, Illinois, p. 13, March 1958.
3. Power Reactors, Volume III, Proceedings of the International Conference in Geneva, August 1955. (Available from the International Documents Service, Columbia University Press, 2960 Broadway, New York 27, N. Y.)
4. Enrico Fermi Fast Breeder Reactor Plant, APDA-115, November 1956. (Unclassified AEC report.)
5. The Dounreay Fast Reactor. Here is How It Works, *Nuclear Power, The Journal of British Nuclear Engineering*, 2(14): 240–241 (June 1957).
6. Dounreay: The Fast Reactor..., *Nuclear Power, The Journal of British Nuclear Engineering*, 2(15): 230–244 (June 1957).

☆ U. S. GOVERNMENT PRINTING OFFICE : 58-4523 07/1

LEGAL NOTICE

This document was prepared under the sponsorship of the U. S. Atomic Energy Commission. Neither the United States, nor the Commission, nor any person acting on behalf of the Commission:

A. Makes any warranty or representation, express or implied, with respect to the accuracy, completeness, or usefulness of the information contained in this document, or that the use of any information, apparatus, method, or process disclosed in this document may not infringe privately owned rights; or

B. Assumes any liabilities with respect to the use of, or for damages resulting from the use of any information, apparatus, method, or process disclosed in this document.

As used in the above, "person acting on behalf of the Commission" includes any employee or contractor of the Commission to the extent that such employee or contractor prepares, handles or distributes, or provides access to, any information pursuant to his employment or contract with the Commission.